

**School of Molecular and Life Sciences**

**Investigating best practices for Structure-from-Motion  
photogrammetry of turbid benthic environments**

**Kesia Louise Savill**

**0000-0002-5507-6841**

**This thesis is presented for the Degree of  
Master of Research (Environmental Science)**

**of**

**Curtin University**

**June 2023**

## **Authors declaration**

To the best of my knowledge and belief, this thesis contains no material previously published by any other person except where due acknowledgement has been made.

This thesis contains no material which has been accepted for the award of any other degree or diploma in any university.

Date: 05/06/2023

## Thesis abstract

Turbid water environments represent ~8-12% of the total area of the global continental shelf, representing a variety of benthic habitats with high ecosystem value, such as turbid coral reefs, which account for 12% of the world's reefs. Yet, turbid reefs are relatively understudied due to their challenging working conditions, such as low light availability. Current climate projections suggest these types of reefs will become more prevalent due to growing evidence of their resilience to increasing sea surface temperatures, that would typically cause bleaching in clear water coral reefs. Their resilience to the effects of climate change can be attributed to their naturally high sediment loads, making them more tolerant to less than optimal growing conditions than their clear water counterparts. Therefore, it is important to understand how these reefs function. Census-based carbonate budgets are a comprehensive method that provides a detailed assessment of reef function, structural complexity and health, that estimates all sources of carbonate production and subtracts mechanical and biological carbonate loss. The Reef Budget method is the most common approach to quantify net carbonate accumulation, which relies on the use of line intercept transects (LIT) to assess the abundance of key carbonate producing organisms on the reef. As corals are typically the main carbonate producer on reefs, an accurate assessment of coral cover and composition is required for an accurate carbonate budget calculation. LIT's are a straightforward method but are time consuming and result in a limited area of reef being surveyed. As turbid reefs are difficult to survey, the use of LIT methods on these reefs results in longer periods *in-situ*, meaning higher costs in time and money. A more advanced approach in collecting data on marine benthic habitats is Structure-from-Motion (SfM) photogrammetry. SfM is the process of estimating the 3D structure of a scene, such as a reef, from a set of 2D photographs. In the last decade, SfM has become increasingly popular and a useful tool in coral reef studies. For instance, SfM has been used to characterise reefs and to extract important metrics, such as coral cover, rugosity and extensions rates, which are critical to improving current knowledge of reef health and can also be used to determine how reefs respond to disturbance events. To date, though,

the vast majority of underwater SfM photogrammetry studies have been conducted in relatively clear water environments, most likely due to the challenges of working in turbid environments. In the first part of this study, SfM photogrammetry techniques were compared with LIT's for collecting metrics for census-based carbonate budgets for a coral reef located in the turbid waters of Exmouth Gulf. The area surveyed in Exmouth Gulf was found to be characterised by patchy reef, dominated by weedy coral species. Moreover, in this experiment, the LIT method was found to give a more accurate assessment of coral metrics for carbonate budget calculations, than the results of SfM photogrammetry. It was concluded that the SfM photogrammetry approach used in the comparison was not optimal for turbid reef environments. Consequently, the aim of the subsequent part of this study was to investigate how SfM photogrammetry could be more successful in turbid environments. This consisted of selected aspects of image acquisition and processing being examined for their effect on the performance of SfM photogrammetry on targets of known dimensions. This included investigating camera types, and the altitude that photos are taken above the survey area, alongside image enhancement techniques in post-processing of photos. This part of the study concluded that a camera with a large sensor size and sensor resolution (e.g., Canon G7X Mark II) performed better in turbid benthic environments, than standard action cameras with lower sensor size and image resolution (e.g., GoPro 5 and GoPro 8) and a DSLR with a high sensor size and lower image resolution (e.g., Nikon D70). It also indicated that the accuracy of 3D models generated from SfM photogrammetry improved when images were taken from multiple altitudes, but this requires further investigation to make more universal conclusions. Image enhancement was found to improve the accuracy of 3D models in turbid benthic environments for the action camera used (GoPro Hero 8), but not for images taken with a higher sensor size (Canon G7X Mark II). However, measurements such as surface area should not be taken alone in assessing 3D model accuracy. Manual reviewing of SfM photogrammetry models can provide a more robust assessment, especially when comparing the SfM photogrammetry model with an above water laser scan or engineering diagram of the object. This study concludes with

recommendations for those carrying out SfM photogrammetry in turbid benthic environments and identifies areas for further research in this area.

## Acknowledgements

This thesis has provided me with the opportunity to explore the remote islands of the Exmouth Gulf, to learn the importance of turbid marine environments and has given me highly valuable experience learning some of the emerging technologies in the field of marine science, which will benefit me greatly in my future career endeavours.

I would not have completed this thesis without the support, guidance and belief of many people. I would firstly like to thank my wonderful supervisors, Dr Iain Parnum, Assoc. Prof. Jennifer McIlwain and Dr David Belton for their valuable knowledge and advice throughout this journey. You have all helped shape me into a better scientist and have been so supportive from the very beginning.

To my Thesis Chair, Dr Nicola Browne, thank you for taking me under your wing during my Honour's year and guiding me to my postgraduate degree. I appreciate all the time you gave me, the many people you introduced me to in the industry and for assisting in the initial creation of this research pathway.

To Assoc. Prof. Andrew Woods and Daniel Adams from Curtin HIVE, and Assoc. Prof. Petra Helmholz and Jack Henharen, thank you for your guidance navigating the world of photogrammetry, for putting up with my endless emails and questions, and for teaching me the essential skills I required for my data analysis.

To my Mum, thank you for always being my number one supporter, always cheering me on the loudest, giving me pep talks, hugs, life advice, telling me how proud you are of me and reminding me why I started down this pathway in the beginning. Forever my biggest inspiration in life, I love you.

To my Nanna, Grandad and brother, James, thank you for your unwavering support and giving me the encouragement to chase my dreams and pursue a career that I love.

To my partner, Dylan, thank you for loving and supporting me, celebrating my achievements, encouraging me and being the anchor that keeps me grounded, I love you!

To the REIF lab group, thank you for your support and guidance through postgraduate study, specifically Shannon Dee and Tahlia Bassett for all your help with learning new skills, programs and equipment.

To Dillon Newman for his underwater photography expertise which was an essential piece of the puzzle.

The Chapter 2 contribution was supported by an Australian Research Council (ARC) Discovery Early Career Research Award (DECRA; DE180100391)

## **Statement of contributions**

### **Chapter 2**

**Prepared for submission:** Savill, K.L., Browne, N.K., Parnum, I. Helmholz, P.

**Author contributions:** KLS, NKB and IP developed the concept for the study. The data was collected by KLS and NKB. Image processing was conducted by KLS with assistance from IP. KLS led the writing of the manuscript. All authors contributed critically to the drafts and gave final approval for publication.

### **Chapter 3**

**Prepared for submission:** Savill, K.L., Parnum, I., McIlwain, J., Belton, D.

**Author contributions:** KLS, IP and JM developed the concept for the study. The data was collected by KLS, IP and JM. Image processing was conducted by KLS with assistance from IP and DB. KLS led the writing of the manuscript. All authors contributed critically to the drafts and gave final approval for publication.

### **Chapter 4**

**Prepared for submission:** Savill, K.L., Parnum, I., McIlwain, J., Belton, D.

**Author contributions:** KLS, IP and JM developed the concept for the study. The data was collected by KLS, IP and JM. Image processing was conducted by KLS with assistance from IP and DB. KLS led the writing of the manuscript. All authors contributed critically to the drafts and gave final approval for publication.



## Table of contents

Authors declaration.....	ii
Thesis abstract.....	iii
Acknowledgments.....	vi
Statement of contributions.....	viii
<i>Chapter 2</i> .....	viii
<i>Chapter 3</i> .....	viii
<i>Chapter 4</i> .....	viii
Table of contents.....	ix
List of figures.....	xii
List of tables.....	xv
List of abbreviations.....	xvii
Chapter 1.....	1
<b>General introduction</b> .....	1
1.1 Turbid marine environments.....	1
1.1.1 Turbid coral reefs.....	1
1.2 Carbonate budgets.....	1
1.2.1 Traditional methodology.....	1
1.2.2 Structure-from-Motion methodology.....	2
1.3 Reseach significance.....	4
1.3.1 Research gaps.....	4
1.4 Research aims and thesis structure.....	4
1.4.1 Research aims.....	4
1.4.2 Thesis structure.....	5
1.5 References.....	8
<b>Chapter 2</b> .....	<b>15</b>
2.1 Abstract.....	15
2.2 Introduction.....	16
2.3 Methods.....	19
2.4 Results.....	29
2.5 Discussion.....	34

2.6 Conclusion.....	38
2.7 References.....	39
2.8 Supplementary material.....	45
<b>Chapter 3.....</b>	<b>46</b>
3.1 Abstract.....	46
3.2 Introduction.....	47
3.3 Materials and methods.....	48
3.4 Results.....	56
3.5 Discussion.....	63
3.6 Conclusions.....	66
3.7 References.....	66
3.8 Supplementary material.....	74
<b>Chapter 4.....</b>	<b>77</b>
4.1 Abstract.....	77
4.2 Introduction.....	78
4.3 Materials and methods.....	79
4.4 Results.....	82
4.5 Discussion.....	85
4.6 Conclusions.....	87
4.7 References.....	87
4.8 Supplementary material.....	91
<b>Chapter 5.....</b>	<b>92</b>
5.1 Summary of findings.....	92
5.1.1 Research finding #1.....	93
5.1.2 Research finding #2.....	94
5.1.3 Research finding #3.....	95
5.2 Limitations and future opportunities.....	97
5.3 Significance of thesis.....	98
5.4 Overall thesis conclusion.....	99
5.5 References.....	99

<b>Appendix A: Copyright statements.....</b>	<b>101</b>
Chapter 2.....	101
Chapter 3.....	102
Chapter 4.....	103

## List of figures

<b>Figure 1.1.</b> Conceptual diagram outlining the background, structure and aims of this research thesis.....	7
<b>Figure 2.1. a.</b> Satellite imagery of the north-east coast of Exmouth Gulf where Eva Island is located and where it is situated relative to the Western Australian coast (in grey). <b>b.</b> Eva Island with survey site location. <b>c.</b> Map of random transects within the site area (20 x 20 m) of LIT (line with direction and angle) and SfM (rectangle indicating 20 photos). <b>d.</b> SfM orthophoto of transect 8.....	20
<b>Figure 2.2. a.</b> Camera frame with GoPro's and GPS and <b>b.</b> Calibration cube and ladder <i>in-situ</i> configuration used to calibrate the cameras prior to photo processing.....	22
<b>Figure 2.3. a.</b> Original photo and image correction for <b>b.</b> Histogram equalization, and c. Z-score normalisation.....	26
<b>Figure 2.4.</b> Polygon creation in QGIS of different coral genera used to create shapefiles for estimation of percentage cover.....	27
<b>Figure 2.5. a.</b> Mean coral cover (%) of total coral cover and four dominant genera for LIT and SfM methods, <b>b.</b> Mean coral cover (%) of all detected genus for LIT and SfM methods (error bars = SE).....	30
<b>Figure 2.6. a.</b> Mean total number of species for LIT and SfM methods, <b>b.</b> Mean diversity index (H index) for LIT and SfM methods (error bars = SE).....	31
<b>Figure 3.1. a.</b> Satellite imagery of the two sites, Fremantle Sailing Club (blue points) and Coogee Maritime Trail (pink point) (Google Earth Pro, 2022). <b>b.</b> Aerial photograph of Coogee Maritime Trail (Seniorocity, 2020). <b>c.</b> Map of artificial reef structures of the Coogee Maritime Trail with red circle indicating surveyed structure (Tomlinson, 2022). <b>d.</b> 3D engineering diagram of Apollo structure (Subcon, 2022).....	49

<b>Figure 3.2.</b> Photos of a <i>Porites</i> coral skeleton taken using the Canon G7X Mark II with <b>a.</b> 100% field of view. <b>b.</b> 75% field of view. <b>c.</b> 50% field of view. <b>d.</b> 25% field of view.....	51
<b>Figure 3.3.</b> Scene setup of calibration ladder, calibration cube, Secchi disk and 2 coral skeletons at Fremantle Sailing Club in 2 m of water.....	52
<b>Figure 3.4.</b> Example of photos taken at <b>a.</b> 1 m above the seafloor, and <b>b.</b> 2 m above the seafloor, of the Apollo artificial reef structure.....	53
<b>Figure 3.5.</b> CloudCompare alignment of <i>Porites</i> skeleton point cloud from Canon G7X Mark II model (brown) overlaid on reference mesh from laser scan (green).....	54
<b>Figure 3.6.</b> CloudCompare alignment of Apollo structure point cloud from Canon G7X Mark II model using photos from 1 m (dark green) overlaid on the reference mesh from the engineering diagram (light green).....	55
<b>Figure 3.7.</b> 3D model of Fremantle Sailing Club scene from <b>a.</b> GoPro Hero 8, <b>b.</b> Canon G7X Mark II, <b>c.</b> Nikon D70. 3D model of scene setup of using a) GoPro Hero 8, b) Canon G7X Mark II, and c) Nikon D70, of the calibration ladder with labelled sides for measurements (Table 4), calibration cube with numbers indicating reference points, Secchi disk and 2 coral skeletons at Fremantle Sailing Club in 2 m of water.....	58
<b>Figure 3.8. a.</b> Laser scan mesh of <i>Porites</i> skeleton. <b>b.</b> Mesh from the 3D model of the <i>Porites</i> skeleton from the Canon G7X Mark II.....	60
<b>Figure 3.9. a.</b> Laser scan mesh of <i>Turbinaria</i> skeleton. <b>b.</b> Mesh from the 3D model of the <i>Turbinaria</i> skeleton from the Canon G7X Mark II. <b>c.</b> Mesh from the 3D model of the <i>Turbinaria</i> skeleton from the Nikon D70.....	60
<b>Figure 3.10. a.</b> Engineering diagram of Apollo structure. <b>B.</b> Mesh from Canon G7X Mark II 3D model from photos at 1 m and 2 m.....	60
<b>Figure 3.11.</b> Modelled accuracy vs measured accuracy.....	62

<b>Figure 3.12.</b> Linear regression (green line) of the measured accuracy against total number of photos with line of best fit using a log relationship (pink line).....	62
<b>Figure 4.1. a.</b> Satellite imagery of the two sites, Fremantle Sailing Club (blue points) and Coogee Maritime Trail (pink point) [19]. <b>b.</b> Aerial photograph of Coogee Maritime Trail [20]. <b>c.</b> Map of artificial reef structures of the Coogee Maritime Trail with red circle indicating surveyed structure [21]. <b>d.</b> 3D engineering diagram of Apollo structure [22].....	80
<b>Figure 4.2. a.</b> Number of features aligned from original, histogram equalisation, and CLAHE enhanced photos taken using a GoPro Hero 8 of the <i>Porites</i> coral skeleton in air and <b>b.</b> underwater.....	82
<b>Figure 4.3.</b> Number of features aligned from original, histogram equalisation, and CLAHE enhanced photos taken using a Canon G7X Mark II of the <i>Porites</i> coral skeleton in air.....	83
<b>Figure 4.4 a.</b> Number of features aligned from original, histogram equalisation, and CLAHE enhanced photos taken using a Canon G7X Mark II of the <i>Porites</i> coral skeleton underwater with automatic settings and <b>b.</b> underwater with custom settings.....	84
<b>Figure S4.1.</b> Example of the original model (light green) at 1 m from Canon G7X Mark II overlaid with CLAHE model (dark green) at 1 m. The CLAHE model can be seen as “noisy” due to the mesh including not just the structure itself.....	92
<b>Figure S4.2.</b> Models from combined altitudes for 1 m and 2 m for <b>a.</b> GoPro Hero 8 original photos. <b>b.</b> GoPro Hero 8 Histogram photos.....	92
<b>Figure 5.1.</b> Concept diagram outlining the outcomes and future research opportunities generated from this thesis.....	96

## List of tables

<b>Table 2.1.</b> Summary of statistical tests for total coral cover, the four dominant coral genera ( <i>Acropora</i> sp., <i>Porites</i> sp., <i>Pavona</i> sp., <i>Pocillopora</i> sp.), richness and diversity (H index). Note that for <i>Acropora</i> sp., <i>Pocillopora</i> sp. and the H index, the non-parametric Mann Whitney U test was used as the data did not meet assumptions. Significant p values are in bold.....	32
<b>Table 2.2.</b> Cost-benefit analysis for LIT and SfM methods.....	33
<b>Table S2.1.</b> GoPro Hero 5 specifications.....	45
<b>Table 3.1.</b> Specifications of cameras used in this study.....	50
<b>Table 3.2.</b> Number of features aligned at each field of view for each camera in air and with 2 different settings underwater. Green highlight indicates high numbers of features aligned between photos.....	57
<b>Table 3.3.</b> Measurements of objects from the scene at Fremantle Sailing Club from each camera and the difference from the actual measurement. Ladder 1 and 2 vertical measurements of longest length of ladder, Ladder 3 and 4 horizontal measurements of top and bottom cross bars (Figure 8b). Top of cube numbers referenced to shape on cube and measured from point to point (Figure 8b). *Actual measurements for Ladder and calibration cube measured using a measuring tape as lengths, Secchi disk measurement as diameter length and coral skeletons measured using surface are of a laser scan of the coral.....	59
<b>Table 3.4.</b> Number of images and surface area measurements (m <sup>2</sup> ) of the Apollo structure from the Canon G7X Mark II and GoPro Hero 8 models created using photos from 1 m, 2 m and combined 1 m & 2 m. Green highlight indicating the most agreeable surface area measurement.....	61
<b>Table S3.1.</b> Turbidity scale from Zweifler et al. (2021).....	74
<b>Table S3.2.</b> Previous SfM photogrammetry studies on benthic environments.....	74

<b>Table 4.1.</b> Specifications of cameras used in this study.....	81
<b>Table 4.2.</b> Surface area comparison of Apollo structure engineering diagram against 3D models created from GoPro Hero 8 and Canon G7X Mark II using original, histogram equalisation and CLAHE photos.....	85
<b>Table S4.1.</b> NTU and SD of Eva Island, Exmouth Gulf, Western Australia for 9 months of the year in 2020/2021.....	91



## **List of Abbreviations**

<b>3D</b>	3 (Three) Dimensional
<b>CCA</b>	Crustose Coralline Algae
<b>CLAHE</b>	Contrast Limited Adaptive Histogram Equalisation
<b>DTM</b>	Degrees of Freedom
<b>DF</b>	Digital Terrain Model
<b>FSC</b>	Fremantle Sailing Club
<b>GPS</b>	Global Positioning System
<b>LIDAR</b>	Light Detection and Ranging
<b>LIT</b>	Line Intercept Transect
<b>NTU</b>	Nephelometric Turbidity Unit
<b>REIF</b>	Reef Ecology and Island Futures
<b>SD</b>	Standard Deviation
<b>SE</b>	Standard Error
<b>SfM</b>	Structure from Motion

# Chapter 1

## General Introduction

### 1.1 Turbid marine environments

#### 1.1.1 Turbid coral reefs

Turbid coral reefs currently represent 12% of the world's reefs (Sully et al., 2020; Zweifler et al., 2021) and are of high biological and economic value (NOAA (a), (b), n.d.). Historically, these reefs were considered to be degraded (Done et al., 2007; Smith et al., 2008; Jupiter et al., 2008), with reduced coral cover and diversity. However, over the past couple of decades, there are studies showing evidence of high coral cover and diversity (Veron 1995; Browne et al., 2010; Palmer et al., 2010; Morgan et al., 2016), and resilience to effects of climate change, such as increasing sea surface temperatures (Perry et al., 2008; Morgan et al., 2017; Browne et al., 2019), which would typically cause bleaching in clear water corals. This suggests that these turbid coral reef environments with naturally high sediment loads, are more tolerant to less optimal growing conditions than clear water corals and could potentially be key refuge sites for future climate change events. Therefore, it is important to understand how these turbid reefs function through monitoring and conservation efforts. Yet, turbid reefs are poorly documented due to the challenging in-water working conditions such as low visibility, resulting in comparatively limited knowledge on turbid reef function (Zweifler et al., 2021). This study aims to assess and improve the techniques used for studying turbid reefs.

### 1.2 Carbonate budgets

#### 1.2.1 Traditional methodology

A comprehensive method that provides a detailed assessment of reef function, structural complexity and health is the census-based carbonate budget (Dee et al., 2020). This approach estimates all sources of carbonate production (e.g., Scleractinian coral, crustose coralline algae (CCA)) and

subtracts mechanical and biological carbonate loss (e.g., parrotfish, microborers, urchins) to calculate the net carbonate accumulation of the reef area per year (Dee et al., 2020). To quantify net carbonate accumulation, the Reef Budget method (Perry et al., 2012) is the most commonly used approach since it was published in 2012, (Browne et al., 2021). This method relies heavily on the use of line intercept transects (LIT) to assess the abundance of key organisms, such as coral, CCA and macroalgae. LITs are used to determine percentage cover of benthic communities as well as colony size, by recording different coral morphologies, and species where possible, that lie directly under the transect tape, whilst also recording (in centimetres) on the tape where morphologies (or species) change (Hill and Wilkinson, 2004). Whilst LITs are a cost efficient and easy to perform, they are limited by the area of reef they can cover in a time efficient manner and the coral identification expertise of the person conducting the survey (Hill and Wilkinson, 2004; Facon et al., 2016). An accurate assessment of coral cover and composition is essential for an accurate carbonate budget calculation as corals typically drive gross carbonate production rates. Whilst they are straightforward to undertake and the equipment required is inexpensive and easy to use, they are time consuming and often cover a limited area of the reef. As turbid reefs are difficult to survey, due to low visibility, this has resulted in visual surveys taking longer to conduct *in-situ* to collect benthic data, which increases the costs of time and money. Hence, researchers need to look for alternative methods and/or new technologies to improve the ability to accurately and more efficiently collect data on these types of reefs.

### **1.2.2 Structure-from-Motion methodology**

The use of photography and video sampling methods have become increasingly popular for monitoring benthic habitats over the past decade. Structure-from-Motion (SfM) photogrammetry is an accessible and non-invasive method, whereby a series of consecutive, overlapping photographs are taken of the survey area (Figueria et al., 2015). The photographs are then processed through photogrammetry software (e.g., Agisoft Metashape,

ContextCapture), where common features from the photographs are detected and aligned to create a 3D model of the survey area (Lange et al., 2020). This method is advantageous over traditional methods as data collection in the field can be conducted over a large area more efficiently and it provides a permanent visual record of the survey area (Leon et al., 2015).

Since 2015, SfM methodology has been used globally in coral reef studies to characterise reefs and to extract important metrics, such as coral cover, extension rates and rugosity (e.g., Burns et al., 2015; Leon et al., 2015; Figueira et al., 2015; Storlazzi et al., 2016; Burns et al., 2016; Ferrari et al., 2016; Ferrari et al., 2017; Bryson et al., 2017; Young et al., 2017; Johnson-Sapp, 2018; Anelli et al., 2019; Magel et al., 2019; Bayley et al., 2019; Fukunaga et al., 2019; Carlot et al., 2020; Rossi et al., 2020; Longo et al., 2020; Lange et al., 2020; Cresswell et al., 2020, Roach et al., 2021; Kornder et al., 2021; Price et al., 2021; Dagum et al., 2021; Bonis-Erickson, 2021; Simmons et al., 2021; Chen and Dai, 2021). These data are central to improving our knowledge on reef health (e.g., Gibson et al., 2021) as well as how they respond to disturbance events such as coral bleaching, disease and hurricanes (e.g., Longo et al., 2020; Kolodziej et al., 2021; Pascoe et al., 2021; Combs et al., 2021; Fukunaga et al., 2022).

To date, most SfM photogrammetry studies of benthic environments have been conducted in relatively clear water environments where conditions are usually favourable for data collection (e.g., Leon et al., 2015; Anelli et al., 2017; Magel et al., 2019; Burns et al., 2019; Creswell et al. 2020, Pascoe et al., 2021; Urbina-Barreto et al., 2021; Fukunaga et al., 2022). Turbidity is defined as a measure of water clarity (US EPA, 2012) and is determined by the amount of light absorbed or scattered by suspended particulate matter in the water column (Zweifler et al., 2021). Turbidity is formally measured as Total Suspended Sediment or Solids (TSS) mg/L, but more commonly a surrogate is used, such as Nephelometric Turbidity Units (NTU) using a turbidity sensor or monitor. In Chapter 2, SfM methods are tested on benthic environments located in Exmouth Gulf, where water circulation causes high turbidity through the resuspension of sediments (Dee et al. 2020). Exmouth

Gulf can exhibit a wide range of turbidity levels but is typically in the range 1-10 NTU (Sutton and Shaw, 2021). Moreover, the turbid reef environments are logistically harder to work in than their clear water counterparts, due to their limited visibility. SfM photogrammetry in these environments have to overcome scattering caused by particulate in the water column, which causes blurring in photos (Lu et al., 2017). The current SfM photogrammetry methodology works successfully in clear water environments, however there are no guidelines for altering the methodology to suit turbid environments where light and/or visibility is low and there is large amounts of particulate in the water column. Therefore, optimising the current SfM photogrammetry methodology can ensure its suitability in turbid environments.

### **1.3 Research significance**

#### **1.3.1 Research gaps**

To the author's knowledge, there are currently no studies which specifically investigate the use and accuracy of SfM photogrammetry in turbid benthic environments. Investigation into optimising current SfM photogrammetry methodologies needs to occur for its application to be successful in these logistically difficult to work in environments. This can be achieved by examining aspects of image acquisition and processing in the SfM photogrammetry workflow that could be optimised for turbid waters. For instance, testing the capabilities of different camera types in turbid environments to determine if there is an optimal camera (or camera properties) that is best suited to these environments. The altitude (i.e., height of the camera lens above the survey target) also needs to be investigated to ensure photos are taken at the optimal altitude for the type of camera used and turbidity of the survey area. Additionally, taking photos of the scene at a mixture of altitudes might also improve the interior orientation parameter estimation, as part of the bundle adjustment. Finally, image enhancement techniques can be investigated to determine if post-processing of photos from turbid environments improves the accuracy of the resulting 3D models and needs to be integrated into SfM methodology for turbid water environments. Image enhancement has been successfully used in previous

SfM photogrammetry studies in underwater environments to improve the quality of the photos and the resulting models (e.g., Hitam et al., 2013; Jawahir Hj Wan Yussof et al., 2013; Yang et al., 2016; Sharma et al., 2019; Abd-Al Ameer et al. 2019; Kanthamma et al., 2020; Sharma et al., 2021;), however it is unclear whether the application of such techniques has been studied in turbid environments specifically.

## **1.4 Research aims and thesis structure**

### **1.4.1 Research aims**

The aim of this thesis is to optimise the use of SfM photogrammetry in turbid underwater environments. This objective will be investigated in three data chapters. Chapter 2 is from the author's Honour's project, which was converted into a Master's study. It was found that SfM photogrammetry was logistically harder than initially thought in turbid environments. It aimed to assess the use of traditional LITs against SfM photogrammetry methods for carbonate budget studies in turbid reef environments. Whilst an orthophoto of the transects was produced from the SfM photogrammetry workflow, the SfM methodology used was inadequate to produce accurate 3D models of an area in turbid water. Consequently, the findings of the Honour's project led to the development of ways to optimise SfM methodology, including investigating camera type, altitude and image enhancement techniques. Chapter 3 aims to determine if the type of camera used significantly affects SfM photogrammetry software's ability to align features, and establish the effect of the distance between the camera and the survey area (i.e., altitude). Chapter 4 aims to determine if image enhancement techniques has a significant effect on SfM photogrammetry software's ability to align features and create a more accurate 3D model.

### **1.4.2 Thesis structure**

This thesis includes five chapters (Figure 1): a general introduction (Chapter 1, this chapter), three data chapters (Chapters 2, 3 and 4) and a general

discussion (Chapter 5). The three data chapters are stand-alone manuscripts. As a result, there is some repetition, particularly with the Methods sections. Chapter 2 (Honour's project) has been prepared for submission to the journal, Coral Reefs. Chapter 3 has been prepared for submission to the journal, Marine and Environmental Research whilst Chapter 4 has been prepared for submission to the journal, Remote Sensing. Chapter 5 is a general discussion that draws together the outcomes and limitations of the findings of this study in terms of SfM photogrammetry in turbid underwater environments, and discusses the considerations required for the successful application in these environments. Chapter 5 concludes with the identification and discussion of future research opportunities for optimising the use of Structure-from-Motion photogrammetry in turbid underwater environments that has arisen from my thesis.

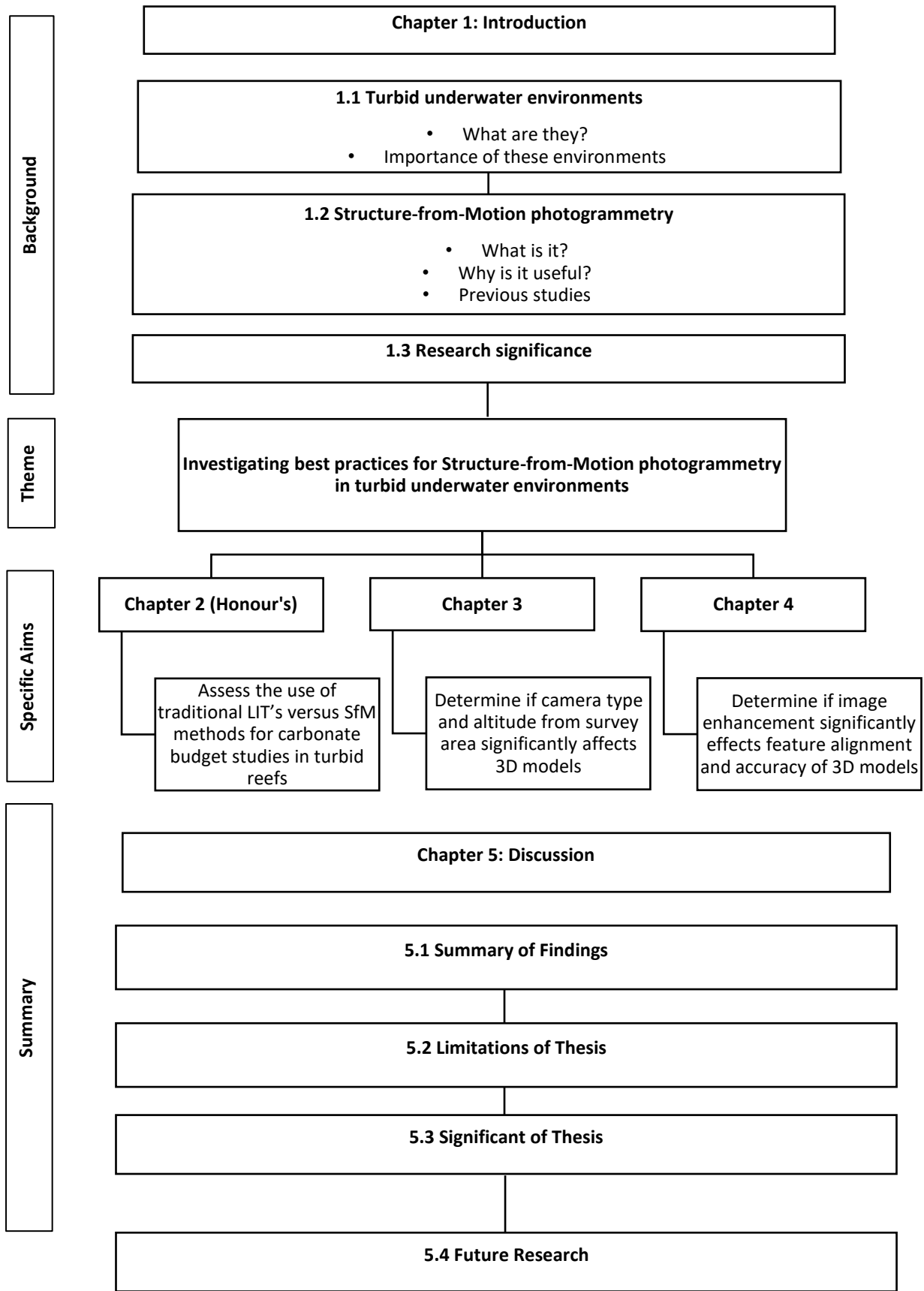


**Figure 1.1.** Conceptual diagram outlining the background, structure and aims of this research thesis



## 1.5 References

- Abd-Al Ameer ZS, Daway HG, Kareem HH. 2019. Enhancement underwater image using histogram equalization based on color restoration. *Journal of Engineering and Applied Sciences*. 14 (2), 641-647
- Anelli M, Julitta T, Fallati L, Galli P, Rossini M, Colombo R. 2017. Towards new applications of underwater photogrammetry for investigating coral reef morphology and habitat complexity in the Myeik Archipelago, Myanmar. *Geocarto International*. 34:5, 459-472
- Bayley DTI, Mogg AOM, Koldewey H, Purvis A. 2019. *PeerJ*. 7, e6540
- Bonis-Ericksen NK. 2021. Examining patterns in coral demographics events in Papahānaumokuākea marine national monument. Master's project, University of Hawai'i At Hilo. Retrieved from [https://dspace.lib.hawaii.edu/bitstream/10790/6860/1/BonisEricksen\\_hilo.hawaii\\_1418O\\_10216.pdf](https://dspace.lib.hawaii.edu/bitstream/10790/6860/1/BonisEricksen_hilo.hawaii_1418O_10216.pdf)
- Browne NK, Smither SG, Perry CT. 2010. Geomorphology and community structure of Middle Reef, central Great Barrier Reef, Australia: an inner-shelf turbid zone reef subject to episodic mortality events. *Coral Reefs* 29:683-689
- Browne N, Braoun C, McIlwain J, Ramasamy N, Zinke J. 2019. Borneo coral reefs subject to high sediment loads show evidence of resilience to various environmental stressors. *PeerJ*. 8, e7382
- Browne NK, Cuttler M, Moon K, Morgan K, Ross CL, Catsro-Sanguino C, Kennedy E, Harris D, Barnes P, Bauman A, Beetham E, Bonesso J, Bozec Y, Cornwall C, Dee S, DeCarlo T, D'Olivio J, Doropoulos C, Evan RD, Eyre B, Gatenby P, Gonzalez M, Hamylton S, Hansen J, Lowe R, Mallela J, O'Leary M, Roff G, Saunders B, Zweilfer A. 2021. Towards predicting responses of reefs and reef-fronted shorelines to climate change: development of a conceptual geo-ecological carbonate reef system model. *Oceanography and Marine biology: Annual Review*. Accepted.
- Bryson M, Ferrari R, Figueira W, Pizarro O, Madin J, Williams S, Byrne M. 2017. Characterization of measurement errors using structure-from-motion

- and photogrammetry to measure marine habitat structural complexity. *Ecology and Evolution*. 15;7 (15):5669-5681
- Burns JHR, Delparte D, Gates RD, Takabayashi M. 2015. Integrating structure-from-motion photogrammetry with geospatial software as a novel technique for quantifying 3D ecological characteristics for coral reefs. *Peer J* 3 [doi: 10.7717/peerj.1077]
- Burns JHR, Delparte D, Kapon L, Belt M. 2016. Assessing the impact of acute disturbances on the structure and composition of a coral community using innovative 3D reconstruction techniques. *Methods in Oceanography*. 15. 10.1016/j.mio.2016.04.001
- Burns JHR, Fukunaga A, Pascoe K, Runyan A. 2019. 3D habitat complexity of coral reefs in the Northwestern Hawaiian Islands is driven by coral assemblage structure. *ISPRS-International Archives of the Photogrammetry, Remote Sensing and Spatial Information Sciences*. XLII-2/W10. 61-67
- Carlot J, Rovere A, Casella E, Harris D, Grellet-Munoz C, Chancerelle Y, Dormy E, Hedouin L, Parravicini V. 2020. Community composition predicts photogrammetry-based structural complexity on coral reefs. *Coral Reefs*. 39, 967-975
- Chen GK, Dai CF. 2021. Using 3D photogrammetry to quantify the subtle differences of coral reefs under the impacts of marine activities. *Marine Pollution Bulletin*. 173, 113032
- Combs IR, Studivan MS, Eckert RJ, Voss JD. 2021. Quantifying impacts of stony coral tissue loss disease on corals in Southeast Florida through surveys and 3D photogrammetry. *PLoS ONE*. 16: e0252593
- Cresswell AK, Orr M, Renton M, Haywood MDE, Giraldo Ospina A, Slawinski D, Austin R, Thomson DP. 2020. Structure-from-motion reveals coral growth is influenced by colony size and wave energy on the reef slope at Ningaloo Reef, Western Australia. *Journal of Experimental Marine Biology and Ecology*. 530-531
- Dagum LJ, Licuanan W, Arceo H, David L. 2021. 3D coral forms: Structural complexity descriptor and potential predictor of fish abundance. *Oceans 2021: San Diego-Porto, 2021*. 1-6

- Dee S, Cuttler M, O'Leary M, Hacker J, Browne N. 2020. The complexity of calculating an accurate carbonate budget. *Coral Reefs* 39:1525-1534
- Done T, Turak E, Wakeford M, DeVantier L, McDonald A, Fisk D (2007) Decadal changes in turbid-water coral communities at Pandora Reef: loss of resilience or too soon to tell? *Coral Reefs* 26:789-805
- Facon M, Pinault M, Obura D, Pioch S, Pothin K, Bigot L, Garnier R and Quod JP. 2016. A comparative study of the accuracy and effectiveness of line and point intercept transect methods for coral reef monitoring in the southwestern Indian Ocean islands. *Ecological Indicators*. 60, 1045-1055
- Ferrari R, McKinnon D, He H, Smith RN, Corke P, Gonzalez-Rivero M, Mumby PJ, Upcroft B. 2016. Quantifying multiscale habitat structural complexity: A cost-effective framework for underwater 3D modelling. *Remote Sensing*. 8(2), 113
- Ferrari R, Figueira WF, Pratchett MS, Boube T, Adam A, Kobelkowsky-Vidrio T, Doo SS, Brooke Atwood T, Byrne M. 2017. 3D photogrammetry quantifies growth and external erosion of individual coral colonies and skeletons. *Scientific Reports*. 7, 16737
- Figueria W, Ferrari R, Weatherby E, Porter A, Hawes S and Byrne M. 2015. Accuracy and precision of habitat structural complexity metrics derived from underwater photogrammetry. *Remote Sensing*. 7(12), 16883-16900
- Fukunaga A, Burns JHR, Craig BK, Kosaki RK. 2019. Integrating three-dimensional benthic habitat characterization techniques into ecological monitoring of coral reefs. *Journal of Marine Science and Engineering*. 7, 27
- Fukunaga A, Pascoe KH, Pugh AR, Kosaki RK, Burns JHR. 2022. Underwater photogrammetry captures the initial recovery of a coral reef at Lalo Atoll. *Diversity*. 12, 39
- Gibson LA. 2021. How large area imagery can be used to quantify growth of a complex branching coral species. Master's project, University of California, San Diego. Retrieved from <https://escholarship.org/uc/item/65k35155>
- Hitam MS, Awalludin EA, Jawahir Hj Wan Yussof WN, Bachok Z. Mixture contrast limited adaptive histogram equalization for underwater image

- enhancement. *2013 International Conference on Computer Applications Technology*. 1-5
- Jawahir Hj Wan Yussof WN, Hitam MS, Awalludin EA, Bachok Z. 2013. Performing contract limited adaptive histogram equalization technique on combined color models for underwater image enhancement. *International Journal of Interactive Digital Media*. 1 (1)
- Johnson-Sapp. 2018. A tale of two reefs: Quantifying the complexity of artificial reefs and natural reefs utilizing Structure-from-Motion 3D modeling. Master's project, Duke University. Retrieved from <https://hdl.handle.net/10161/16560>
- Jupiter S, Roff G, Marion G, Henderson M, Schrameyer V, McCulloch M, Hoegh-Guldberg O. 2008. Linkages between coral assemblages and coral proxies of terrestrial exposure along a cross-shelf gradient on the southern Great Barrier Reef. *Coral Reefs* 27:887–903
- Kanthamma K, Geetha G, Keerthi D, Uday Kiran D, Vinod Kumar CH. 2020. Improved CLAHE enhancement technique for underwater images. *International journal of Engineering Research and Technology*. 9 (7)
- Kolodziej G, Studivan MS, Gleason ACR, Langdon C, Enochs IC, Manzella DP. 2021. Impacts of Stony Coral Tissue Loss Disease (SCTLD) on coral community structure at an inshore patch reef of the Upper Florida Keys using photomosaics. *Frontiers in Marine Science*. 8, 682163
- Kornder NA, Cappelletto J, Mueller B, Zalm MJL, Martinez SJ, Vermeij MJA, Huisman J, de Goeij JM. 2021. Implications of 2D versus 3D surveys to measure the abundance and composition of benthic coral reef communities. *Coral Reefs*. 40, 1137-1153
- Lange ID, Perry CT. 2020. A quick, easy and non-invasive method to quantify coral growth rates using photogrammetry and 3D model comparisons. *Method Ecol Evol* 11:714-726
- Leon JX, Roelfsema CM, Saunders MI, Phinn SR. 2015. Measuring coral reef terrain roughness using 'structure-from-motion' close range photogrammetry. *Geomorphology* 242:21-28
- Longo GO, Correia LFC, Mello TJ. 2020. Coral recovery after a burial event: insights on coral resilience in a marginal reef. *Marine Biodiversity*. 50, 92

- Lu H, Li Y, Zhang Y, Chen M, Serikawa S, Kim H. 2017. Underwater optical image processing: A comprehensive review. *Mobile Networks and Applications*. 22, 1204-1211
- Magel JMT, Burns JHR, Gates RD, Baum JK. 2019. Effects of bleaching-associated mass coral mortality on reef structural complexity across a gradient of local disturbance. *Scientific Reports*. 9, 2512
- Morgan, K.M.; Perry, C.T.; Smithers, S.G.; Johnson, J.A.; Daniell, J.J. 2016. Evidence of extensive reef development and high coral cover in nearshore environments: Implications for understanding coral adaptation in turbid settings. *Sci. Rep.* 6, 29616.
- Morgan KM, Perry CT, Johnson JA, Smither SG. 2017. Nearshore turbid-zone corals exhibit high bleaching tolerance on the Great Barrier Reef following the 2016 ocean warming event. *Front Mar Sci* 4:224
- National Oceanic and Atmospheric Administration (a). No Date. The importance of coral reefs. Retrieved from [https://oceanservice.noaa.gov/education/tutorial\\_corals/coral07\\_importance.html](https://oceanservice.noaa.gov/education/tutorial_corals/coral07_importance.html)
- National Oceanic and Atmospheric Administration (b). No Date. How to coral reefs benefit the economy? Retrieved from [https://oceanservice.noaa.gov/facts/coral\\_economy.html](https://oceanservice.noaa.gov/facts/coral_economy.html)
- Palmer, S.E.; Perry, C.T.; Smithers, S.G.; Gulliver, P. 2010. Internal structure and accretionary history of a nearshore, turbid-zone coral reef: Paluma Shoals, central Great Barrier Reef, Australia. *Mar. Geol.* 276, 14–29.
- Pascoe KH, Fukunaga A, Kosaki RK, Burns JHR. 2021. 3D assessment of a coral reef at Lalo Atoll reveals varying responses of habitat metrics following a catastrophic hurricane. *Scientific Reports*. 11, 12050
- Perry, C.T.; Smithers, S.G.; Palmer, S.E.; Larcombe, P.; Johnson, K.G. 2008. 1200 year paleoecological record of coral community development from the terrigenous inner shelf of the Great barrier reef. *Geology*. 36, 691–694
- Perry CT, Edinger EN, Kench PS, Murphy GN, Smithers SG, Steneck RS, Mumby PJ. 2012. Estimating rates of biologically driven coral reef framework production and erosion: a new census-based carbonate budget methodology and applications to the reefs of Bonair. *Coral Reefs* 31:853-868

- Price DM, Lim A, Callaway A, Eichhorn MP, Wheeler AJ, Lo Iacano C, Huvenne VAI. 2021. Fine-scale heterogeneity of a cold-water coral reef and its influence on the distribution of associated taxa. *Frontiers in Marine Science*. 8:556313
- Roach TNF, Yadav S, Caruso C, Dilworth J, Foley CM, Hancock JR, Huckeba J, Huffmyer AS, Hughes K, Kahkejian VA, Madin EMP, Matsuda SB, McWilliam M, Miller S, Santoro EP, Rocha de Souza M, Torres-Pullizaa D, Drury C, Madin JS. 2021. A field primer for monitoring benthic ecosystems using Structure-from-Motion photogrammetry. *Journal of Visualized Experiments*. 170, e61815
- Rossi P, Castagnetti C, Capra A, Brooks AJ, Mancini F. 2020. Detecting change in coral reef 3D structure using underwater photogrammetry: critical issues and performance metrics. *Applied Geomatics*. 12, 3-17
- Sharma V, Kulshrestha A, Barot P. 2019. A study on underwater image enhancement using histogram equalization. *International Journal of Scientific and Engineering Research*. 10 (5)
- Simmons KR, Bohnenstiehl DR, Eggleston DB. 2021. Spatiotemporal variation in coral assemblages and reef habitat complexity among shallow fore-reef sites in the Florida Keys National Marine Sanctuary. *Diversity*. 14, 153
- Smith LD, Gilmour JP, Heyward AJ. 2008. Resilience of coral communities on an isolated system of reefs following catastrophic mass-bleaching. *Coral Reefs* 27:197-205
- Storlazzi CD, Dartnell P, Hatcher GA. 2016. End of the chain? Rugosity and fine-scale bathymetry from existing underwater digital imagery using structure-from-motion (SfM) technology. *Coral Reefs* 35:889–894
- Sully S, van Woesik R. 2020. Turbid reefs moderate coral bleaching under climate-related temperature stress. *Global Change Biology*. 26(3), 1367-1373
- Sutton AL, Shaw JL. 2021. Cumulative pressures on the distinctive values of Exmouth Gulf. First draft report to the Department of Water and Environmental Regulation by the Western Australian Marine Science Institution, Perth, Western Australia. 272 pages.

- Urbina-Barreto I, Garnier R, Elise S, Pinel R, Dumas P, Mahamadaly V, Facon M, Bureau S, Peignon C, Quod JP, Dutriex E, Penin L and Adjeroud M. 2021. Which method for which purpose? A comparison of line intercept transect and underwater photogrammetry methods for coral reef surveys. *Frontier in Marine Science*. 8
- US EPA. 2012. Water: Monitoring and Assessment. 5.5 Turbidity, US Environmental Protection Agency, Washington, D.C.
- van Woesik R, Houk P, Isechal AL, Idechong JW, Victor S, Golbuu Y. 2012. Climate-change refugia in the sheltered bays of Palau: analogs of future reefs. *Ecology and Evolution*. 2(10), 2474-2484
- Veron JEN. 1995. Corals in space and time: The biogeography and evolution of the *Scleractinia*. Sydney, Australia: University of New South Wales Press, 321p
- Wagner DE, Kramer P, van Woesik R. 2010. Species composition, habitat and water quality influence coral bleaching in southern Florida. *Marine Ecology Progress Series*. 408, 65-78
- Yang W, Xu Y, Qiao X, Rao W, Li D, Li Z. 2016. Method for image intensification of underwater sea cucumber based on contrast-limited adaptive histogram equalization. *Transactions of the Chinese Society of Agricultural Engineering*. 32, 197-203
- Young G, Dey S, Rogers AD, Exton D. 2017. *PLoS ONE*. 12. 10.1371.0175341
- Zweifler A, O'Leary M, Morgan K, Browne NK. 2021. Turbid coral reefs: Past, present and future-A review. *Diversity*. 13(6), 251

## Chapter 2

### **A comparative and cost-benefit analysis of Structure-from-Motion in determining coral cover and diversity in turbid reef environments.**

Kesia L. Savill, Nicola K. Browne, Iain M. Parnum and Petra Helmholz

#### **2.1 Abstract**

Inshore reefs exposed to naturally high volumes of sediment are termed “turbid zone reefs”, whose geographic range is likely to increase due to changing climates, sea level rise and poor land management practices. Yet, these reefs are poorly studied, limiting our knowledge and understanding of how these reefs function. Census-based carbonate budgets provide a detailed assessment of reef function using line intercept transects (LIT’s) to determine key coral metrics (cover, diversity). However, they are time-consuming and require a high level of expertise in coral identification. Recently, Structure-from-Motion (SfM) photogrammetry has been employed as an alternative method to survey changes in reef habitat. This study examined the effectiveness of SfM in turbid coral reef environments by comparing coral metrics used in carbonate budget studies against the traditional LIT method. Species richness was greater for SfM, but mean coral cover was significantly higher for LIT’s (LIT = 41.75%  $\pm$  1.2, SfM = 21.9%  $\pm$  2.77). Importantly, differences in coral cover were driven by SfM’s limited ability to resolve small, low lying coral colonies, specifically *Pavona* sp., which was the only coral genera of the four most abundant corals (*Acropora*, *Porites*, *Pocillopora*), whose cover was significantly different between methods. The low in-water visibility conditions combined with the complex surface topography were the key factors that impacted the accuracy of the SfM data acquisition. Further, a cost-benefit analysis found that LIT’s are cheaper and quicker to conduct. To enhance the future application of SfM to these types of environments, we provide several recommendations, such as the addition of technology (e.g., GPS, LIDAR, acoustic and echo sounding)



and cameras suited to low light environments. But for now, LIT's are currently the less resource intensive and more scientifically robust approach for collecting carbonate budget coral metrics within turbid and/or rugose coral reef environments.

## **2.2 Introduction**

Coral reefs are one of the most biodiverse and productive ecosystems that support and promote biodiversity, and provide essential ecosystem services, such as coastal protection and food security. Reefs are largely composed of calcium carbonate deposited by carbonate producing organisms (Hubbard et al., 1986; Mallela & Perry, 2007; Hubbard, 2008). Scleractinian corals are typically the main producers of calcium carbonate (Herran et al., 2017), and therefore drive rates of reef accretion (Hubbard et al., 1986; Mallela & Perry, 2007; Hubbard, 2008). These organisms also provide the structural complexity of the reef (Graham and Nash, 2013), providing shelter for other reef-dwelling organisms (Lange et al., 2020). Thus, the accretionary potential and ability of reefs to maintain their structural integrity and associated ecosystem services is heavily dependent on corals and their rate of calcium carbonate production. However, local stressors (e.g., sediments, nutrients) and anthropogenic climate change (e.g., warming oceans) threaten coral function and growth, which to date has resulted in a global decline in coral cover (Veron, 2009; Hoegh-Guldberg et al., 2017; Lange et al., 2020), reef complexity and reef accretionary potential (Lange et al., 2020).

There is growing evidence that inshore reefs exposed to naturally high volumes of sediments are more resilient to warming ocean events than their offshore clear-water counterparts. These reefs, termed "turbid zone reefs", are frequently exposed to sediment resuspension events resulting in elevated turbidity and sediment accumulation (Perry & Smithers, 2006). This can lead to a reduction in photosynthesis and energy production due to low light availability, a reduction of larval settlement, and potentially increased coral mortality if corals are smothered in sediments (Browne et al., 2013) and

consequently may be described as degraded. Yet, over the past 20 years there is growing evidence that many turbid coral reefs have high coral cover and diversity (Veron, 1995; Browne et al., 2010), are highly adaptive to sedimentary regimes and are, therefore, more resilient than previously considered (Veron, 1995; Ayling & Ayling, 1999; Perry & Smither, 2006). For example, Morgan et al (2017) reported significantly less bleaching at Paluma Shoals, a turbid reef on the inshore Great Barrier Reef, than clear-water reefs nearby. The mechanisms that provide these reefs with increased resilience to such events is unclear, but its likely due to one or both of the following: 1) high suspended sediment concentrations can shield turbid reef corals from high light intensity alleviating radiative stress (Storlazzi et al., 2015), and 2) the ability to effectively use heterotrophic and autotrophic feeding mechanisms thereby maintaining a positive energy budget even when bleached (Anthony & Fabricius, 2000; Morgan et al., 2017). Regardless of the mechanism, it is important to better understand how these under-studied reefs are functioning given that they are likely to increase in geographic range in coming years due to sea level rise, changing climates (e.g., increased rainfall) and poor land management practices (Guinotte et al., 2003; Oppenheimer et al., 2019) and could be important refuge sites for future large-scale climate-change events (Morgan et al., 2017).

A comprehensive method that provides a detailed assessment of coral reef function is the census-based carbonate budget. This approach measures all known sources of carbonate accumulation (e.g., coral, crustose coralline algae (CCA)) and biological carbonate removal (e.g., parrotfish, urchins, microborers), to provide a rate of net carbonate production (Dee et al., 2020). The most widely used method for quantifying net carbonate production is the Reef Budget (Perry et al 2012), which to date has been employed in 44% (17 out of 38) of published census-based carbonate budget studies since it was published in 2012 (Browne et al., 2021). It has been used to assess reef health (e.g., Manzello et al., 2018), reef response to acute disturbance events (e.g., Lange and Perry, 2019) and assess a reef's ability to keep up through reef accretion with future sea level rise (e.g., Perry et al., 2018).

However, the method heavily relies on the line intercept transect (LIT) to assess the abundance of key organisms (e.g., coral cover, CCA cover, macroalgal cover), which are recorded *in-situ* on dive slates or using photographs and/or videos as photo transects (Jonker et al., 2008). Photo-transects can be used as an alternative to *in-situ* recordings, by taking photos at regular intervals along the transect, then selecting random images to perform image analysis, reducing the amount of time required in the field as identification can be done using automated software (Jonker et al., 2008). Although *in-situ* transects and photo-transects are easy and cheap to conduct, they cover a limited area of the reef and may, therefore, not provide a true representation of habitat area. Photo-transects, also known as ortho-mosaics, can only determine percentage cover (Urbina-Barreto et al., 2021), not surface area, as they do not capture the 3D information required for surface area calculation, required for carbonate budget calculations. Limitations of LIT's and photo-transects are likely to be more of a concern for reefs that are characterized by heterogenous habitats (patchy coral community), such as on turbid zone reefs. An accurate assessment of coral cover and composition is critical for reliable carbonate budget calculations given that corals typically drive reef gross carbonate production rates, as coral cover and composition alongside carbonate production rates can indicate the stability of the coral community (Browne et al., 2013).

As technology evolves, researchers look for more efficient ways to collect *in-situ* benthic cover data over larger three-dimensional (3D) areas of the reef. In recent years, Structure-from-Motion (SfM) photogrammetry has been used as a non-invasive, alternative method to survey changes in the reef habitat (e.g., coral cover) (Lange et al., 2020). SfM photogrammetry involves taking a series of overlapping photographs (Lange et al., 2020) which are then analysed using Structure-from-Motion software (e.g., ContextCapture, Australis, Agisoft Photoscan). The SfM software detects common features or points from multiple photos to create a high-resolution digital terrain model (DTM) and orthophoto mosaic (Leon et al., 2015), which can be used to create a 3D model (Lange et al., 2020). To date, no published carbonate budget study has employed the use of SfM photogrammetry to assess key

coral carbonate production metrics (cover and composition). Yet, this method offers many advantages over the traditional LIT including quicker data collection in the field, the ability to work over a large area more efficiently and providing a permanent record of coral reef habitat (Lange et al., 2020). The potential disadvantage of this technique is the cost of equipment (camera setup, computational power, computer software) and specific expertise required to calibrate the cameras, if programs such as ContextCapture require manual calibration, and experience in using photogrammetry software to process the photographs.

This study assesses the use of traditional LIT's versus SfM photogrammetry methods for carbonate budget studies in turbid reef environments, by comparing data collected on key variables for carbonate budget estimates (coral cover and composition) and resources required to effectively collect and analyse the data (time, expertise, cost). Specifically, the aims of this study are to: 1) assess if coral cover and diversity are significantly different between methods, 2) evaluate associated resources required to carry out LIT and SfM photogrammetry methods, and 3) determine whether SfM can be used to better estimate carbonate budgets in turbid reef environments than the commonly used LITs.

## **2.3 Methods**

### **Study site**

This study was conducted in Exmouth Gulf, on the central coast of Western Australia. The Gulf is a large embayment (2600 km<sup>2</sup>) (Brunskill et al., 2001) that is relatively shallow (mean depth ~11.9 m) and experiences south to south-westerly winds for most of the year (Bonesso et al., 2020; Dee et al., 2020). Turbidity, which varies from ~1m of visibility to ~5-10m is high in the region due to episodic sediment resuspension from prevailing winds, local wind-driven waves and net tidal currents, therefore, reefs in this area are naturally turbid (Bonesso et al, 2020).

Benthic data was collected at the northern reef of Eva Island ( $21^{\circ}55'19''S$ ,  $114^{\circ}25'55''E$ ), located on the eastern side of the Gulf (Fig 2.1a, b). The reef is characterised by shallow reef flats that are ~3-4m in depth to the north, sandbars dominated by macro-algae to the south and coral bombies dispersed around the island (Dee et al., 2020). Due to the turbid nature of the area, with visibility usually ranging from ~1-2m to ~5-6m, the reefs are mainly dominated by sediment tolerant corals (e.g., *Porites*, *Turbinaria*; Dee et al., 2020).

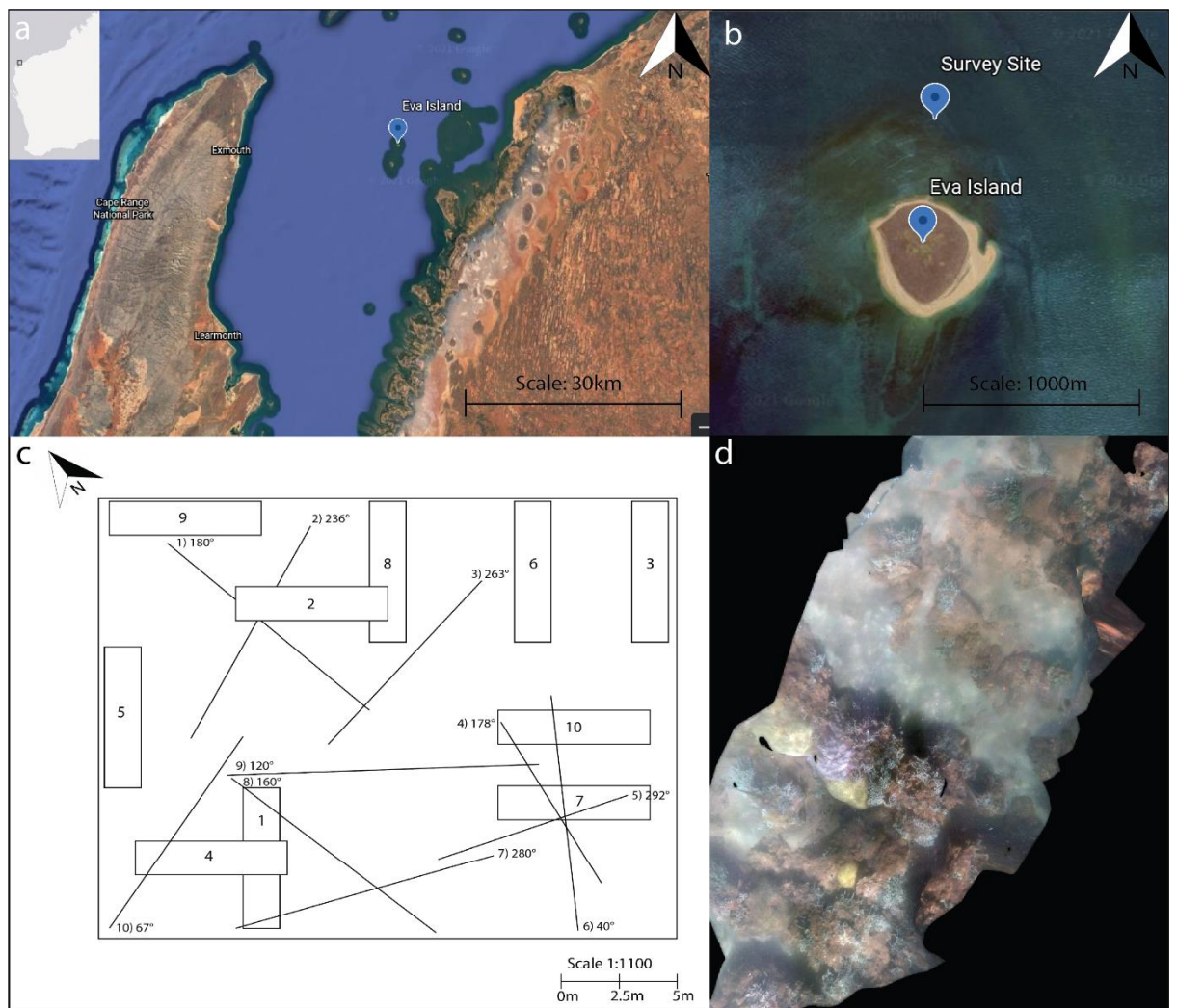


**Fig 2.1.** **a.** Satellite imagery of the north-east coast of Exmouth Gulf where Eva Island is located and where it is situated relative to the Western Australian coast (in grey). **b.** Eva Island with survey site location. **c.** Map of random transects within the site area (20 x 20 m) of LIT (line with direction and angle) and SfM (rectangle indicating 20 photos). **d.** SfM orthophoto of transect 8.

### **Line intercept transects**

To compare between LITs and SfM photogrammetry, a site on the reef was selected where the coral cover was relatively high (~23%; Dee et al., 2020). High-resolution LiDAR data at Eva reef (Dee et al., 2020) was used to remotely select a 20 x 20 m site. Prior to entering the water, the start point and compass direction of 10 randomly placed transects (10 m) were assigned for the LIT's at the site (Fig 2.1c). This was done by using a random number generator to generate coordinates within the 20 x 20 m area and provide the compass direction. If transects crossed the 20 x 20 m boundary, a new compass direction was randomly generated. Once in the water, transect start points were marked with a flagged stake. Divers were directed where to place the marker by a snorkeler with a GPS (Garmin eTrex 10) to ensure that the transects were laid out correctly. Along each transect, a diver recorded data on benthic cover (e.g., coral genus, algae/sponge, substrate) that lay directly below the tape and recorded the length of tape that it occurred.

### **Structure-from-Motion photogrammetry**

The 20 x 20 m site area was marked out using string to ensure that the data collected was contained within the same site as the LIT's. Sixteen control points (stainless steel markers with a black dot in the centre) were used to provide a reference point for photo processing and alignment. These were randomly placed on the benthos within the area and reference marked using a GPS.

### *Camera frame*

The camera frame prototype used was constructed using anodised aluminium square tube for the arms, and machine aluminium and stainless steel for the centre boss and hinge assembly. The frame was assembled in the shape of an X, with a single GoPro Hero 5 at each end, which made a 1.5 m<sup>2</sup> array (Figure 2.2a). The cameras were angled at 20° down from horizontal towards the centre of the frame, with the front two cameras facing backwards and the back two facing forwards. This arrangement was used to ensure the area could be covered with enough overlap in an efficient manner.

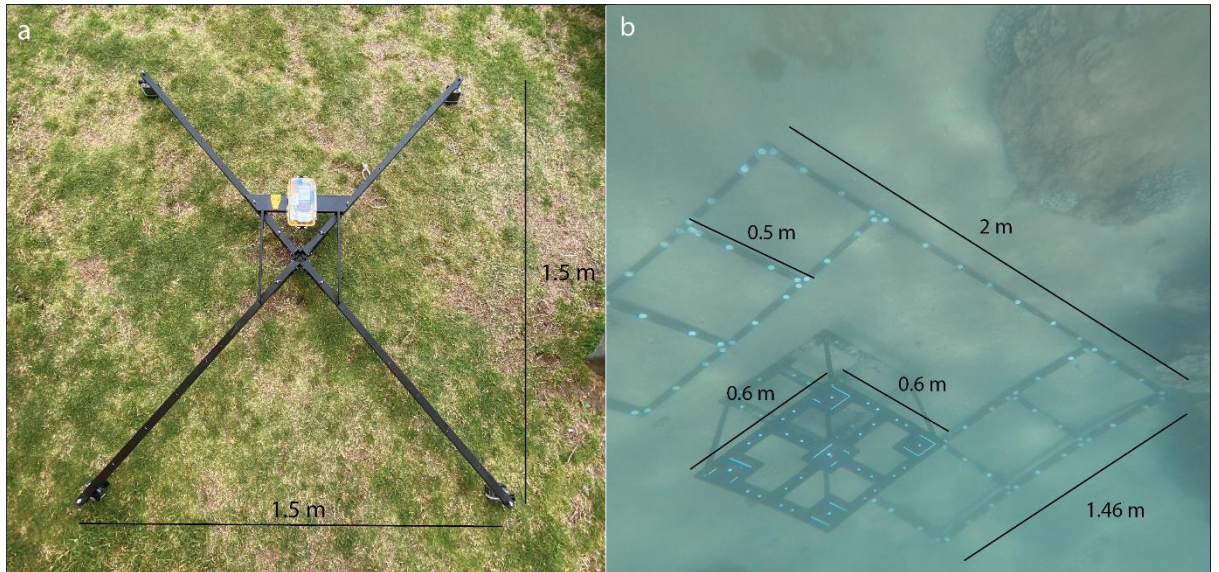


**Figure 2.2.** **a.** Camera frame with GoPro's and GPS and **b.** Calibration cube and ladder *in-situ* configuration used to calibrate the cameras prior to photo processing.

### *Camera settings*

Each GoPro Hero 5 (see Supplementary Table S2.1) was set to a 'Linear' field of view so that the cameras would not do an internal adjustment of the radial distortion. The cameras were then set to capture one photo every second and were all connected to the Wi-Fi GoPro remote, allowing all cameras to be turned on and record simultaneously.

### *Data collection*

Once the divers were in the water, all 4 GoPros were started simultaneously from the boat with the use of a GoPro wireless remote. The calibration cube and ladder were placed on a sandy patch within the 20 m by 20 m site (Figure 2.2b). Distortion can occur in an image due to photographic processing, therefore, the calibration cube is essential to solve the interior orientation (IO) parameters of the camera, most importantly, radial distortion, decentering distortion, and principal point offset (Helmholz, 2021). It is beneficial to calibrate the cameras to prevent systematic bias of photographic measurements. Calibration was performed as ContextCapture requires

manual calibration for image processing. It should be noted that calibration is not required for all photogrammetry programs.. A single diver swam over the cube and ladder with the camera frame, maneuvering it in an arc-like motion to provide photos from multiple angles. This is necessary information for calibration in a photogrammetry program (e.g., ContextCapture) and is critical for the construction of the 3-dimensional view of the benthos from the photos.

Once the cameras were calibrated, the diver with the frame swam parallel lines across the site. The frame was positioned 1 m above the benthos and each line was swam 1.5 m apart to ensure sufficient overlap of photos (1.5 m was the width of the frame so moving the frame over 'one frame length' was the most accurate way to do this). Once the diver reached the end of the site, this was repeated with lines perpendicular to the first ones.

### *Photo analysis*

Photos of the calibration cube and ladder were imported into ContextCapture for camera calibration as described in Bentley (2019). 10-11 photos were selected based on the quality of the photo and ensuring all angles of the cube were captured. ContextCapture was used as it is a more manual program and therefore can be used to manually assist in the processing of images with features such as camera calibration to manually solve the interior orientation of the cameras.

### *Image enhancement*

Due to the turbid conditions (1-2 m vertical visibility) at the time of the survey, image enhancement was investigated to improve image clarity. Two algorithms were considered: histogram equalisation and z-score normalisation. Fig 3 shows an example of an image before correction, and after histogram equalization, and z-score normalisation and stretching. From visual assessment, the "z-score" method ("pers.comm" 2021) was chosen to enhance the images (see Supplementary Data S2.2). In the z-score method, the z-score was calculated for each image band (i.e., red, green and blue).



The z-score is where data ( $z$ ) are normalised by subtracting the mean of the data from each value then dividing the residuals by the standard deviation of the values. After this transformation, the data have a mean of 0 and units of standard deviation. Visual assessment of the distribution of image values in each of the image bands concluded they could be adequately approximated by a normal distribution. For a normal distribution, 99.7% of the data are within  $\pm 3$  standard deviations, values in the image bands greater than this were concluded to be predominantly noise and provide little information about the scene. So, the normalised image values between -3 and 3 were stretched over the values 0-255 in each band assuming a normal distribution. The enhanced images improved the ability of the photogrammetry programs to align photographs together during the orthophoto creation.

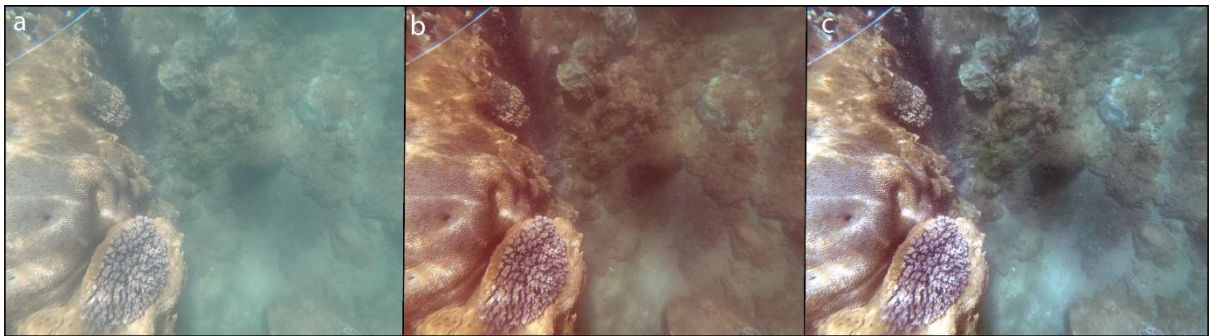


**Figure 2.3.** **a.** Original photo and image correction for **b.** Histogram equalization, and **c.** Z-score normalisation.

#### *Orthophoto creation*

An orthophoto is an aerial or satellite image that is geometrically corrected (orthorectified) so that the scale is uniform. Due to the high rugosity of the reef, refraction of light and particulate in the water column, there were photos from sections of the reef that could not be accurately aligned together to provide a complete 20 m by 20 m orthophoto. Instead, 20 photos from 10 areas of the reef where ContextCapture was able to identify similarities and correctly align the photographs providing an orthophoto were selected (e.g., Fig 2.1d). This provided sufficient cover of the study site (Fig 2.1c).

### *Segmenting coral types and estimating percentage cover*

To determine the percentage cover of each of the coral genera, using manual classification and ensuring all colonies were accounted for, shapefiles were created in QGIS (Fig 2.4). Classification was not standardized due to time constraints of training others in coral identification. These shapefiles were then imported into MATLAB and a code was created to extract the percentage cover for each species (see Supplementary Data S2.3). The code determines the size of one pixel in the reference frame (image), adds the number of non-zero pixels (i.e., excludes blank space) and multiplies them together to determine the total area. The program determines the area of each entry (polygon) in the shapefiles, adds them together for the total cover (for each coral genera), then divides by the total area of the orthomosaic to give the percentage cover.

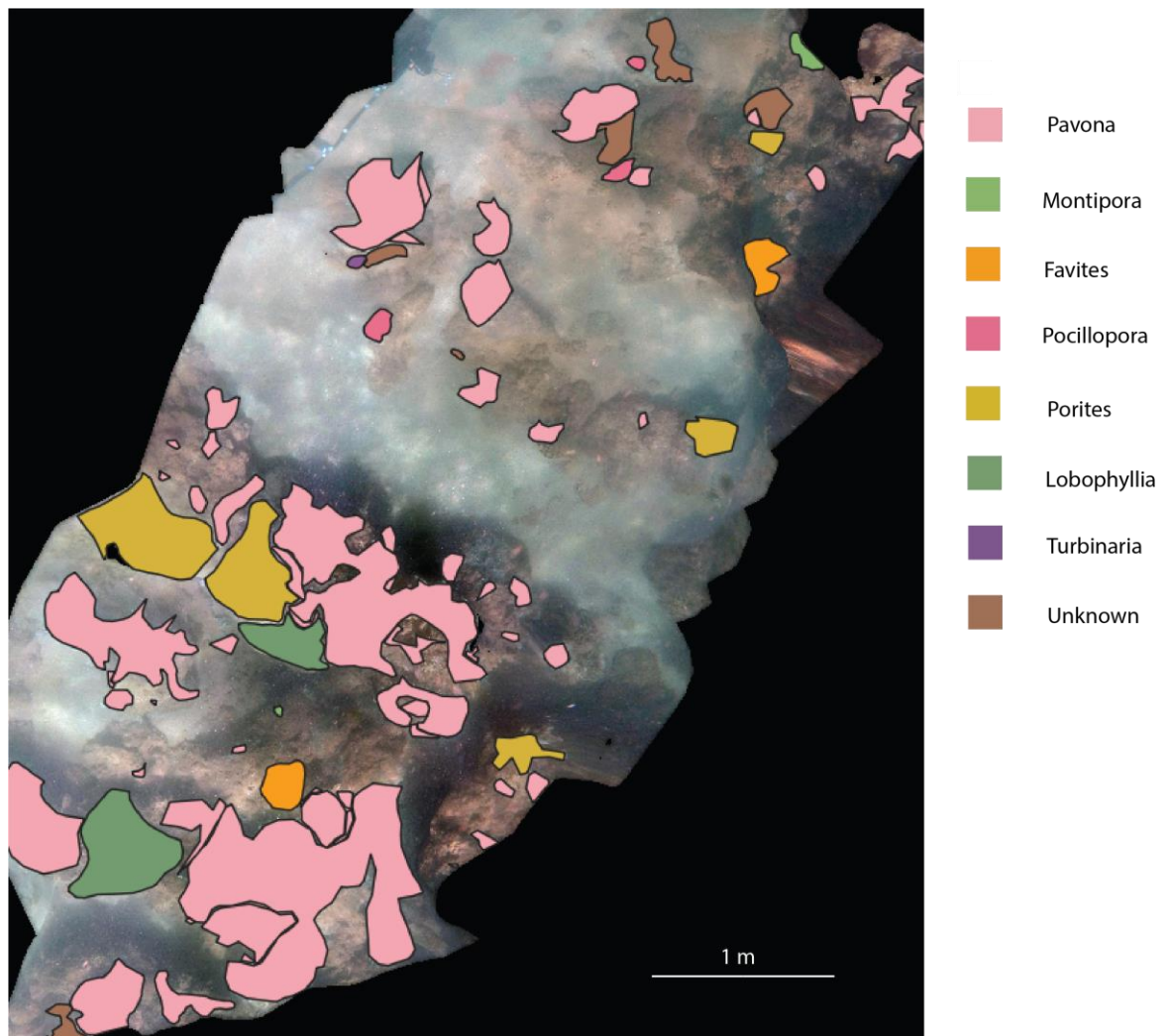


**Figure 2.4.** Polygon creation in QGIS of different coral genera used to create shapefiles for estimation of percentage cover.

### **Cost-benefit and statistical analysis**

Cost-benefit analysis data for each method was collected throughout the study. This included the cost of equipment, time in the field, data input, analysis/processing of photographs and statistical analyses. There was a lot of trial and error during the photo processing, however, only the time it took to produce the results using the method outlined in this study has been presented.

Independent t-tests were conducted in R Studio to determine whether LIT's and SfM coral metric data differed significantly. Where data did not fit the assumptions for the parametric test, the non-parametric statistical hypothesis

test of Wilcoxon signed-rank test was used. The coral metrics recorded were number of species, coral cover (% cover) and diversity (Shannon-Weiner Index). In addition, statistical analysis of percent cover in *Acropora* sp., *Pocillopora* sp., *Porites* sp. And *Pavona* sp. Was conducted to assess if coral morphology was an influencing factor on potential differences in measured total coral cover between the two techniques. These corals were the most abundant corals observed on the reef and included branching, foliose and massive growth forms.

## 2.4 Results

### Coral cover

Mean coral cover was significantly higher ( $df=18$ ,  $t=4.21$ ,  $p<0.01$ ; Table 2.1) with the LIT method ( $41.75\% \pm 1.2$ ) than with the SfM method ( $21.9\% \pm 2.77$ ; Figure 2.5a). The most abundant corals across both methods included *Pavona* sp. (LIT;  $26.9\% \pm 3.98$ , SfM;  $14.02\% \pm 2.00$ ) and *Porites* sp. (LIT;  $5.1\% \pm 1.88$ , SfM;  $3.52\% \pm 0.77$ ; Figure 2.5b). The next most abundant corals using the LIT method included *Pocillopora* sp. ( $2.75\% \pm 1.12$ ), *Acropora* sp. ( $1.2\% \pm 0.51$ ), *Turbinaria* sp. ( $1.3\% \pm 0.57$ ) and *Lobophyllia* sp. ( $1.3\% \pm 0.94$ ). In contrast, *Pocillopora* sp. And *Turbinaria* sp. Were less abundant using the SfM ( $1.2\% \pm 0.33$  &  $0.6\% \pm 0.14$ ), although similar coverage of *Acropora* sp. ( $1.2\% \pm 0.14$ ) and *Lobophyllia* sp. ( $1.47\% \pm 0.29$ ) were detected.

To determine which coral species might be driving the significant differences in coral cover between the two methods, four coral species were selected for further statistical analysis. These included the most abundant foliose and massive corals (e.g., *Pavona* sp. And *Porites* sp.) as well as two branching corals (*Acropora* sp. And *Pocillopora* sp.). Only coral cover in *Pavona* sp. Was significantly different between the two methods ( $df=18$ ,  $t=2.87$ ,  $p\text{-value}=0.009$ ), with higher coverage detected using the LIT method (Figure 2.5a; Table 2.1).

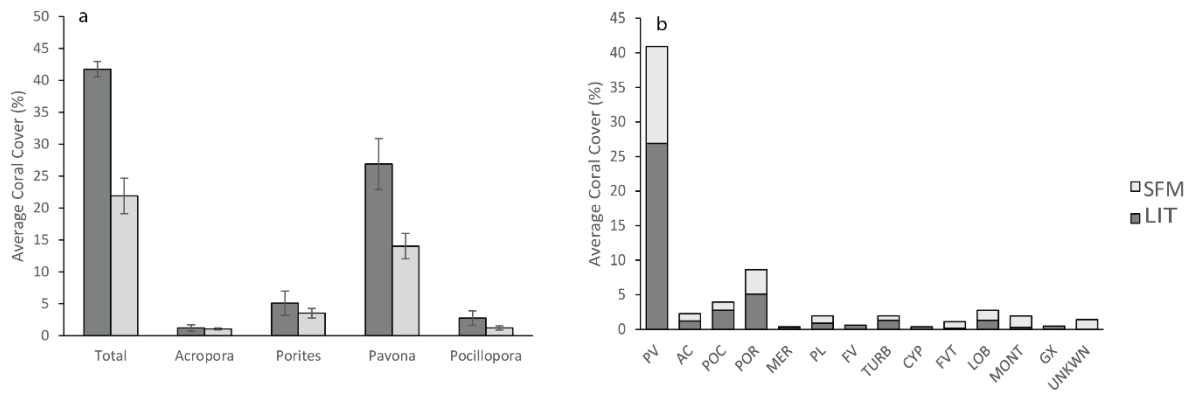


**Figure 2.5. a.** Mean coral cover (%) of total coral cover and four dominant genera for LIT and SfM methods **b.** Mean coral cover (%) of all detected genus for LIT and SfM methods (error bars = SE)

### Number of species & Shannon's diversity index

The total number of species detected using the traditional LIT method and SfM method were significantly different ( $df=18$ ,  $t=-2.31$ ,  $p=0.03$ ; Table 2.1), with SfM (average of 5.5) detecting a higher number of species than the LIT (average of 4.2; Figure 2.6a). However, the Shannon's diversity index (H index) was not significantly different between the two methods ( $W=58$ ,  $p=0.57$ ) with an H index of 0.71 reported for LIT and 0.65 for SfM (Figure 4b).

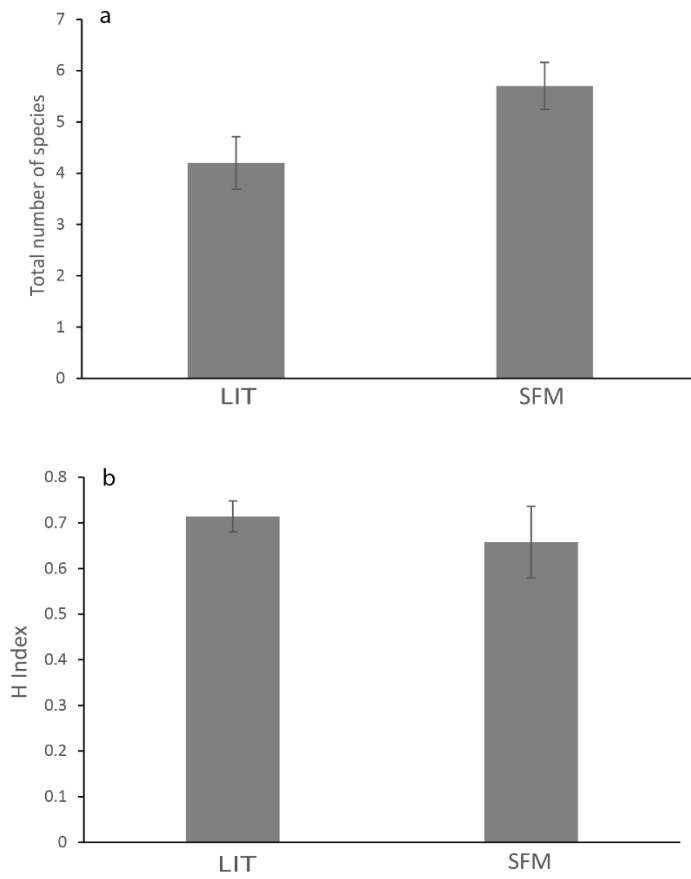


**Figure 2.6. a.** Mean total number of species for LIT and SfM methods. **b.** Mean diversity index (H index) for LIT and SfM methods (error bars = SE).

**Table 2.1.** Summary of statistical tests for total coral cover, the four dominant coral genera (*Acropora* sp., *Porites* sp., *Pavona* sp., *Pocillopora* sp.), richness and diversity (H index). Note that for *Acropora* sp., *Pocillopora* sp. And the H index, the non-parametric Mann Whitney U test was used as the data did not meet assumptions. Significant p values are in bold.

		T-value	DF	P-Value	W	Mean	SE
Coral cover (%)	LIT	4.21	18	<b>&lt;0.01</b>		41.75	1.2
	SfM					21.9	2.77
<i>Acropora</i> sp. (%cover)	LIT			0.52	58	1.2	0.51
	SfM					1.08	0.14
<i>Porites</i> sp. (%cover)	LIT	0.23	18	0.81		5.1	1.88
	SfM					3.52	0.77
<i>Pavona</i> sp. (%cover)	LIT	2.87	18	<b>&lt;0.01</b>		26.9	4.68
	SfM					14.02	2
<i>Pocillopora</i> sp. (%cover)	LIT			0.73	45	2.75	1.12
	SfM					1.21	0.33
Total species	LIT	-2.31	18	<b>0.03</b>		4.2	0.51
	SfM					5.7	0.45
H Index	LIT			0.57	58	0.71	0.03
	SfM					0.65	0.07

### Cost-benefit analysis

A comparison of the time and costs required for each method found that both the cost and time required was greater using SfM. The greater SfM costs (x9 LIT) were largely driven by the outlay costs for the cameras and the camera frame (Table 2.2). Time in the field was higher for LIT's, but the considerable post-processing of the imagery required for SfM, resulted in over twice the amount of time required to extract the data (Table 2.2).

**Table 2.2.** Cost-benefit analysis for LIT and SfM methods.

<b>Method</b>	<b>Line Intercept Transect</b>	<b>Structure-from-Motion</b>
<b>Data record</b>	<i>In-situ</i>	<i>In-situ</i> , computer system
<b>Equipment</b>	Dive slate, pencil, transect tape, measuring tape, marker poles, GPS	Custom-made camera frame, x4 GoPro Hero 5 cameras, GoPro Smart Remote, GPS, x4 20m measuring tapes, x17 control point markers
<b>Equipment cost</b>	\$228.45 (\$20 for dive slate, \$0.65 for pencil, \$24 for transect tape, \$15 for measuring tape, \$9.80 for marker poles, \$159 for Garmin eTrex 10 handheld GPS)	\$2038 (\$360 for frame (including labour), \$1400 for cameras (~\$350 per GoPro Hero 5), \$119 for GoPro Smart Remote, \$159 for Garmin eTrex 10 handheld GPS)
<b>Transect length (m)</b>	10 x 10 m transects	10 transects (20 images)
<b>Area covered (m<sup>2</sup>)</b>	20	20
<b>Survey time (mins)</b>	131	76
<b>Spread sheet Data Entry (mins)</b>	80	20
<b>Excel data Analysis (mins)</b>	100	10
<b>Sorting of images (mins)</b>	N/A	70 (10 min per camera + 30 min calibration photos)
<b>Camera calibration (ContextCapture) (mins)</b>	N/A	240
<b>Z-score stretch (MATLAB) (mins)</b>	N/A	112 (~ 5 seconds per photo, 56 min per camera)
<b>Orthophoto creation (ContextCapture) (mins)</b>	N/A	100 (10 per photo/transect)
<b>Polygon creation (QGIS) (mins)</b>	N/A	92 (~9 mins per orthophoto)
<b>Statistical analysis (mins)</b>	20	20
<b>Total time (mins)</b>	331	740



## 2.5 Discussion

Here we found that the LIT method recorded almost double the total coral cover compared to SfM. Previous research suggests that LIT's over-represent coral cover when compared to quadrat mapping (e.g., Weinberg 1981, Ohlhorst et al. 1988) and video transects (e.g., Saufan et al. 2015, Leujak & Ormond 2007). The difference in accuracy of the different sampling methods has largely been attributed to the contour effect, proportion of substrate sampled, viewing angle, image resolution, observer bias and data calculation (Leujak & Ormond, 2007). For example, Saufan et al. (2015) conducted a comparison of the LIT technique with a video transect in Malaysia and found that LIT's overestimated coral cover by 5-10%. They suggested this was likely due to the contour effect of the transect tape whereby the tape closely followed the contour of large coral colonies. Where there are a number of large domed corals, overestimates may, therefore, be based off the circumference of these large colonies instead of recording the planar area as if viewed from an aerial point of view. Here, large domed corals did not dominate the benthos, with small *Porites* sp. (~30 cm) covering ~5% of the benthos. Hence, the contour effect is not likely to be an influencing factor. Similarly, it is unlikely that the area sampled and observer bias will have inflated LIT coral coverage estimates given that we used a number of transects within a defined area, which were also randomly selected pre-entry into the water. As such, we consider that our LIT coral coverage estimates provide a comparatively accurate assessment of the benthos within the selected area.

The difference in coral estimates between LIT and SfM in this study was considerably larger than previously recorded (typically ~ 5-10%; e.g., Carleton and Done, 1994; Leujak et al., 2007; Saufan et al., 2015). Importantly, this difference in total cover was driven by the significant difference in *Pavona* sp. Coral cover only. In turbid coral reef environments, this foliose coral tends to grow in patches, often with once large patches of *Pavona* sp. Partly covered in sediments. In contrast, the branching corals (*Acropora* sp. And *Pocillopora* sp.) and the massive corals (*Porites* sp.) are

more visible due to their morphology and colouring. As such, the reduced ability to detect small low-lying patches of coral using cameras in low visibility environments has resulted in an under-estimation of *Pavona* sp. And total coral cover.

Complex surface topography is another likely cause for the underestimation of total coral cover by SfM. The 20 x 20 m survey area was in a highly rugose environment, characterised by large boulders and overhangs interspersed with sand patches (Figure 1d). *Pavona* sp. Tended to grow on top of and down the side of these large boulders, which was not captured well by the cameras. Previous SfM studies have used a single DSLR camera (Burns et al., 2015; Bryson et al., 2017; Burns and Delparte, 2017), often with a hemispheric dome port, which has been proven to reduce refraction and enhance the software's ability to process and align the photographs (Burns et al., 2015; Burns and Delparte, 2017). This not only improves the quality of the photo, but also allows for a diver to follow the contours of the reef closely. In contrast, the setup used here was too large to manoeuvre through the tight spaces and a rugose environment. However, due to the limited visibility, multiple camera angles were beneficial in assisting with the alignment of photographs as the multiple angle shots filled in gaps in features. As such, to improve SfM in turbid, rugose environments, the multi-camera setup should be kept to assist in the infilling of features, but a smaller frame should be considered to improve manoeuvrability.

Significantly more coral genera (richness) were detected using SfM than the LIT despite the low visibility and issues regarding surface complexity. SfM detected an average of  $5.7 \pm 0.45$  genera compared to  $4.2 \pm 0.51$  with LIT. LIT's are known to be limited in their capacity to detect the abundance of rare and small species as they cover a smaller area (Hill and Wilkinson, 2004). Here, we conducted 10 x 10 m LIT's while the SfM covered an average of 24.66 m<sup>2</sup> per transect (~247 m<sup>2</sup> total). As such, it is not surprising that more coral genera were detected using the SfM. However, the H index (H') was not significantly different between the two methods. The H' takes into account both the abundance and evenness of the species present, thereby providing

more information about the coral community structure than species richness alone (Kiernan, 2021). For both methods, the H' was low (<1) indicating that the community is uneven, in this case dominated by *Pavona* sp. (~50% of the total coral cover). Given that the SfM was unable to detect as many of the coral colonies of the more abundant coral genera present compared to the LIT, this resulted in a lower H' despite a higher species richness.

In turbid, rugose coral reef environments we suggest that LIT's should be used over SfM to calculate coral cover and diversity for carbonate budgets. SfM determined the coral cover to be half that of LIT's, which will have a significant impact on carbonate budget assessments where the abundance of corals typically drive rates of gross carbonate production on a reef (Browne et al., 2013; Perry and Alvarez-Filip, 2018; Perry et al., 2018; Dee et al., 2020). The rates of carbonate production indicate the stability of the coral community and potential for reef growth (Browne et al., 2013). Hence, if coral cover is under-represented, the gross coral carbonate production will yield a rate of carbonate production that is lower than the true carbonate production for that reef and, therefore, provide an inaccurate assessment of reef stability and reef growth potential. Although LIT's might be overestimating coral cover, it is likely that the error for LIT's (previously recorded at 5-10%; e.g., Carleton and Done, 1994; Leujak et al., 2007; Saufan et al., 2015) is not as great as for SfM in these highly turbid and rugose environments. SfM has the potential to be useful for carbonate budgets as it can cover a larger reef area but until the method is improved, this technique requires higher in-water visibility, and lower reef complexity with limited overhanging reef structures.

Future improvements to both the *in-situ* data collection and camera array would likely increase the capacity of the technique to better capture the benthos in low light, rugose reef environments. The production of a 3-dimensional benthic mosaic of a coral reef relies on the computer program to align photos in the correct order. Here, 16 ground control points for geo-positioning and scale were used, however, in low visibility conditions, it was found that the program struggled to find enough similar points between images to align them. This could be improved by using at least three ground

control points and a scale bar (e.g., transect tape) in each image, maintaining a slower swim speed (e.g.,  $0.5 \text{ m}\cdot\text{s}^{-1}$ ) to ensure better overlap between images and using a high-resolution camera that works well in low light environments (e.g., Pentax K-5 DSLR camera (Burns et al., 2015)), which will allow for higher quality images. In addition, the application of a hemispheric dome port will reduce light refraction to assist image alignment software. Alterations to the camera frame are also recommended to improve the development of a 3D mosaic. For example, lights could be added to the frame to improve the visibility of coral colonies and reduce shadows cast from the sun, waves, and diver. Furthermore, more time could be spent optimising the camera configuration (i.e., distance of cameras from each other and angle of the camera to the reef), running multiple pre-survey simulations, and reducing the frame size to increase its manoeuvrability.

As SfM can create a permanent, visual record of a reef, geo-positioning of the site is a critical factor for the implementation of long-term monitoring programmes. To achieve better results in the future, additional equipment could be used to provide more detailed information to assist the construction of a benthic habitat map. A GPS towed on the surface, along with underwater positioning options, such as acoustic positioning (e.g., Short Base Line (SBL) or Ultrashort Base Line (UBL)), and/or Inertial Navigation System (INS) coupled with a speed sensor (e.g., Doppler Velocity Log (DVL)) would provide adequate information of the study site and would enhance the repeatability of survey. The addition of an echosounder would provide accurate depth values, a critical component for the reconstruction process. As this technique is still relatively new and as technology continually improves, the SfM technique employed in this study could be compared with a circular survey (as opposed to the parallel transects) to determine the best way to capture photographs of the reef for the creation of the photo mosaic. A central pole would be placed in the middle of the survey site with a rope attached from the pole to the camera frame, and a tape measure would be placed on the benthos, extending out from the middle. A diver would swim in an orbit around the central pole, and after each orbit, let out a pre-determined amount of rope each time, until the entire site had been photographed in a

circular motion. This technique could provide better overlap of photographs, and coupled with additional equipment for positioning and depth, could produce a more accurate 3-dimensional habitat map.

Cost-benefit analysis of the two methods found that the LIT method was cheaper and quicker to conduct. LIT's require less expensive equipment and, although more time in the field is required, post processing time is considerably less than with SfM. However, there are some important advantages to using the SfM. SfM allows for larger areas to be surveyed and photographs provide a permanent record of the data that can be: 1) verified for quality control, 2) compared to future surveys to provide a more accurate estimate of change over time, and 3) further analysed to provide additional metrics such as coral volume and reef rugosity (Storlazzi et al., 2016). Yet, the initial outlay costs for the cameras and frames (\$1879) is relatively expensive, and the computing requirements and expertise required for post processing may not be available. Resources, such as time and funding, are essential to consider when designing a coral reef monitoring program, however, it is also important to assess the quality of the science. This study found that for turbid, rugose environments characterised by a patchy coral community, SfM may not provide the most accurate assessment of coral cover, and as such, the LIT method is currently the more scientifically robust and less resource intensive approach for these reef environments.

## **2.6 Conclusion**

SfM is a novel and progressive technique that can provide multiple metrics for a large area of reef. However, in turbid reef environments, with patchy coral reefs dominated by weedy coral species, current techniques for applying SfM will not provide the most accurate assessment of coral metrics for carbonate budget calculations. Further, SfM requires a large set-up budget and more time for processing data and, therefore, may not be a feasible option for many research studies and monitoring projects. However, it does allow for less experienced divers to perform a survey and importantly, allows for repeatability assessments. Here, we recommend the addition of

technologies such as GPS, LIDAR, acoustic positioning and echo sounding to create a more accurate 3-dimensional reconstruction of the reef. This would provide exact locations on the reef (per photo), a depth gradient and, if scaled accurately, would allow calculations such as rugosity and coral volume to be extracted, further improving carbonate budget assessments.

## 2.7 References

Anthony KRN, Fabricius KE (2000) Shifting roles of heterotrophy and autotrophy in coral energetics under varying turbidity. *J Exp Mar Biol Ecol* 252:221–253

Ayling AM, Ayling AL (1999) Medium term changes in coral populations of fringing reefs at Cape Tribulation. Townsville, Great Barrier Reef Marine Park Authority. Research Publication No. 59

Babcock RC, Thomson DP, Haywood MDE, Vanderklift MA, Pillans R, Rochester WA, Miller M, Speed CW, Shedrawi G, Field S, Evans R, Stoddart J, Hurley TJ, Thompson A, Gilmour J, Depczynski M (2020) Recurrent coral bleaching in north-western Australia and associated declines in coral cover. *Mar Freshw Res* 72:620-632

Bentley (2019) ContextCapture User Guide. Retrieved from ContextCapture Master (bentley.com)

Bonesso JL, Cuttler MVW, Browne N, Hacker J, O’Leary M (2020) Assessing reef island sensitivity based on LiDAR-derived morphometric indicators. *Remote Sensing* 12:3033 [doi: 10.3390/rs12183033]

Browne NK, Smither SG, Perry CT (2010) Geomorphology and community structure of Middle Reef, central Great Barrier Reef, Australia: an inner-shelf turbid zone reef subject to episodic mortality events. *Coral Reefs* 29:683-689

Browne NK, Smithers SG, Perry CT (2013) Spatial and temporal variations in turbidity on two inshore turbid reefs on the Great Barrier Reef, Australia. *Coral Reefs* 32:195-210

Browne NK, Cuttler M, Moon K, Morgan K, Ross CL, Catsro-Sanguino C, Kennedy E, Harris D, Barnes P, Bauman A, Beetham E, Bonesso J, Bozec Y, Cornwall C, Dee S, DeCarlo T, D'Olivio J, Doropoulos C, Evan RD, Eyre B, Gatenby P, Gonzalez M, Hamylton S, Hansen J, Lowe R, Mallela J, O'Leary M, Roff G, Saunders B, Zweilfer A (2021) Towards predicting responses of reefs and reef-fronted shorelines to climate change: development of a conceptual geo-ecological carbonate reef system model. *Oceanography and Marine biology: Annual Review*. Accepted.

Brunskill GJ, Orpin AR, Zagorskis I, Woolfe KJ (2001) Geochemistry and particle size of surface sediments of Exmouth Gulf, Northwest Shelf, Australia. *Cont Shelf Res* 21:157-201

Bryson M, Ferrari R, Figueira W, Pizarro O, Madin J, Williams S, Byrne M (2017) Characterization of measurement errors using structure-from-motion and photogrammetry to measure marine habitat structural complexity. *Ecol Evol* 7:5669-5681

Burns JHR, Delparte D (2017) Comparison of commercial structure-from-motion photogrammetry software used for underwater three-dimensional modelling of coral reef environments. *ISPRS-International Archives of the Photogrammetry, Remote Sensing and Spatial Information Sciences*. XLII-2/W3. 127-131 [doi: 10.5194/isprs-archives-XLII-2-W3-127-2017]

Burns JHR, Delparte D, Gates RD, Takabayashi M (2015) Integrating structure-from-motion photogrammetry with geospatial software as a novel technique for quantifying 3D ecological characteristics for coral reefs. *Peer J* 3 [doi: 10.7717/peerj.1077]

Carleton JH, Done TJ (1995) Quantitative video sampling of coral reef benthos: large-scale application. *Coral Reefs* 14:35-46

Dee S, Cuttler M, O'Leary M, Hacker J, Browne N (2020) The complexity of calculating an accurate carbonate budget. *Coral Reefs* 39:1525-1534

Done T, Turak E, Wakeford M, DeVantier L, McDonald A, Fisk D (2007) Decadal changes in turbid-water coral communities at Pandora Reef: loss of resilience or too soon to tell? *Coral Reefs* 26:789-805

- Graham NAJ, Nash KL (2013) The importance of structural complexity in coral reef ecosystems. *Coral Reefs* 32:315-326
- Guinotte JM, Buddemeier ARW, Kleypas AJA (2003) Future coral reef habitat marginality: Temporal and spatial effects of climate change in the Pacific Basin. *Coral Reefs* 22:551
- Helmholz P (2021) Lecture 2: Interior Orientation [Powerpoint slides]. Retrieved from SPAT3002, Curtin University Blackboard Online, <http://www.lms.curtin.edu.au/>
- Herrán N, Narayan GR, Raymond CE, Westphal H (2017) Calcium carbonate production, coral cover and diversity along a distance gradient from Stone Town: A case study from Zanzibar, Tanzania. *Front Mar Sci* 4:1-14
- Hill J and Wilkinson C (2004) Methods for Ecological Monitoring of Coral Reefs. Australian Institute of Marine Science. Version 1
- Hoegh-Guldberg O, Poloczanska ES, Skirving W, Dove S (2017) Coral reef ecosystems under climate change and ocean acidification. *Front Mar Sci* 4:1-20
- Hubbard DK (2008) Depth and species-related patterns of Holocene reef accretion in the Caribbean and Western Atlantic: A critical assessment of existing models. *Spec Publ Int Assoc Sedimentol* 40:1-18
- Hubbard DK, Burke RB, Gill IP (1986) Styles of reef accretion along a steep, shelf-edge reef, St. Croix, U.S. Virgin Islands. *J Sediment Res* 56:848-861
- Jonker M, Johns K, Osborne K (2008) Surveys of benthic reef communities using underwater digital photography and counts of juvenile corals. Long-term monitoring of the Great Barrier Reef, Standard Operational Procedure Number 10 [doi: 10.25845/jjzj-0v14]
- Jupiter S, Roff G, Marion G, Henderson M, Schrameyer V, McCulloch M, Hoegh-Guldberg O (2008) Linkages between coral assemblages and coral proxies of terrestrial exposure along a cross-shelf gradient on the southern Great Barrier Reef. *Coral Reefs* 27:887–903



Kiernan D (2021) Introduction Simpson's Index and Shannon-Weiner Index. <https://stats.libretexts.org/@go/page/2932>

Lange ID, Perry CT (2019) Bleaching impacts on carbonate production in the Chagos Archipelago: influence of functional coral groups on carbonate budgets trajectories. *Coral Reefs* 38:619-624

Lange ID, Perry CT (2020) A quick, easy and non-invasive method to quantify coral growth rates using photogrammetry and 3D model comparisons. *Method Ecol Evol* 11:714-726

Leon JX, Roelfsema CM, Saunders MI, Phinn SR (2015) Measuring coral reef terrain roughness using 'structure-from-motion' close range photogrammetry. *Geomorphology* 242:21-28

Leujak W, Ormond RFG (2007) Comparative accuracy and efficiency of six coral community survey methods. *J Exp Mar Bio Ecol* 351:168-187

Mallela J, Perry CT (2007) Calcium carbonate budgets for two coral reefs affected by different terrestrial runoff regimes, Rio Bueno, Jamaica. *Coral Reefs* 26:129-145

Manzello DP, Enochs IC, Kolodziej G, Carlton R, Valentine L (2018) Resilience in carbonate production despite three coral bleaching events in 5 years on an inshore patch reef in the Florida Keys. *Mar Biol* 165:99

Moore JA, Bellchambers LM, Depczynski MR, Evans RD, Evans SN, Field SN, Friedman KJ, Gilmour JP, Holmes TH, Middlebrook R, Radford BT, Ridgway T, Shedrawi G, Taylor H, Thomson DP, Wilson SK (2012) Unprecedented mass bleaching and loss of coral across 12° of latitude in Western Australia in 2010-11. *PLoS One* 7(12):e51807 [doi: 10.1371/journal.pone.0051807]

Morgan KM, Perry CT, Johnson JA, Smither SG (2017) Nearshore turbid-zone corals exhibit high bleaching tolerance on the Great Barrier Reef following the 2016 ocean warming event. *Front Mar Sci* 4:224

Ohlhorst SL, Liddell WD, Taylor RJ, Taylor JM (1988) Evaluation of reef census techniques. *Proc 6th Int Cor Reef Symp* 2:319-324

Oppenheimer M, Glavovic GJ, van de Wal R, Magnan AK, Abd-Elgawad A, Cai R, Cifuentes-Jara M, DeConto RM, Ghosh T, Hay J, Isla F, Marzeion B, Meyssignac B, Sebesvari Z (2019) Sea level rise and implications for low lying islands, coasts and communities, in IPCC Special Report on the Ocean and Cryosphere in a Changing Climate

Perry CT, Alvarez-Filip L (2018) Changing geo-ecological functions of coral reefs in the Anthropocene. *Funct Ecol* 33:976– 988

Perry CT, Alvarez-Filip L, Graham NAJ, Mumby PJ, Wilson SK, Kench PS, Manzello DP, Morgan KM, Slangen ABA, Thomson DP, Januchowski-Hartley F, Smithers SG, Steneck RS, Carlton R, Edinger EN, Enochs IC, Estrada-Saldivar N, Haywood MDE, Kolodziej G, Murphy GN, Perez-Cervantes E, Suchley A, Valentino L, Boenish R, Wilson M, Macdonald C (2018) Loss of coral reef growth capacity to track future increases in sea level. *Nature* 558:396-400

Perry CT, Edinger EN, Kench PS, Murphy GN, Smithers SG, Steneck RS, Mumby PJ (2012) Estimating rates of biologically driven coral reef framework production and erosion: a new census-based carbonate budget methodology and applications to the reefs of Bonair. *Coral Reefs* 31:853-868

Perry CT, Smithers SG (2006) Taphonomic signatures of turbid-zone reef development: Examples from Paluma Shoals and Lugger Shoal, inshore central Great Barrier Reef, Australia. *Palaeogeography, Palaeoclimatology, Palaeoecology* 242:1–20

Saufan M, Boo WH, Siang HY, Chark LH, Bachok Z (2015) Optimization of coral video transect technique for coral reef survey: Comparison with intercept transect technique. *Open Journal of Marine Science* 5:379-397

Smith LD, Gilmour JP, Heyward AJ (2008) Resilience of coral communities on an isolated system of reefs following catastrophic mass-bleaching. *Coral Reefs* 27:197-205

Speed CW, Babcock RC, Bancroft KP, Beckley LE, Bellchambers LM, Depczynski M, Field SN, Friedman KJ, Gilmour JP, Hobbs JP, Kobryn HT, Moore JA, Nutt CD, Shedrawi G, Thomson DP, Wilson SK (2013) Dynamic

stability of coral reefs on the West Australian coast. PLoS One 8(7):e69863  
[doi: 10.1371/journal.pone.0069863]

Storlazzi CD, Norris BK, Rosenberger KJ (2015) The influence of grain size, grain colour and suspended-sediment concentration on light attenuation: Why fine-grained terrestrial sediment is bad for coral reef ecosystems. Coral Reefs 34:967-975

Storlazzi CD, Dartnell P, Hatcher GA (2016) End of the chain? Rugosity and fine-scale bathymetry from existing underwater digital imagery using structure-from-motion (SfM) technology. Coral Reefs 35:889–894

Urbina-Barreto I, Garnier R, Elise S, Pinel R, Dumas P, Mahamadaly V, Facon M, Bureau S, Peignon C, Quod JP, Dutrieux E, Penin L and Adjeroud M. (2022). Which method for which purpose? A comparison of line intercept transect and underwater photogrammetry methods for coral reef surveys. Front. Mar. Sci 8

Veron JEN (1995) Corals in space and time: The biogeography and evolution of the *Scleractinia*. Sydney, Australia: University of New South Wales Press, 321p

Veron JEN, Hoegh-Guldberg O, Lenton TM, Lough JM, Obura DO, Pearce-Kelly P, Sheppard CRC, Spalding M, Stafford-Smith MG, Rogers AD (2009) The coral reef crisis: The critical importance of <350ppm CO<sup>2</sup>. Mar Pollut Bull 58:1428-1436

Veron JEN, Stafford-Smith MG, Turak E, DeVantier LM (2016) Corals of the World. Version 0.01  
[http://www.coralsoftheworld.org/coral\\_geographic/interactive\\_map/results/?version=0.01](http://www.coralsoftheworld.org/coral_geographic/interactive_map/results/?version=0.01)

Weinberg S (1981) A comparison of coral reef survey methods. Bijdragen tot de Dierkunde 51:19

## 2.8 Supplementary Material

**Table S2.1.** GoPro Hero 5 specifications

<i>Go Pro Hero 5</i>	
<b>Mode</b>	Linear
<b>Focal Length</b>	3 mm
<b>Sensor Size</b>	7.66 mm
<b>35 mm eq.</b>	14.0922 mm

**Data S2.** AdjustPhotosUsingZscore.m

Z-score normalisation and stretch of photos was executed in MATLAB prior to alignment. Relevant code is available on figshare [doi: 10.6084/m9.figshare.14685768]

**Data S3.** EstimatingPercentageCover.m

Percentage cover was calculated in MATLAB using shapefiles created in QGIS. Relevant code is available on figshare [doi: 10.6084/m9.figshare.14685801]

## Chapter 3

### Effect of camera type and altitude on SfM photogrammetry for application in turbid benthic environments.

Kesia L. Savill, Iain M. Parnum, Jennifer McIlwain and David Belton

#### 3.1 Abstract

Over the last decade, Structure-from-Motion (SfM) photogrammetry has successfully been used to survey marine benthic environments, including quantifying 3D characteristics of coral reefs. However, the application of this technique in turbid benthic environments is in its infancy. Sessile organisms in these environments, such as scleractinian corals, are adapted to low-light conditions and high sediment loads, and have a higher chance of survival with increasing sea surface temperatures due to climate change. This study further develops SfM photogrammetry methodology by improving its performance in turbid benthic environments, using different camera types, and optimising camera settings and distances between the camera and the survey area. To assess the performance of the SfM workflow in these comparisons, firstly, the number of features aligned in the SfM photogrammetry software were examined in a “single shot” experiment. Then SfM photogrammetry model accuracy was assessed by measuring objects of known dimensions (including coral skeletons) contained in an artificial scene set up. Finally, SfM photogrammetry models of an artificial “Apollo” reef structure were compared with the engineering diagram of the structure. Three types of cameras were compared, action cameras (GoPro Hero 5 and 8), a compact camera (Canon G7X Mark II) and a DSLR (Nikon D70). In addition, the automatic and custom settings were examined in the compact and DSLR cameras. The number of features aligned for photos taken of a *Porites* coral skeleton, with the coral skeleton taking up different percentages of the field of view were examined. The Canon G7X Mark II had the highest number of features aligned for most fields of view underwater with automatic settings and custom settings. The Canon G7X Mark II produced the most complete and accurate 3D model of the artificial scene at Fremantle Sailing

Club, and alongside the Nikon D70, were the only cameras to successfully reconstruct the coral skeletons within the scene. Of the different 3D models produced of an Apollo artificial reef structure, the Canon G7X Mark II provided the most agreeable model compared to the engineering diagram, with an accuracy of 98.2%. Regression analysis found the accuracy of the SfM photogrammetry 3D models could be well approximated using the total number of photos used in the SfM workflow, with the best visual fit using a log relationship. Multilinear regression (using a log function) found that photos taken at a altitude of 1 m from the object had more bearing on the accuracy of the model compared with photos taken at 2 m.

Recommendations from this study for the application of SfM photogrammetry in turbid benthic environments are 1) to use a camera with a large sensor size and high sensor resolution, 2) select custom camera settings (over automatic ones) to suit current conditions on the day of surveying and 3) take photos at a close altitude from the object (e.g.,  $\leq 1$  m), and ideally from multiple altitudes to increase model accuracy. These recommendations agree with previous photogrammetry recommendations for clear waters.

### **3.2 Introduction**

A novel and emerging methodology to survey marine benthic environments, such as coral reefs, has been used in studies over the last decade. Structure-from-Motion (SfM) photogrammetry is a non-invasive, low-cost method, that creates high-resolution models which can be easily repeated to monitor change over time (Lange et al., 2020; Roach et al. 2021). These models can be used to extract data from coral reefs such as surface area, volume and rugosity (e.g., Burns et al., 2015; Figueria et al., 2015; Ferrari et al., 2016; Magel et al., 2019), as well as data on community structure (e.g., Anelli et al., 2019; Roach et al., 2021; Kornder et al., 2021; Kolodziej et al., 2021). This method has been developed to quantify 3D characteristics of coral reefs (e.g., Burns et al., 2019), allowing assessments of reef health (e.g., Gibson, 2021), response to disturbance events (e.g., Longo et al., 2020; Fukunaga et al., 2022) and monitoring of reefs (e.g., Lange et al., 2020; Rossi et al.,

2020). Yet, previous studies using this technique have mostly taken place in clear water environments, with little evidence to suggest its application has been applied in turbid benthic environments.

Despite turbid water environments representing ~8 to 12% of the total area of the global continental shelf (Shi and Wang, 2010), they are relatively understudied and pose challenges to methods that use underwater photography. While underwater environments pose challenges to photography, such as low light, low contrast, loss of colour and noise (Arnold, 2022), turbid water environments have significantly less light availability, limited visibility and a significant amount of particulate in the water column (IADC, n.d.) compared to clear water environments. This means that the use of SfM photogrammetry in these environments can be challenging.

This study aims to investigate aspects of image collection in turbid benthic environments to help improve the performance of SfM photogrammetry, in particular the accuracy of 3D reconstructions. This study compared different camera types, camera settings and distances between the camera and the survey area. The results help provide recommendations for the successful use of SfM photogrammetry, specifically for turbid benthic environments.

### **3.3 Material and Methods**

#### **3.3.1 Study sites**

This study was conducted at two locations: the Fremantle Sailing Club in Perth, Western Australia (-32.0707962, 115.7509938), and the Coogee Maritime Trail at Coogee Beach, Perth, Western Australia (-32.1054588, 115.7625571) (Figure 3.1). These sites were chosen due to their low visibility and turbid conditions, with in-water visibility ranging from 2-3 m at both locations during the time of imaging. The turbidity of these locations is due to the constant movement of boats leaving and returning to their pens at Fremantle Sailing Club, and due to prevailing winds and local wind-driven waves at Coogee Maritime Trail. Another reason for selecting the Coogee

Maritime Trail as a study site was it contains prefabricated structures (artificial reefs) with known dimensions, such as Apollo cluster structures (Fig 3.1d).

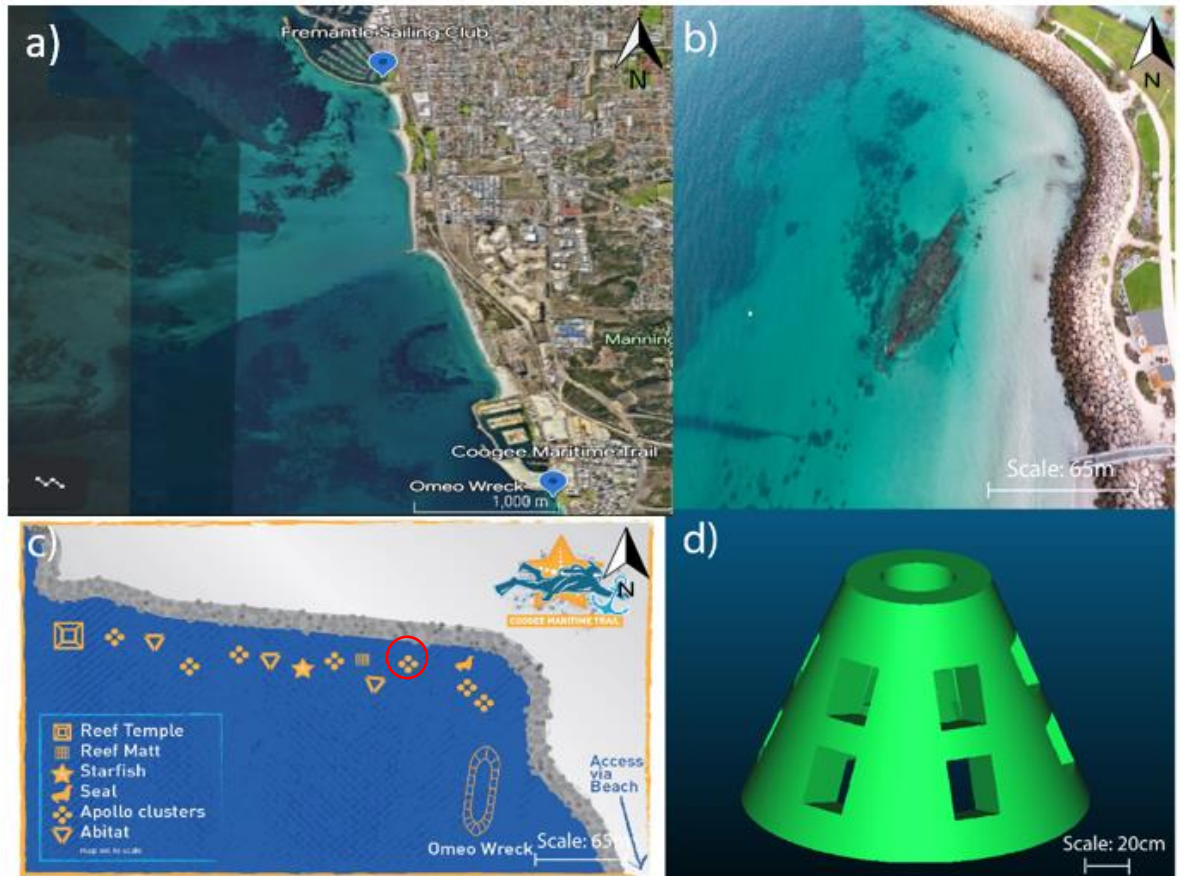


**Figure 3.1.** a. Satellite imagery of the two sites, Fremantle Sailing Club and Coogee Maritime Trail (Google Earth Pro, 2022). b. Aerial photograph of Coogee Maritime Trail (Seniorocity, 2020). c. Map of artificial reef structures of the Coogee Maritime Trail with red circle indicating surveyed structure (Tomlinson, 2022). d. 3D engineering diagram of Apollo structure (Subcon, 2022).

### 3.3.2 Data collection

#### 3.3.2.1 Laser scanning

A laser scan of the *Porites* (massive morphology) and *Turbinaria* (foliose morphology) skeletons were performed using an Artec Space Spider 3D scanner, which can achieve 3D point accuracies up to 0.05 mm, which exceeds the expected precision of underwater Structure-from-Motion



photogrammetry techniques, allowing the laser scans to be used as “real world” measurements for comparison (Saunders, 2020). Only one of each was used as that was what we had access to at the time and given time restraints, could not incorporate replicates. The laser scans were compared with measurements of the same skeletons placed in a scene at the Fremantle Sailing Club.

### Cameras

3 different types of cameras were selected to represent the different types of cameras typically used in underwater photogrammetry of coral reefs, an action camera, compact camera and DSLR. Photos taken using the GoPro Hero 8 in its protective housing (Table 3.1) were taken in linear mode with continuous automatic capture settings of 1 image per second. Photos taken using the Canon G7X Mark II (with Ikelite housing) (Table 3.1) set to a focal length of 24mm and Nikon D70 (with Sea & Sea DX-D70 housing) (Table 3.1) set to a focal length of 18mm were taken using 2 settings, 1) the camera’s automatic settings and 2) with a shutter speed of 1/400, an aperture of f/8 and an ISO of 200. Photos taken using the Canon G7X Mark II and Nikon D70 were manually captured.

**Table 3.1.** Specifications of cameras used in this study.

Camera type	Sensor resolution (MegaPixels)	Sensor size (mm)	Image size (pixels)	Focal length (35mm equivalent)
GoPro Hero 8 	12	6.17 x 4.55	4000x3000	19-39 mm (Linear mode)
Canon G7X Mark II 	20	13.2 x 8.8	5472x3648	24-100 mm
Nikon D70 	6	23.7 x 15.6	3008x2000	18-50 mm

### 3.3.2.2 Water quality

The environmental conditions, i.e., turbidity, of the study sites were taken into consideration when selecting the camera settings. Turbidity sensors, along with a CTD, were deployed for each survey to measure the turbidity during the survey.

### 3.3.2.3 Fremantle Sailing Club

As part of the aim to investigating the feature matching capability of the structure-from-motion photogrammetry software for different cameras and at different altitudes, three consecutive photos were taken of a *Porites* coral skeleton using the four different cameras (described in Table 3.1), at four different fields of view with the coral filling the frame at different percentages (100%, 75%, 50% and 25%), e.g., Figure 3.2. Number of features matched for each photo were recorded which would indicate which altitude was most likely to produce a better model based on the number of features the program is able to identify on the more complex structure of a coral skeleton.

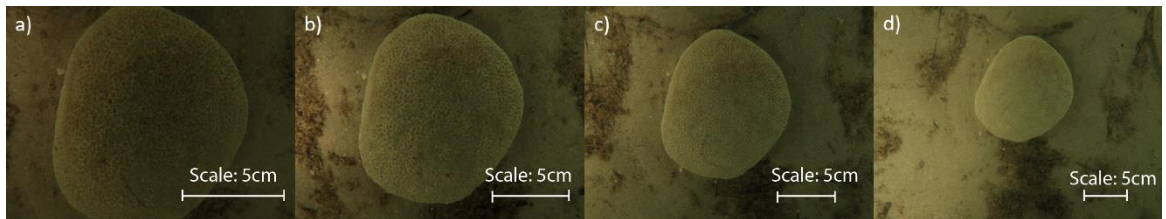


**Figure 3.2.** Photos of a *Porites* coral skeleton taken using the Canon G7X Mark II with **a.** 100% field of view. **b.** 75% field of view. **c.** 50% field of view. **d.** 25% field of view.

To compare the performance of the four cameras to create 3D models using structure from motion photogrammetry in turbid benthic environments, several objects with known measurements were set up in a scene that were then photographed (Figure 3.3). Using one camera at a time, photos were taken continuously while swimming in a boustrophodonic pattern above the scene at a depth of 1m above the substrate. The same swim pattern was used for all cameras. The seafloor here was at a depth of 1.5 m.

Measurements were taken from the resulting model to compare to the real world measurements as an indicator of camera performance.

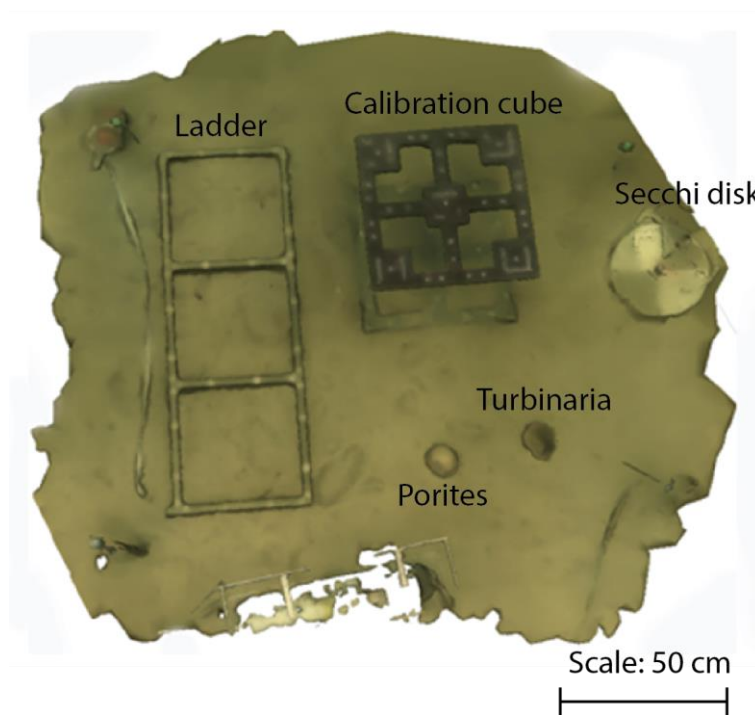


**Figure 3.3.** Scene setup of calibration ladder, calibration cube, Secchi disk and 2 coral skeletons at Fremantle Sailing Club in 2m of water.

#### 3.3.2.4 Omeo Wreck Dive Trail

Due to time restraints and the time it takes to process the images and extract required data, the two best performing cameras from the experiment at Fremantle Sailing Club (GoPro Hero 8 and Canon G7X Mark II), were used to collect photos and produce a 3D model of an Apollo structure from the Coogee Maritime Trail (Fig 3.1d). The GoPro Hero 8 captured photos using the automatic settings of the camera whilst in linear mode at one image per second and the Canon G7X Mark II captured photos using the custom settings previously used at the Fremantle Sailing Club and images were captured at roughly one image per second (this was manually done so would not be as many images as the GoPro's automatic image taking). Photos were taken continuously while swimming in a boustrophodonic pattern, to simulate photo collection for a broadscale survey, above the Apollo structure, firstly at a depth of 1m above the substrate, followed by a depth of 2m above the

substrate (Figure 3.4) with the camera facing directly downwards to the substrate.

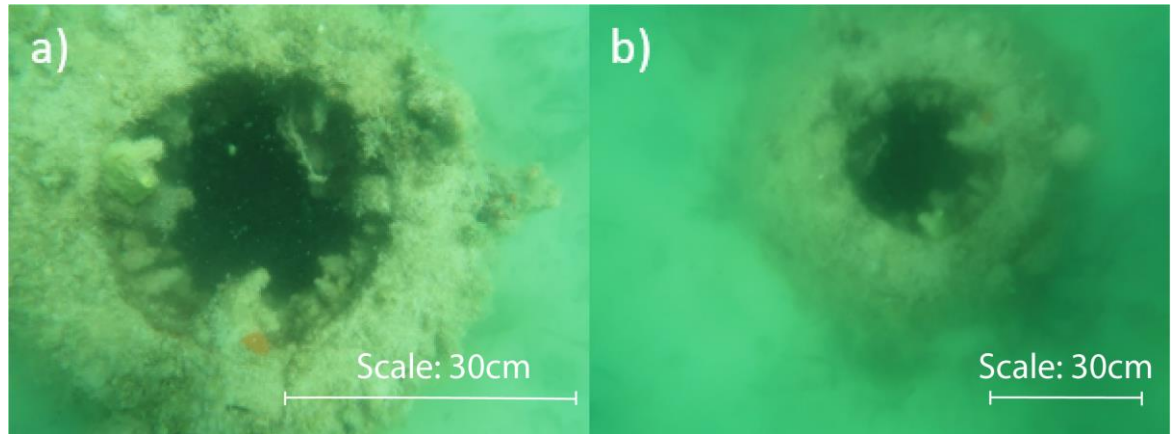


**Figure 3.4.** Example of photos taken using the Canon G7X Mark II at **a.** 1m above the seafloor, and **b.** 2m above the seafloor, of the Apollo artificial reef structure.

### 3.3.3 Data processing

#### 3.3.3.1 Feature matching

In Agisoft Metashape, photos for each dataset were aligned individually. This produced key points/features aligned across photos. These were recorded for each dataset as an indication of camera performance and image quality before 3D models were created. For the photos of the coral at different fields of view, the surrounding area was masked out, so when comparing the number of features aligned, they were just from the coral structure.

#### 3.3.3.2 3D model creation

The 3D model creation of the scene at Fremantle Sailing Club and the Apollo structure at Coogee Maritime Trail was performed using Agisoft Metashape, using the photos taken *in-situ*. Each data set from each location was processed individually, with camera calibration and optimization completed within the program, which resolves the optical characteristics of the camera lens within the software, using the image metadata and Brown's distortion model to perform the calibration (Burns et al., 2015).

### **3.3.4 Data analysis**

The open source 3D point processing software, CloudCompare v.2.12, was used to perform comparisons of surface area measurements of the coral skeletons point cloud from Fremantle Sailing Club and the Apollo point cloud from Coogee Maritime Trail (Saunders, 2020). The model was scaled using the top of the calibration cube measurements as they were accurate to real world measurements. This is a valid methodology as different approaches (cameras) are being tested and this allows uniformity. This allows for assessment of the ability of the program to create a 3D model and how well that model is produced. To allow for a comparative analysis, the models and their respective laser scan (coral skeletons) or engineering diagram (Apollo structure) needed to be aligned.

#### **3.3.4.1 Coral skeleton alignment**

The coral skeleton point cloud from photos collected at Fremantle Sailing Club was imported into CloudCompare and any seafloor was trimmed manually and independently of each other, so only the coral skeleton was visible. The laser scan mesh of the coral was imported and having already been scaled in a previous study by Saunders (2021), the photogrammetry-generated point cloud was then scaled to match the laser scan mesh. The photogrammetry point cloud and the laser scan mesh were overlaid (Figure 3.5) using the match bounding box centres feature, then they were aligned using the fine alignment tool.

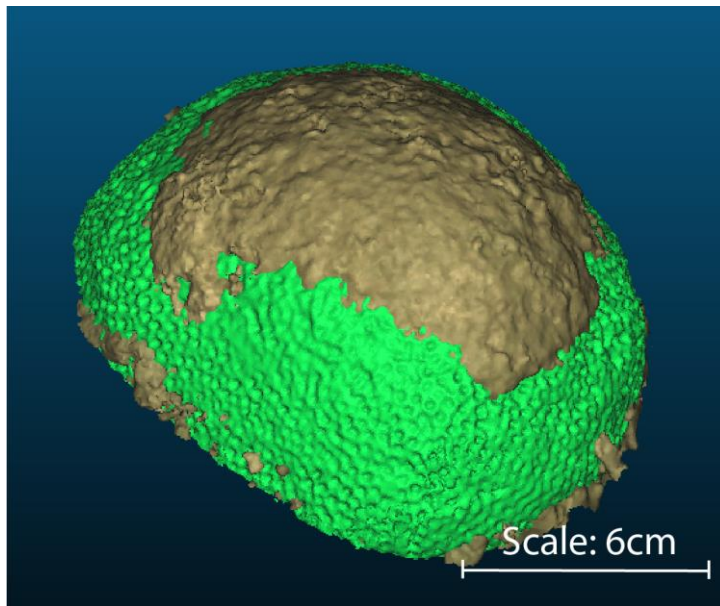


**Figure 3.5.** CloudCompare alignment of *Porites* skeleton point cloud from Canon G7X Mark II model (brown) overlaid on reference mesh from laser scan (green).

#### **3.3.4.2 Apollo structure alignment**

The Apollo structure point clouds were imported into CloudCompare and the same steps for trimming were applied, as they were for the coral skeletons. The engineering diagram of the Apollo cluster (Figure 1d) was imported, and as the Apollo point cloud had been scaled in Metashape, this was used to scale the engineering diagram mesh. Once scaled, the bounding box centres were aligned and the point cloud and the mesh were aligned (Figure 3.6) using the fine alignment tool. The engineering diagram mesh that was scaled using the Canon G7X Mark II point cloud was used as the comparison mesh for all of the Apollo structure point clouds.

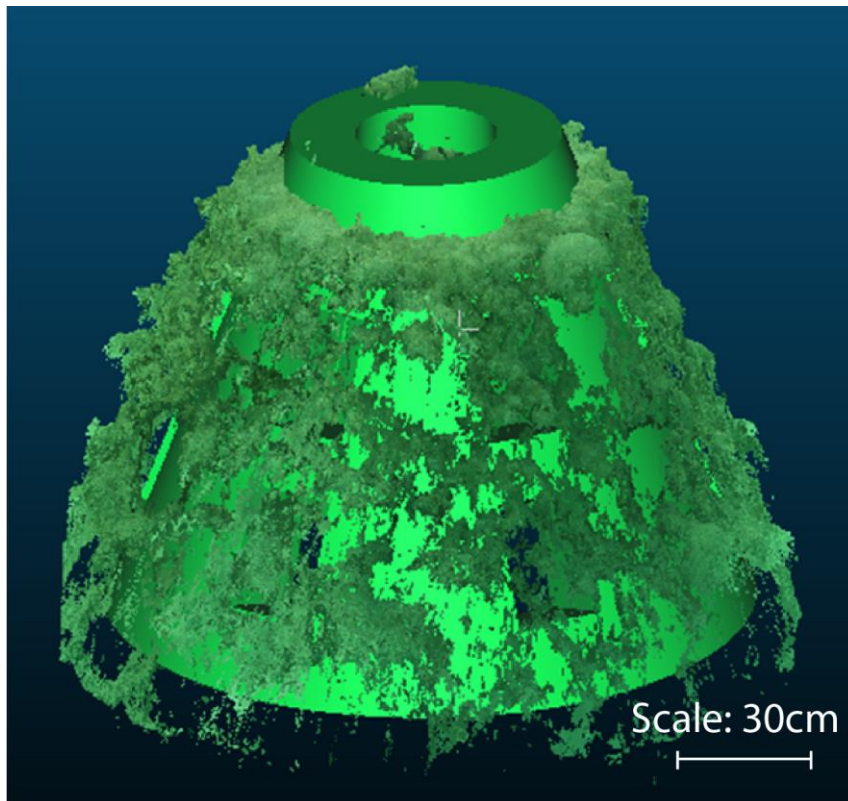


**Figure 3.6.** CloudCompare alignment of Apollo structure point cloud from Canon G7X Mark II model using photos from 1m (dark green) overlaid on the reference mesh from the engineering diagram (light green).

#### **3.3.4.3 Surface area comparison**

To determine the surface area of the point cloud measurements, it was transformed into a mesh using the surface reconstruction tool. The Poisson surface reconstruction tool was used following the methodology of Saunders (2020) that used the same coral skeleton laser scan and similar methodology. The measure surface tool was then used to calculate the surface area of each individual mesh for data set.

#### **3.3.4.4 Regression analysis**

For the Apollo datasets, a multi-linear regression analysis was conducted to determine whether the number of photos taken at 1 m and/or 2 m, had a bearing on the accuracy of the 3D model, and linear regression was carried out to determine if overall accuracy could be approximated using total number of photos. To carry this out, 3D models of the Apollo structure were

created using various combinations of photos from 1 m and 2 m. The resulting 3D models were then compared to see how well the surface area agreed with the engineering diagram which determined the accuracy of the model. The percentage agreement was used as a proxy for accuracy and regression analysis was carried out in MATLAB using the built in “regress” function. The Root-Mean-Squared-Error (RMSE) was used to assess regression model performance (Denis, 2020).

### **3.4 Results**

#### **3.4.1 Water quality**

During data collection, Fremantle Sailing Club harbour ranged in NTU between 0 and 3 and average of < 0.5, and Coogee Maritime Trail had a NTU range of 9-16 and average of 11.5. These values are relatively low considered the in-water conditions (visibility) and therefore could be an inaccurate indication of the turbidity of the area during the time of imaging. Due to this, the secchi disk was used to determine the turbidity of the survey areas, with Fremantle Sailing Club and Coogee Maritime Trail having visibility of 2m and 2.5m respectively on the day of imaging, which was less than the water depth.

#### **3.4.2 Feature matching from coral skeletons**

For the number of features aligned for the photos of corals taken with different percentages of the coral being in the frame with the four cameras, generally it showed more features aligned using the custom settings than compared to the automatic settings (Table 3.2). Of the three cameras compared, the Canon G7X Mark II had the highest number of features aligned for most photos underwater with automatic camera settings and underwater with custom camera settings (Table 3.2). For both the Canon G7X Mark II and Nikon D70, custom settings resulted in more features aligned underwater compared to the automatic settings. For the GoPro camera, the number of features aligned dropped considerably when the coral



was in 25 or 50% of the image, whereas this was relatively independent for Canon G7X Mark II and Nikon D70.

**Table 3.2.** Number of features aligned at each field of view for each camera with 2 different settings underwater. Green highlight indicates high numbers of features aligned between photos.

Underwater (auto) (%)	GoPro 8	G7X MII	D70
100	1858	N/A	1012
75	1942	3759	190
50	559	3840	2915
25	752	304	1609
Underwater (setting 1) (%)	GoPro 8	G7X MII	D70
100	N/A	5292	1313
75		5450	1953
50		5755	4434
25		4562	4447

### 3.4.3 Measurement comparison across 3D models

The Canon G7X Mark II produced the most complete and accurate 3D model of the artificial scene created at FSC, based on the visual model (Figure 3.7b) and the measurements of the objects within the model (Table 3.3). Only the Canon G7X Mark II and the Nikon D70 models reconstructed the coral skeletons (Figure 3.7b, c) from the scene.

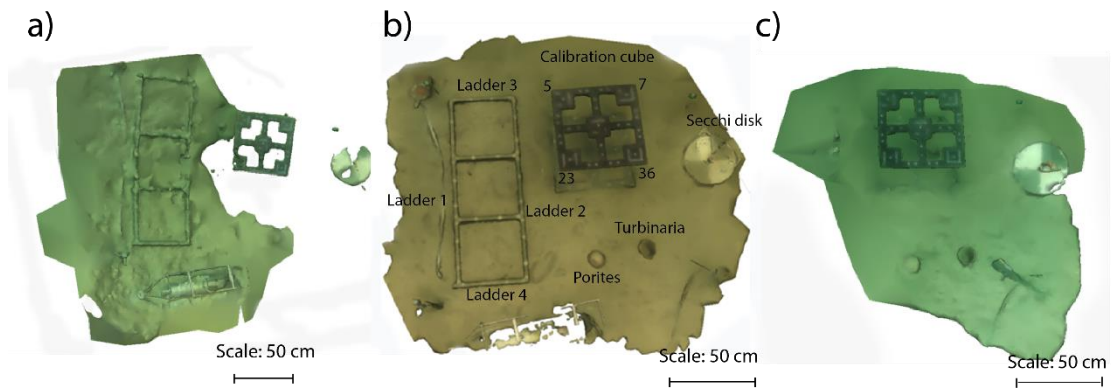


**Figure 3.7.** Screen capture of 3D model of Fremantle Sailing Club scene from **a.** GoPro Hero 8 (automatic settings), **b.** Canon G7X Mark II (custom settings), **c.** Nikon D70 (custom settings).

**Table 3.3.** Measurements of objects from the scene at Fremantle Sailing Club from each camera and the difference from the actual measurement. Ladder 1 and 2 vertical measurements of longest length of ladder, Ladder 3 and 4 horizontal measurements of top and bottom cross bars (Figure 8b). Top of cube numbers referenced to shape on cube and measured from point to point (Figure 8b). \*Actual measurements for Ladder and calibration cube measured using a measuring tape as lengths, Secchi disk measurement as diameter length and coral skeletons measured using surface area of a laser scan of the coral.

Object	Actual*	G7X	Difference	D70	Difference	GoPro8	Difference
Ladder 1	1.38m	1.39m	+0.01m	N/A	N/A	1.7m	+0.32m
Ladder 2	1.38m	1.38m	0m	N/A	N/A	1.71m	+0.33m
Ladder 3	0.426m	0.419m	0.007m	N/A	N/A	0.532m	+0.106m
Ladder 4	0.425m	0.42m	+0.005m	N/A	N/A	0.527m	+0.102m
Secchi disk	0.38m	0.38m	0m	0.406m	+0.026m	0.45m	+0.07m
Top of cube (23 to 36)	0.45m	0.45m	0m	0.451m	+0.001m	0.451m	+0.001m
Top of cube (36 to 7)	0.45m	0.449m	0.001m	0.457m	+0.007m	0.45m	0m
Top of cube (7 to 5)	0.45m	0.449m	0.001m	0.453m	+0.003m	0.455m	+0.005m
Top of cube (5 to 23)	0.45m	0.452m	+0.002m	0.443m	0.007m	0.462m	+0.012m
Porites (surface area)	0.0276m	0.0281m	+0.0005m	N/A	N/A	N/A	N/A
Turbinaria (surface area)	0.0361m	0.0285m	0.0076m	0.0274m	0.0087m	N/A	N/A
Turbinaria (highest point to floor)	0.113m	0.115m	+0.002m	0.115m	+0.002m	N/A	N/A

### 3.4.4 Surface area comparisons

The 3D models of the *Porites* and *Turbinaria* coral skeletons created in the scenes with the Canon G7X Mark II (Figure 3.8b, 3.9b), and for the *Turbinaria* with Nikon D70 (Figure 3.9c), were compared with the in-air laser scan models (Figures 3.8a and 3.9a). The 3D mesh produced by the Canon G7X Mark II of the *Porites* skeleton (Figure 3.8b) had a surface area similar to the laser scan (101.8% agreement); whereas the one of the *Turbinaria* skeleton (Figure 3.9b) had an agreement of 78.9% (Table 3.3). The Nikon D70 produced a mesh of the *Turbinaria* skeleton that had an agreement of 75.9% with the laser scan mesh for the *Turbinaria* skeleton (Table 3.3).

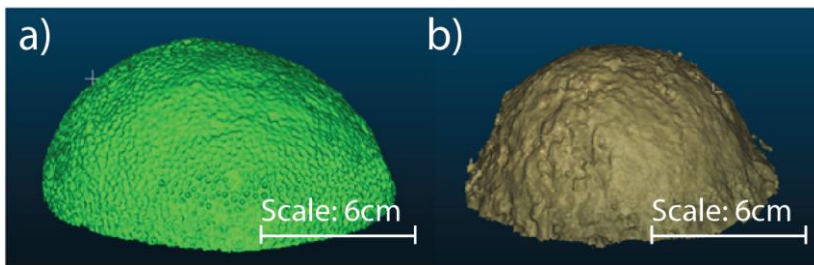


**Figure 3.8.** **a.** Laser scan mesh of *Porites* skeleton. **b.** Mesh from the 3D model of the *Porites* skeleton from the Canon G7X Mark II.

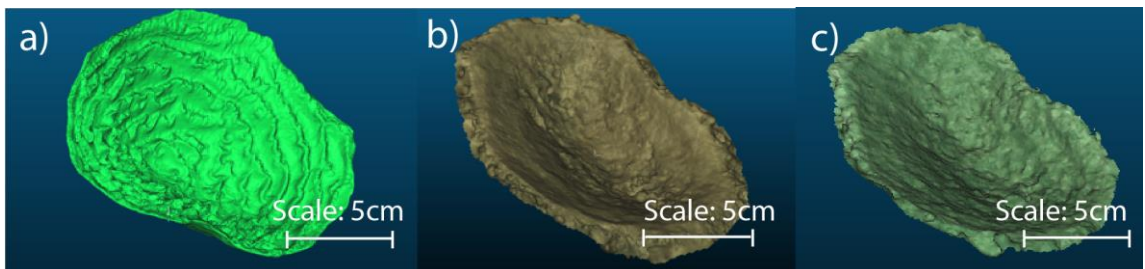


**Figure 3.9.** **a.** Laser scan mesh of *Turbinaria* skeleton. **b.** Mesh from the 3D model of the *Turbinaria* skeleton from the Canon G7X Mark II. **c.** Mesh from the 3D model of the *Turbinaria* skeleton from the Nikon D70.

From the 3D models of the Apollo structure, the Canon G7X Mark II provided a model (Figure 3.10b) that most agrees with the surface area measurements of the engineering diagram, with an accuracy of 98.2% (Table 3.4).

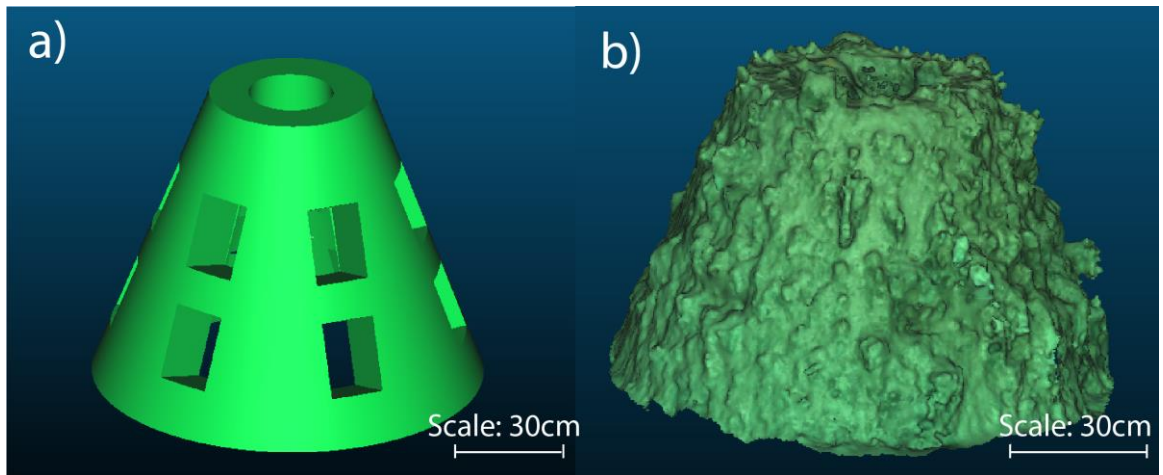


**Figure 3.10. a.** Engineering diagram of Apollo structure. **B.** Mesh from Canon G7X Mark II 3D model from photos at 1m and 2m.

**Table 3.4.** Number of images and surface area measurements ( $m^2$ ) of the Apollo structure from the Canon G7X Mark II and GoPro Hero 8 models created using photos from 1m, 2m and combined 1m & 2m. Green highlight indicating the most agreeable surface area measurement.

<i>Surface Area Comparison</i>	Number of images	$m^2$
<b>Apollo (actual)</b>		22.46
<b>Canon G7X Mark II @ 1m</b>	94	21.22
<b>Canon G7X Mark II @ 2m</b>	66	18.76
<b>Canon G7X Mark II (all images)</b>	160	22.06
<b>GoPro Hero 8 @ 1m</b>	766	18.83
<b>GoPro Hero 8 @ 2m</b>	227	16.88
<b>GoPro Hero 8 (all images)</b>	993	20.96

### 3.4.5 Regression analysis

Predicted accuracy of 3D models from linear and multilinear regression compared with data was investigated (Figure 3.11) to determine if the number of photos taken would increase the accuracy of the subsequent 3D model creation. Accuracy could be well approximated using linear regression

on the total number of photos (Figure 3.12). Although the RMSE for a linear and log functions were both 5%, the best visual fit was using a log relationship (Figure 3.12). Therefore, multilinear regression used a log function, and found that photos taken at an altitude of 1 m (77%) had more bearing on the accuracy of the 3D model, than photos taken at 2 m (23%). The resulting model from MLR (Figure 3.12) had an RMSE of 5% as well.

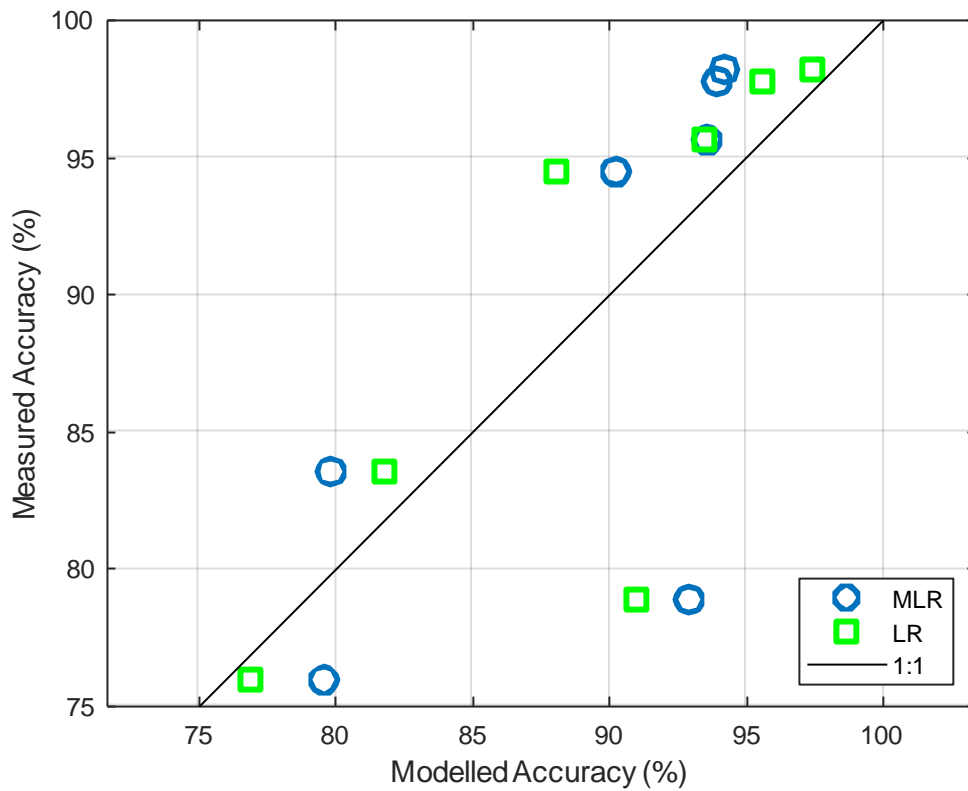


**Figure 3.11.** Modelled accuracy vs measured accuracy.

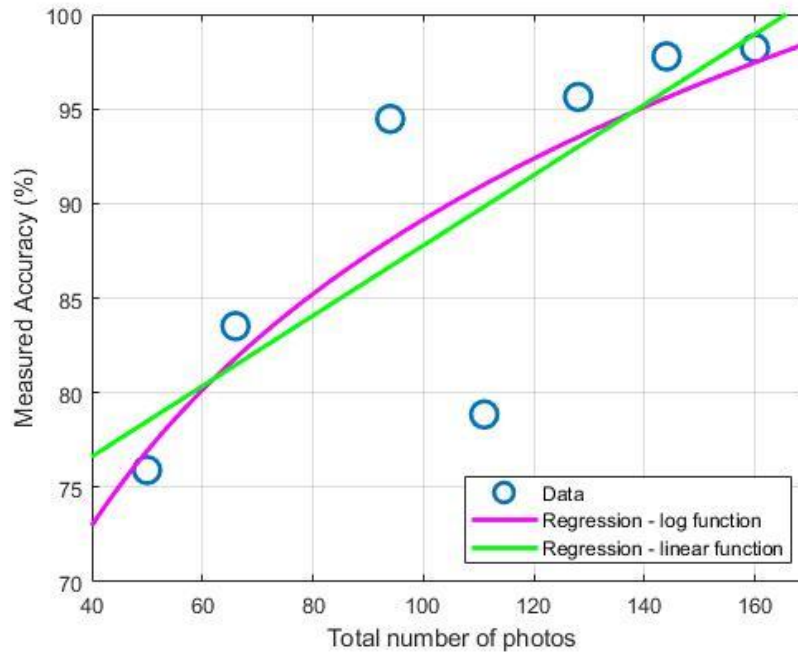


**Figure 3.12.** Linear regression (green line) of the measured accuracy against total number of photos with line of best fit using a log relationship (pink line).

### 3.5 Discussion

#### 3.5.1 Water quality

The turbidity, as indicated as an NTU value, of the sites were similar to that of the turbid coral reefs of the island in the Exmouth Gulf, which were surveyed in Chapter 2. The northern turbid reef of Eva Island in the Exmouth Gulf had on average 1.9 NTU during a 9 month period (Table S3.1), which is within the range of turbidity that the Exmouth Gulf experiences as reported by Sutton and Shaw (2021). Both Fremantle Sailing Club and Coogee Maritime Trail have NTU values that are comparable to Exmouth Gulf and therefore the resulting workflow should increase the accuracy of 3D models from surveys of the Gulf's turbid reefs.

#### 3.5.2 Camera selection

Of the cameras compared in this study (Table 3.1), it was found that the Canon G7X Mark II, a compact camera, out-performed the action camera (GoPro 8) and the digital single lens reflex (DSLR) (Nikon D70). For instance,

photos of a *Porites* coral skeleton taken with the Canon G7X Mark II were found to align more features in the SfM software than photos from the other cameras. Moreover, photos from the Canon G7X Mark II resulted in more accurate 3D models: one of a low relief scene including the coral skeletons of known dimensions (at Fremantle Sailing Club), and the other of an artificial reef structure of known dimensions (at Coogee Maritime Trail). It is likely the reasons for this include the camera's sensor and image size, and the custom settings used.

A camera with a large sensor size, like the Canon G7X Mark II (13.2 x 8.8 mm), is ideal for turbid benthic environments, as it has larger photosites, a light sensitive element on the sensor (McCarty, n.d.), giving the camera the ability to take good quality photos in low light situations (Maio, 2020). So, it is understandable that a camera like the Canon G7X Mark II, outperformed cameras that had sensors that were more than four times smaller, i.e., the GoPro camera (6.17 x 4.55 mm). However, the Nikon D70 has a larger sensor size (23.7 x 15.6 mm) than the Canon G7X Mark II, but the Canon G7X Mark II has a higher sensor resolution (20 megapixels) than the Nikon D70 (6.1 megapixels).

From 43 previous studies from open-access journals from 2015 to 2022 (Table S3.2), only eight of those studies used a camera similar to the Canon G7X Mark II. The most commonly used cameras were a version of the GoPro (from Hero 3 to Hero 7), which were used in 17 studies, and a range of DSLR cameras, used in 19 studies. Of these studies, most were conducted in clear water environments, where conditions are less challenging for the use of SfM photogrammetry than in turbid benthic environments. Only Roach et al. (2021) investigated camera performance from an action camera and a DSLR camera, however the action camera was used in video mode. It was found that they were both able to 3D models with < 0.5 mm/pixel resolution and suggested that an action camera be used in homogenous environments (e.g., seagrass meadows, dead coral habitats) or where only broad scale community metrics (e.g., abundance, diversity) are required (Roach et al.,

2021). The same study suggests a DSLR camera be used in more complex environments or where fine scale analysis (e.g., coral extension rates) is required. The findings from this study are in agreement with Roach et al. (2021) in regard to camera selection, based on the camera properties of large sensor size and high sensor resolution, which allow for high quality photos and fine scale metrics, such as surface area, to be extracted. This is important to consider as automatic settings would adjust for each photo taken, which would be problematic for photogrammetry as the photos would be less uniform and harder to align due to inadequate photo quality.

### **3.5.3 Camera settings**

This study found that customised settings performed better than the automatic settings. For instance, the Canon G7X Mark II aligned the greatest number of features in most fields of view for air, underwater with automatic camera settings and underwater with custom camera settings. Previous studies using compact and/or DSLR cameras have used custom settings to suit the environment they are surveying in (e.g., Burns et al., 2015; Burns et al., 2017; Fukunaga et al., 2019; Suka et al., 2020; Roach et al., 2021; Pascoe et al., 2021). This would suggest that if a camera has customisable settings, it is beneficial to use these to suit the environment, rather than rely on the automatic settings that will self-adjust every time you take a photo.

### **3.5.4 Altitude from objects**

This study found evidence that photos taken at closer altitude (1 m vs 2 m) in a turbid benthic environment, helped improve the accuracy of 3D models produced from SfM photogrammetry software. However, in general it was found that more photos from either altitude increased model accuracy, to a point, as it was found that a log function based on number of photos could be used adequately account for 3D model accuracy, i.e., the rate of increase of model accuracy eventually decreases with number of photos. It is possible, though, that the mixture of altitudes from the target improved the estimation of the camera's internal orientation parameters as part of the SfM



photogrammetry bundle adjustment, but this was not conclusive. A more dedicated study is required to determine this aspect more conclusively.

### **3.5.5 Uncertainty in findings**

The models created of the Apollo structure at Coogee Maritime Trail showed that the Canon G7X Mark II produced the most agreeable model of the structure, with high surface area accuracy. Whilst the model still slightly underestimated the surface area, the results were questionable as you would expect the surface area of the Apollo structure to have increased since its installation, due to the growth from algae, tunicates and other organisms. It is unclear as to whether CloudCompare's surface area calculation from the engineering diagram took into account the holes in the structure of the Apollo, which could have affected the calculation, potentially alluding to a greater surface area than it actual is. If this was the case, the surface area from the models created from the cameras could be more accurate than initially assumed.

### **3.6 Conclusion**

This study quantifies the effects of photogrammetry in turbid underwater environments as opposed to other studies that have been qualitative. It determines that camera quality is the most important thing to consider for photogrammetry in these environments. Recommendations from this study would suggest that for Structure-from-Motion photogrammetry to be successful in turbid benthic environments, a camera with a large sensor size and large sensor resolution should be used. As the accuracy increases with the number of photos which eventually results in diminishing returns, it is recommended that photos taken at two altitudes (e.g., 1 m and 2 m) above the survey area, would assist in creating the most visually complete and accurate model. If time is limited, images taken 1 m above the survey area would be most suitable than images taken further away (e.g., 2 m).

Potentially, a frame could allow cameras to be mounted at different altitudes. There is scope for further study to determine the optimal camera and altitude

based on the topography, i.e., seagrass meadows or low lying reefs versus rugose coral reefs, to further develop this method in turbid benthic environments.

### 3.7 References

Anelli M, Julitta T, Fallati L, Galli P, Rossini M, Colombo R. 2017. Towards new applications of underwater photogrammetry for investigating coral reef morphology and habitat complexity in the Myeik Archipelago, Myanmar. *Geocarto International*. 34:5, 459-472

Arnold B. 2022. Dive into underwater photography: A guide for beginners. *Modula*. <https://wp-modula.com/underwater-photography/#:~:text=%20Challenges%20of%20shooting%20underwater%20%201%20Low,particulate%20in%20the%20water%2C%20it%20will...%20More%20>

Askey P. 2004. Nikon D70 review: Digital Photography Review. <https://www.dpreview.com/reviews/nikond70/>

Bayley DTI, Mogg AOM, Koldewey H, Purvis A. 2019. *PeerJ*. 7, e6540

Browne NK, Smither SG, Perry CT. (2010). Geomorphology and community structure of Middle Reef, central Great Barrier Reef, Australia: an inner-shelf turbid zone reef subject to episodic mortality events. *Coral Reefs*. 29:683-689

Browne, N.K.; Smithers, S.G.; Perry, C.T. 2013. Carbonate and terrigenous sediment budgets for two inshore turbid reefs on the central Great Barrier Reef. *Mar. Geol.* 346, 101–123.

Bryson M, Ferrari R, Figueira W, Pizarro O, Madin J, Williams S, Byrne M. 2017. Characterization of measurement errors using structure-from-motion and photogrammetry to measure marine habitat structural complexity. *Ecology and Evolution*. 15;7 (15):5669-5681

Burns JHR, Delparte D, Gates RD, Takabayashi M. 2015 (a). Integrating structure-from-motion photogrammetry with geospatial software as a novel

technique for quantifying 3D ecological characteristics of coral reefs. *PeerJ*. 3. 10.7717/peerj.1077

Burns JHR, Delparte D, Gates RD, Takabayashi M. 2015 (b). Utilizing underwater three-dimensional modelling to enhance ecological and biological studies of coral reefs. *ISPRS-International Archives of the Photogrammetry, Remote Sensing and Spatial Information Sciences*. XL-5/W5. 61-66

Burns JHR, Delparte D, Kapon L, Belt M. 2016. Assessing the impact of acute disturbances on the structure and composition of a coral community using innovative 3D reconstruction techniques. *Methods in Oceanography*. 15. 10.1016/j.mio.2016.04.001

Burns JHR, Delparte D. 2017. Comparison of commercial Structure-from-Motion photogrammetry software used for underwater three-dimensional modeling of coral reef environments. *ISPRS-International Archive of the Photogrammetry, Remote Sensing and Spatial Information Sciences*. XLII-2/W3. 10.5194/isprs-archives-XLII2-W3-127-2017

Burns JHR, Fukunaga A, Pascoe K, Runyan A. 2019. 3D habitat complexity of coral reefs in the North-Western Hawaiian Islands is driven by coral assemblage structure. *ISPRS-International Archives of Photogrammetry, Remote Sensing and Spatial Information Sciences*. XLII-2/W10. 61-67

Cahyono AB, Wibisono AC, Saptarini D, Permadi RI, Budisusanto Y, Hidayat B. 2020. Underwater photogrammetry application for coral reef mapping and monitoring. *International Journal on Advanced Science Engineering and Information Technology*. 10, 293

Carlot J, Rovere A, Casella E, Harris D, Grellet-Munoz C, Chancerelle Y, Dormy E, Hedouin L, Parravicini V. 2020. Community composition predicts photogrammetry-based structural complexity on coral reefs. *Coral Reefs*. 39, 967-975

Chen GK, Dai CF. 2021. Using 3D photogrammetry to quantify the subtle differences of coral reefs under the impacts of marine activities. *Marine Pollution Bulletin*. 173, 113032

- Combs IR, Studivan MS, Eckert RJ, Voss JD. 2021. Quantifying impacts of stony coral tissue loss disease on corals in Southeast Florida through surveys and 3D photogrammetry. *PLoS ONE*. 16: e0252593
- Couch CS, Oliver TA, Suka R, Lamirand M, Asbury M, Amir C, Vargas-Angel B, Winston M, Huntington B, Lichowski F, Halperin A, Gray A, Garriques J, Samson J. 2021. Comparing coral colony surveys from in-water observations and Structure-from-Motion imagery shows low methodological bias. *Frontiers in Marine Science*. 8, 622
- Cresswell AK, Orr M, Renton M, Haywood MDE, Giraldo Ospina A, Slawinski D, Austin R, Thomson DP. 2020. Structure-from-motion reveals coral growth is influenced by colony size and wave energy on the reef slope at Ningaloo Reef, Western Australia. *Journal of Experimental Marine Biology and Ecology*. 530-531, 151438
- Denis DJ. (2020). Univariate, bivariate, and multivariate statistics using R: Quantitative tools for data analysis and data science. Logistic regression and the generalized linear model. John Wiley & Sons Ltd
- Done T, Turak E, Wakeford M, DeVantier L, McDonald A, Fisk D. (2007). Decadal changes in turbid-water coral communities at Pandora Reef: loss of resilience or too soon to tell? *Coral Reefs* 26:789-805
- Ferrari R, McKinnon D, He H, Smith RN. 2016. Quantifying multiscale habitat structural complexity: A cost-effective framework for underwater 3D modelling. *Remote Sensing*. 8(2):113
- Figueira WF, Ferarri Legoretta R, Weatherby E, Porter A. 2015. Accuracy and precision of habitat structural complexity metrics derived from underwater photogrammetry. *Remote Sensing*. 7, 16883-16900
- Frosin K. 2021. Evaluating damselfish distribution patterns and benthic habitat complexity associations using SFM-photogrammetry. Master's project, Bangor University. Retrieved from <https://research.bangor.ac.uk/portal/files/38920590/2021FrosinKFMScRes.pdf>

Fukunaga A, Burns JHR, Craig BK, Kosaki RK. 2019. Integrating three-dimensional benthic habitat characterization techniques into ecological monitoring of coral reefs. *Journal of Marine Science and Engineering*. 7, 27

Fukunaga A, Pascoe KH, Pugh AR, Kosaki RK, Burns JHR. 2022. Underwater photogrammetry captures the initial recovery of a coral reef at Lalo Atoll. *Diversity*. 12, 39

George EE, Mulliniz JA, Meng F, Bailey BA. 2021. Space-filling and benthic competition on coral reefs. *PeerJ*. 9:e11213

Gibson LA. 2021. How large area imagery can be used to quantify growth of a complex branching coral species. Master's project, University of California, San Diego. Retrieved from <https://escholarship.org/uc/item/65k35155>

Google Earth Pro V 7.3.48642. (June 8<sup>th</sup>, 2022). Map of South Fremantle and Coogee, Perth.

International Association of Dredging Companies (IADC). No date. Turbidity: Turbidity is a leading factor in causing underwater disturbances to marine life and must be minimised and monitored during a dredging project.

International Association of Dredging Companies. <https://www.iadc-dredging.com/subject/environment/turbidity/#:~:text=Turbidity%20is%20an%20optical%20quality%20of%20water%20and,or%20thick%20%E2%80%93%20when%20it%20contains%20suspended%20silt>.

Johnson-Sapp. 2018. A tale of two reefs: Quantifying the complexity of artificial reefs and natural reefs utilizing Structure-from-Motion 3D modeling. Master's project, Duke University. Retrieved from <https://hdl.handle.net/10161/16560>

Jupiter S, Roff G, Marion G, Henderson M, Schrameyer V, McCulloch M, Hoegh-Guldberg O. (2008). Linkages between coral assemblages and coral proxies of terrestrial exposure along a cross-shelf gradient on the southern Great Barrier Reef. *Coral Reefs* 27:887–903

Kolodziej G, Studivan MS, Gleason ACR, Langdon C, Enochs IC, Manzella DP. 2021. Impacts of Stony Coral Tissue Loss Disease (SCTLD) on coral

community structure at an inshore patch reef of the Upper Florida Keys using photomosaics. *Frontiers in Marine Science*. 8, 682163

Kornder NA, Cappelletto J, Mueller B, Zalm MJL, Martinez SJ, Vermeij MJA, Huisman J, de Goeij JM. 2021. Implications of 2D versus 3D surveys to measure the abundance and composition of benthic coral reef communities. *Coral Reefs*. 40, 1137-1153

Lange ID, Perry CT. 2020. A quick, easy and non-invasive method to quantify coral growth rates using photogrammetry and 3D model comparisons. *Methods in Ecology and Evolution*. 11, 714-726

Lechene MAA, Haberstroh AJ, Byrne M, Figueira W, Ferrari R. 2019. Optimising sampling strategies in coral reefs using large-area mosaics. *Remote Sensing*. 11, 2907

Leon JX, Roelfsma CM, Saunders MI, Phinn SR. 2015. Measuring coral reef terrain roughness using Structure-from-Motion close-range photogrammetry. *Geomorphology*. 242, 21-28

Light on LED. 2022. LED light lux levels and light measurement and brightness. Light on LED. Retrieved from <https://www.liteonled.com.au/buying-guide/understanding-led-lighting/led-lux-levels>

Longo GO, Correia LFC, Mello TJ. 2020. Coral recovery after a burial event: insights on coral resilience in a marginal reef. *Marine Biodiversity*. 50, 92

Maio A. 2020, April 19. Camera sensor sizes explained: What you need to know. Studio Binder. Retrieved from <https://www.studiobinder.com/blog/camera-sensor-size/#:~:text=%20Sensor%20size%20chart%20%201%20Full%20Frame,a%202x%20crop%20factor.%20The%20four...%20More%20>

McCarty L. No Date. Photosites. Lisa McCarty. Retrieved from <http://lisamccarty.com/about-photosites>

- Magel JMT, Burns JHR, Gates RD, Baum JK. 2019. Effects of bleaching-associated mass coral mortality on reef structural complexity across a gradient of local disturbance. *Scientific Reports*. 9, 2512
- Million WC, O'Donnell S, Bartels E, Kenkel CD. 2021. Colony-level 3D photogrammetry reveals that total linear extension and initial growth do not scale with complex morphological growth in the branching coral, *Acropora cervicornis*. *Frontiers in Marine Science*. 8, 10.3389/fmars.2021.646475
- Morgan, K.M.; Perry, C.T.; Smithers, S.G.; Johnson, J.A.; Daniell, J.J. 2016. Evidence of extensive reef development and high coral cover in nearshore environments: Implications for understanding coral adaptation in turbid settings. *Sci. Rep.* 6, 29616.
- Morgan KM, Perry CT, Johnson JA, Smither SG. (2017). Nearshore turbid-zone corals exhibit high bleaching tolerance on the Great Barrier Reef following the 2016 ocean warming event. *Front Mar Sci*. 4:224
- Palma M, Casado MR, Pantaleo U, Cerrano C. 2017. High resolution orthomosaics of African coral reefs: A tool for wide-scale benthic monitoring. *Remote Sensing*. 9(7), 705
- Palma M, Magliozzi C, Casado MR, Pantaleo U, Fernandes J, Coro G, Cerrano C, Leinster P. 2019. Quantifying coral reef composition of recreational diving sites: A Structure-from-Motion approach at seascape scale. *Remote Sensing*. 11(24), 3027
- Palmer, S.E.; Perry, C.T.; Smithers, S.G.; Gulliver, P. 2010. Internal structure and accretionary history of a nearshore, turbid-zone coral reef: Paluma Shoals, central Great Barrier Reef, Australia. *Mar. Geol.* 276, 14–29.
- Pascoe KH, Fukunaga A, Kosaki RK, Burns JHR. 2021. 3D assessment of a coral reef at Lalo Atoll reveals varying responses of habitat metrics following a catastrophic hurricane. *Scientific Reports*. 11, 12050
- Peck M, Tapilatu RF, Kurniati E, Rosado C. 2021. Rapid coral reef assessment using 3D modelling and acoustics: acoustic indices correlate to fish abundance, diversity and environmental indicators in West Papua, Indonesia. *PeerJ*. 9: 210761

- Perry, C.T.; Smithers, S.G.; Palmer, S.E.; Larcombe, P.; Johnson, K.G. 2008. 1200 year paleoecological record of coral community development from the terrigenous inner shelf of the Great barrier reef. *Geology*. 36, 691–694
- Raber G, Schill SR. 2019. Reef rover: A low-cost autonomous unmanned surface vehicles (USV) for mapping and monitoring coral reefs. *Drones*. 3, 38
- Raoult V, David PA, Dupont SF, Matthewson CP, O'Neill SJ, Powell NN, Williamson JE. 2016. GoPros as an underwater photogrammetry tool for citizen science. *PeerJ* 4:e1960
- Roach TNF, Yadav S, Caruso C, Dilworth J, Foley CM, Hancock JR, Huckeba J, Huffmyer AS, Hughes K, Kahkejian VA, Madin EMP, Matsuda SB, McWilliam M, Miller S, Santoro EP, Rocha de Souza M, Torres-Pullizaa D, Drury C, Madin JS. 2021. A field primer for monitoring benthic ecosystems using Structure-from-Motion photogrammetry. *Journal of Visualized Experiments*. 170, e61815
- Rossi P, Castagnetti C, Capra A, Brooks AJ, Mancini F. 2020. Detecting change in coral reef 3D structure using underwater photogrammetry: critical issues and performance metrics. *Applied Geomatics*. 12, 3-17
- Saunders R. 2020. Three-dimensional modelling of coral reef using underwater photogrammetry.
- Seniorocity. 2020. *Coogee Maritime Trail and Omeo Shipwreck*.  
<https://seniorocity.com.au/coogee-maritime-trail-and-omeo-shipwreck/>
- Simmons KR, Bohnenstiehl DR, Eggleston DB. 2021. Spatiotemporal variation in coral assemblages and reef habitat complexity among shallow fore-reef sites in the Florida Keys National Marine Sanctuary. *Diversity*. 14, 153
- Smith LD, Gilmour JP, Heyward AJ. (2008). Resilience of coral communities on an isolated system of reefs following catastrophic mass-bleaching. *Coral Reefs* 27:197-205
- Suka R, Huntington B, Morioka J, O'Brien K, Acoba T. 2020. Successful application of a novel technique to quantify negative impacts of derelict



fishing nets on North-Western Hawaiian Island reefs. *Marine Pollution Bulletin*. 157, 111312

Sutton AL, Shaw JL. 2021. Cumulative pressures on the distinctive values of Exmouth Gulf. First draft report to the Department of Water and Environmental Regulation by the Western Australian Marine Science Institution, Perth, Western Australia. 272 pages.

Tomlinson A. 2022. *Arrivals and Departures: New dive and snorkel trail for Coogee*. West Travel Club. <https://westtravelclub.com.au/stories/new-dive-snorkel-trail-for-coogee>

Urbina-Barreto I, Chiroleu F, Pinel R, Frechon L, Mahamadaly V, Elise S, Kulbicki M, Quod JP, Dutriex E, Garnier R, Bruggemann JH, Penin L, Adjerous M. 2021. Quantifying the shelter capacity of coral reefs using photogrammetric 3D modeling: from colonies to reefscape. *Ecological Indicators*. 121, 107151

Veron JEN. (1995). Corals in space and time: The biogeography and evolution of the Scleractinia. Sydney, Australia: University of New South Wales Press, 321p

Young G, Dey S, Rogers AD, Exton D. 2017. *PLoS ONE*. 12. 10.1371.0175341

### 3.8 Supplementary material

**Table S3.1.** NTU and SD of Eva Island, Exmouth Gulf, Western Australia for 9 months of the year in 2020/2021.

Location	Month/Year	Average NTU	SD
Eva Island	October 2020	1.90	± 1.13
Eva Island	November 2020	1.21	± 0.35
Eva Island	December 2020	1.55	± 1.05
Eva Island	January 2021	1.33	± 0.79
Eva Island	February 2021	2.49	± 2.31
Eva Island	March 2021	2.46	± 4.87
Eva Island	April 2021	3.77	± 5.57
Eva Island	May 2021	1.72	± 1.83
Eva Island	June 2021	1.14	± 0.41

**Table S3.2.** Previous SfM photogrammetry studies on benthic environments.

Author	Year	Camera type	Location
Leon et al.	2015	Lumix DMC Ft3	Heron Reef, Great Barrier Reef, Australia
Burns et al.	2015	Pentax K5	French Frigate Shoals
Figueira et al.	2015	GoPro Hero 4 Black	Shelly Beach, Sydney
Burns et al.	2015	Canon 5D Mark III	Tide pools in Southeast Hawaii
Storlazzi et al.	2016	Sony FCB H11	Forereef off Lahaina, West Central Maui, Hawaii
Burns et al.	2016	Canon 5D Mark III	Waiopae, Southeast Hawaiian Island
Ferrari et al.	2016	Canon Powershot G2	Pool environment
Raoult et al.	2016	GoPro Hero 3 Black	Heron Island Southern reef flats, Great Barrier Reef, Australia
Burns et al.	2017	Canon 5D Mark III	Unknown
Bryson et al.	2017	Prosilica GC1380	Lizard Reef, Great Barrier

			Reef, Australia
Young et al.	2017	GoPro Hero 3/3+/4	Caribbean Islands of Honduras
Palma et al.	2017	GoPro Hero 3 Silver	Partial marine park reserve of Ponta do Ouro, Mozambique
Johnson-Sapp	2018	Canon T6l	Natural and artificial reefs, Miami
Anelli et al.	2019	Olympus TG4	Lampi, Southern Myanmar
Palma et al.	2019	GoPro Hero 3 Silver	Partial marine park reserve of Ponta do Ouro, Mozambique
Bayley et al.	2019	Nikon D750	Danajon Bank double barrier reef, Phillipines
Burns et al.	2019	Canon 5D Mark III	French Frigate Shoals
Magel et al.	2019	Nikon D750	Forereefs of Kirimati, Republic of Kirimati
Fukunaga et al.	2019	Canon EOS Rebel SL1	Northwestern Hawaiian Islands atoll
Raber et al.	2019	GoPro Hero 6 Black & Sony a6300	West Bay, Grand Cayman
Lechene et al.	2019	GoPro Hero 4	Reef slopes of Heron Reef, Great Barrier Reef, Australia
Suka et al.	2020	Canon SL2	Unknown
Cresswell et al.	2020	GoPro Hero 4	Northern Ningaloo Reef, Australia
Cahyono et al.	2020	GoPro Hero 4 Silver	Pasir Putih beach, East Java
Carlot et al.	2020	GoPro Hero 4	Wave exposure sites, Moorea
Rossi et al.	2020	Lumix DMC GH4	Unknown
Lange et al.	2020	Canon Powershot G7X Mark II	Chagos Archipelago, Indian Ocean

Longo et al.	2020	GoPro Hero 6	Fernando de Noronha, Northeast Brazil
Couch et al.	2021	Canon EOS Rebel SL2	Hawaiian Island
Roach et al.	2021	Canon EOS Rebel SL3 & GoPro Hero 7 Black	Unknown
Kornder et al.	2021	GoPro Hero 6 Black	Leeward shore of Curacao
Kolodziej et al.	2021	GoPro Hero 4 Black	Cheeca Rocks Reef, Florida Keys
Gibson	2021	Nikon D7000	Palmyra Atoll, Central Pacific
George et al.	2021	Canon Rebel T4i	Island of Curacao
Pascoe et al.	2021	Canon 5D III	Lalo Atoll, Northwest Hawaii
Frosin	2021	GoPro Hero 5	Grand Cayman
Simmons et al.	2021	GoPro Hero 3/4	Lower Florida Keys
Peck et al.	2021	GoPro Hero 7	West Papua
Combs et al.	2021	Canon G16	Southeast Florida
Chen et al.	2021	Olympus tough camera	Wanlitong, South Taiwan
Million et al.	2021	Olympus TG4/5	Lower Florida Keys
Urbina-Barreto et al.	2021	Sony Alpha 7II & Sony FE16	Islands of French oversea territory
Fukunaga et al.	2022	Sony a7IIIR	Lalo Atoll, Northwest Hawaii

## Chapter 4

### Image enhancement can improve the accuracy of 3D models in turbid benthic environments.

Kesia L. Savill, Iain M. Parnum, Jennifer McIlwain and David Belton

#### 4.1 Abstract

An important tool in marine environment conservation is benthic habitat mapping. Within the last decade, Structure-from-Motion (SfM) photogrammetry has been used to survey marine benthic environments, however there is little evidence that this technique has been extensively applied to turbid benthic environments. A variety of benthic habitats with high ecosystem value are found in turbid waters, such as coral reefs which represent 12% of reefs globally. The use of SfM photogrammetry in these environments is difficult due to low light conditions and backscatter from suspended sediment. In this study, image enhancement of photos from an action camera and a compact camera is investigated to determine if it has a significant effect on SfM photogrammetry software's ability to align features and create a more accurate 3D model in turbid benthic environments. Two image enhancement techniques are tried: histogram equalisation and contrast limited adaptive histogram equalisation (CLAHE). Both the histogram equalisation and the CLAHE image enhancement, were able to improve the number of features aligned from photos of a *Porites* coral skeleton, with the skeleton in different percentage fields of view in air and underwater using automatic and custom camera settings. The 3D model from photos using the GoPro Hero 8 that had a histogram equalisation enhancement provided the most agreeable surface area measurement to the engineering model, with 100.6% accuracy. In contrast, the 3D model from photos using the Canon G7X Mark II that had most agreeable surface area measurement to the engineering model with 98.2% accuracy was from the original photos that were not enhanced. Therefore, image enhancement

improved the accuracy of the models from the action camera (GoPro Hero 8), but not for the compact camera (Canon G7X Mark II). Whilst the accuracy was improved, measurements, such as surface area, can be obscured by inaccurate visual representations from the 3D model. This could be attributed to pseudo-feature creation due to the histogram stretching of the photos and the software not recognising structural gaps in the artificial reef structure.

## 4.2 Introduction

Benthic habitat mapping is an important tool in marine environment conservation and management. Within the last decade, a new method has been used to survey marine benthic environments, such as coral reefs, called Structure-from-Motion (SfM) photogrammetry. It is a non-invasive method, which involves taking overlapping photos of an area of interest which is then processed through software, such as Agisoft Metashape, to create 3D models and orthomosaics of the survey area [1]. While there have been many studies using SfM photogrammetry to study benthic habitats [e.g., 2,3,4,1,5,6] there are little published studies in turbid environments as opposed to clear water environments.

Turbid waters account for ~8% to 12% of the total global continental shelf area [7]. A variety of benthic habitats are found in turbid waters, including those considered to have high ecosystem value. For instance, turbid coral reefs represent 12% of reefs globally and yet they are relatively understudied [8,9]. However, photos taken in turbid environments can suffer from a variety of problems, such as low contrast from reduced light, and backscatter from suspended sediment in the water column. Methods to improve photography in low light environments can be applied in acquisition (e.g., optimising settings) and post-processing (e.g., image enhancement). Yet, there are limited studies that have investigated whether these improve results from SfM photogrammetry, let alone from turbid environments. In the previous chapter, the effect of photo acquisition tactics on SfM photogrammetry results

was investigated. This chapter investigates the effect of image enhancement of photos used for SfM photogrammetry.

Image enhancement of photos has been shown to improve certain aspects of an image, whilst removing redundant aspects according to specific needs [10]. As underwater imagery is affected by light absorption, reflection, scattering of light rays, bending, and often poor visibility, images tend to lose contrast [11]. Image enhancement techniques can mitigate these issues. Two common image enhancement techniques have previously been used in studies on underwater image enhancement, a histogram equalisation [11,12], and a contrast limited adaptive histogram equalisation (CLAHE) [13,14,15,16]. Histogram equalisation is a technique in image processing of contrast adjustment using the image's histogram, increasing the global contrast of an image when the image is represented by a narrow range of intensity values [11]. Compared to the CLAHE technique, which divides an image into sections, called tiles, and applies a histogram equalisation to each tile using a pre-defined clip limit [13,11]. The resulting tiles are stitched together using bilinear interpolation to generate an output image with improved contrast [16,17].

Previous studies [e.g., 18,19,20,21,22] have used image enhancement techniques to improve 3D models created using SfM photogrammetry. In a study by Alasal et al. [30], it was found that the histogram equalisation image enhancement had a great impact on the image's contrast, which was reflected in the quality of the resulting 3D model. Another study by Mertes et al. [23] used CLAHE on images of shipwrecks, which greatly increased the quality of the images and subsequent 3D models. This suggests that image enhancement, such as histogram equalisation and CLAHE, should improve the quality of images and resulting 3D models independent of camera type.

This study investigates if histogram equalisation and/or CLAHE image enhancements have a significant effect on SfM photogrammetry software's ability to align features and create a more accurate 3D model from photos taken in turbid underwater environments. The author is not aware of any

previous studies to focus on image enhancement techniques in SfM photogrammetry of turbid underwater environments, which are notorious for producing poorer quality photos compared to their clear water counterparts.

### **4.3 Materials and Methods**

#### *Study site*

This study was conducted at two locations: the Fremantle Sailing Club in Perth, Western Australia (-32.0707962, 115.7509938), and the Coogee Maritime Trail at Coogee Beach, Perth, Western Australia (-32.1054588, 115.7625571) (Figure 4.1). These sites were chosen due to their low visibility and turbid conditions, with in-water visibility ranging from 2-3 m at both locations during the time of imaging. The turbidity of these locations is due to the constant movement of boats leaving and returning to their pens at Fremantle Sailing Club, and due to prevailing winds and local wind-driven waves at Coogee Maritime Trail. Another reason for selecting the Coogee Maritime Trail as a study site was it contains prefabricated structures (artificial reefs) with known dimensions, such as Apollo cluster structures (Fig 4.1d).



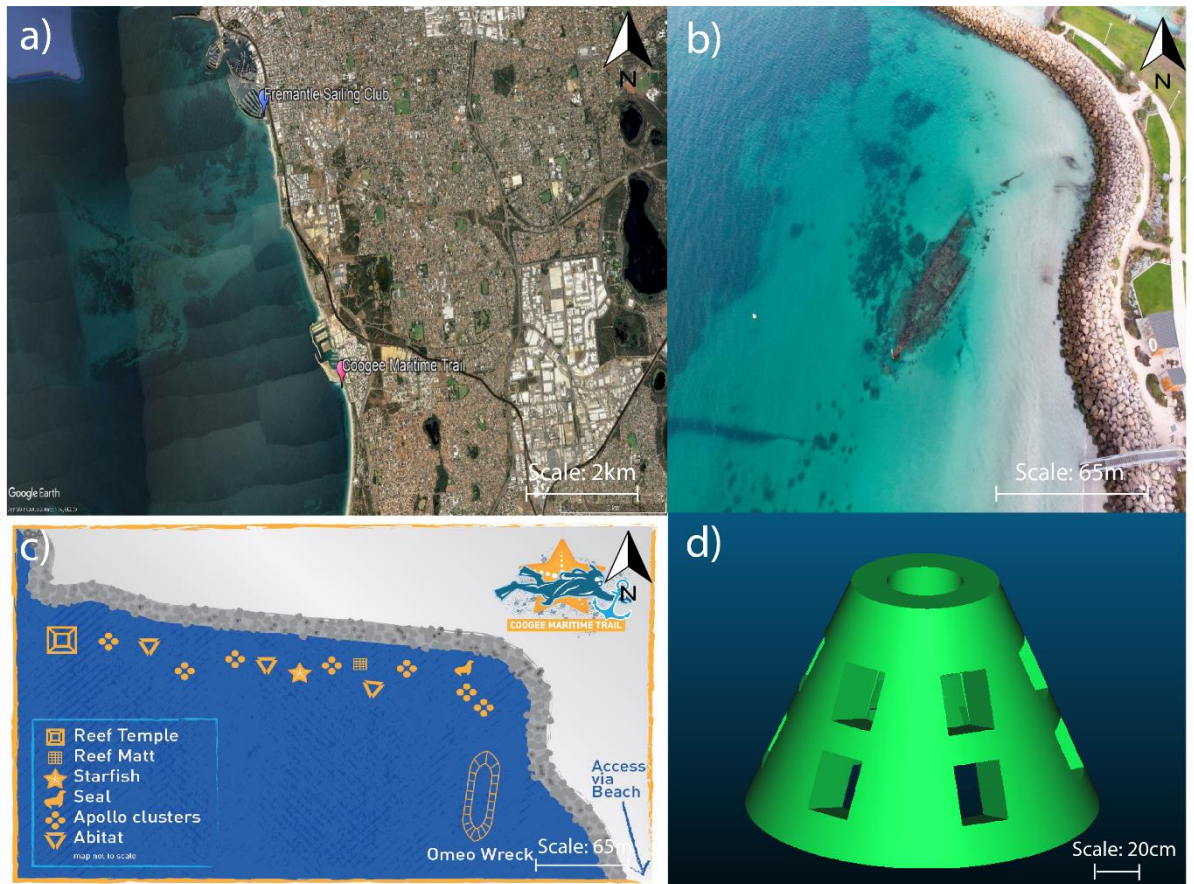




**Figure 4.1.** a. Satellite imagery of the two sites, Fremantle Sailing Club and Coogee Maritime Trail [24]. b. Aerial photograph of Coogee Maritime Trail [25]. c. Map of artificial reef structures of the Coogee Maritime Trail with red circle indicating surveyed structure [26]. d. 3D engineering diagram of Apollo structure [27].

### Data collection

Data collection is detailed in Chapter 3, but in summary, a laser scan was taken of the two coral skeletons, *Porites* and *Turbinaria*, to be used as a “real world” measurement for comparison. The camera settings used were the same as in Chapter 3, however, only the GoPro Hero 8 and the Canon G7X Mark II (Table 4.1) were used. Water quality was assessed with light and turbidity loggers, alongside a CTD. Feature matching from photos of the coral skeletons and camera performance at Fremantle Sailing Club and 3D model generation at Fremantle Sailing Club and Coogee Maritime Trail were assessed as in Chapter 3, with the addition of image enhancement in post-processing.

## Cameras

**Table 4.1.** Specifications of cameras used in this study.

Camera type	Sensor resolution (MegaPixels)	Sensor size (mm)	Image size (pixels)	Focal length (35mm equivalent)
GoPro Hero 8 	12	6.17 x 4.55	4000x3000	19-39 mm (Linear mode)
Canon G7X Mark II 	20	13.2 x 8.8	5472x3648	24-100 mm

## Image processing

### *Image enhancement*

Two different image enhancement techniques were conducted on the photos taken at both Fremantle Sailing Club and Coogee Maritime Trail: histogram equalisation and contrast limited adaptive histogram equalisation (CLAHE). In this study, histogram equalisation of photos was carried out in MATLAB (see Supplementary Data S4.1), and CLAHE was applied to the photos taken using Jupyter Notebook (Python) (see Supplementary Data S4.2).

## Data analysis

Data analysis is detailed as in Chapter 3, but in summary, CloudCompare was used to perform comparisons of surface area measurements using the coral skeleton laser scans and Apollo engineering diagram against created 3D model point clouds, using the methods detailed by Saunders [28].

## 4.4 Results

### *Water quality*

During data collection, Fremantle Sailing Club harbour ranged in NTU between 0 and 3 and average of < 0.5 , and Coogee Maritime Trail had a NTU range of 9-16 and average of 11.5.

### *Feature matching*

The histogram equalisation image enhancement improved the number of features aligned from the photos taken by the GoPro Hero 8 of the *Porites* coral skeleton taken in air at 25% and 50% field of view (Figure 4.2a). The CLAHE image enhancement improved the number of features aligned from the photos taken by the GoPro Hero 8 of the *Porites* coral skeleton taken in air at 75% and 100% field of view (Figure 4.2a), and for all fields of view for photos taken underwater (Figure 4.2b).

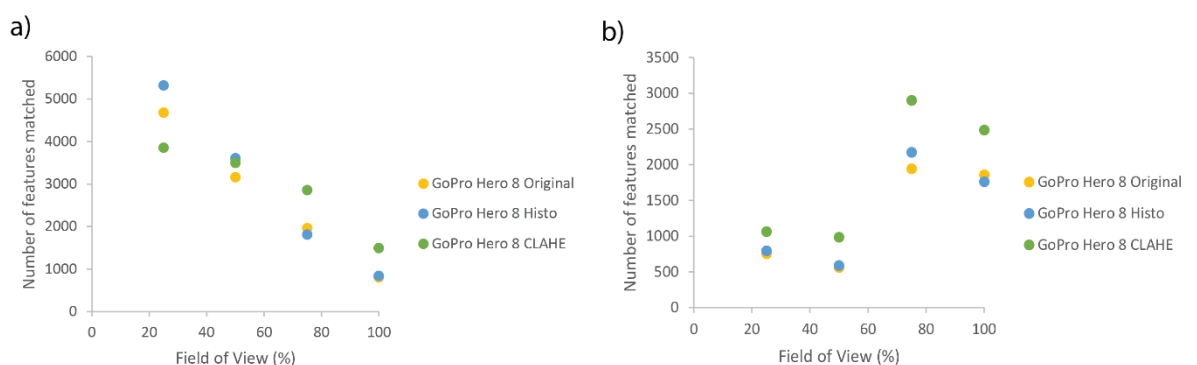


**Figure 4.2. a.** Number of features aligned from original, histogram equalisation, and CLAHE enhanced photos taken using a GoPro Hero 8 of the *Porites* coral skeleton in air and **b.** underwater.

The CLAHE image enhancement improved the number of features aligned from the photos taken using the Canon G7X Mark II of the *Porites* coral skeleton in air for 25% and 75% field of view (Figure 4.3a). The original images taken in air provided the greatest number of features aligned in air for 50% and 100% field of view (Figure 4.3).

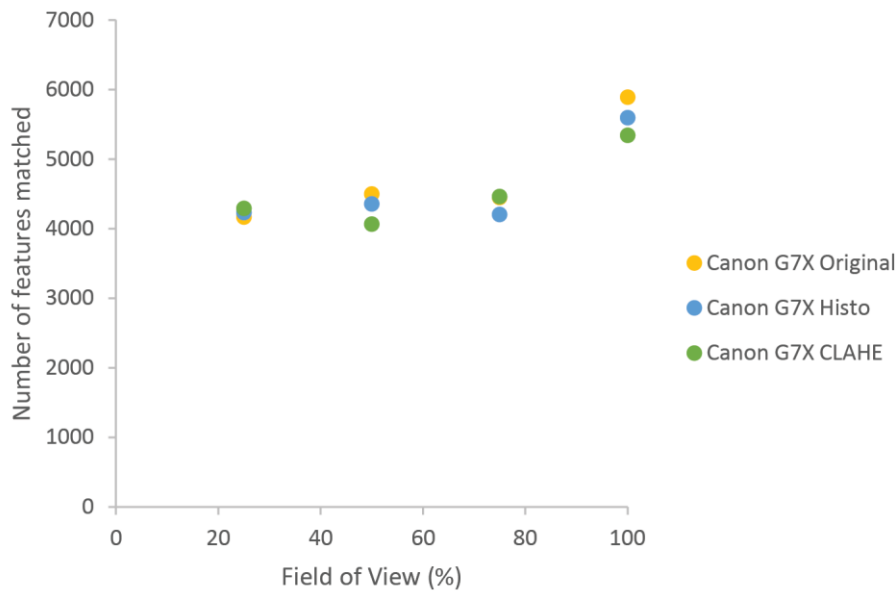


**Figure 4.3.** Number of features aligned from original, histogram equalisation, and CLAHE enhanced photos taken using a Canon G7X Mark II of the *Porites* coral skeleton in air.

The histogram equalisation improved the number of features aligned from photos taken using the Canon G7X Mark II of the *Porites* coral skeleton underwater using automatic settings for 25% field of view (Figure 4.4a). The CLAHE image enhancement improved the number of features aligned for 50% and 75% field of view from photos taken underwater using the automatic settings. Photos taken at 100% field of view were unable to be aligned for any photos taken underwater with the automatic settings, including the image enhanced photos. The original images taken at 25% field of view underwater using custom settings provided the greatest number of features aligned (Figure 4.4b). The CLAHE image enhancement improved the number of features aligned at 50%, 75% and 100% field of view for photos taken underwater using custom settings (Figure 4.4b).

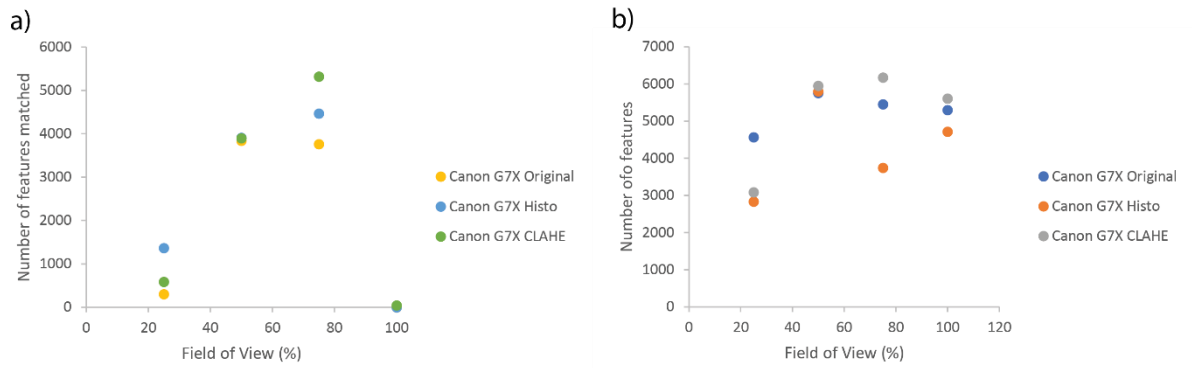


**Figure 4.4 a.** Number of features aligned from original, histogram equalisation, and CLAHE enhanced photos taken using a Canon G7X Mark II of the *Porites* coral skeleton underwater with automatic settings and **b.** underwater with custom settings.

#### Surface area comparison

The 3D model created using photos taken using the GoPro Hero 8 at 1 m above the seafloor with a histogram equalisation applied to the photos, provided the most agreeable surface area measurement to the engineering model, with 100.6% (Table 4.2). The 3D model created using the Canon G7X Mark II using the original photos taken at both 1 m and 2 m above the seafloor, provided the second most agreeable surface area measurement to the engineering model, with 98.2% (Table 4.2).

**Table 4.2.** Surface area comparison of Apollo structure engineering diagram against 3D models created from GoPro Hero 8 and Canon G7X Mark II using original, histogram equalisation and CLAHE photos.

Surface Area Comparison	Number of images	$m^2$		
		Original	Histogram	CLAHE
<b>Apollo (actual)</b>		<b>22.46</b>		
<b>G7X @ 1m</b>	94	21.22	47.58	15.38
<b>G7X @ 2m</b>	66	18.76	28.4	19.62
<b>G7X (all images)</b>	160	<b>22.06</b>	16.52	19.06
<b>GoPro 8 @ 1m</b>	766	18.83	<b>22.6</b>	42.8
<b>GoPro 8 @ 2m</b>	227	16.88	7.46	52.06
<b>GoPro 8 (all images)</b>	993	20.96	8.11	<b>24.09</b>

## **4.5 Discussion**

This study examined the effect of image enhancement of photos taken in turbid benthic environments, on 3D models generated from them using SfM photogrammetry software. In the previous chapter, it was found that a compact camera (Canon G7X Mark II) performed better than two GoPro model action cameras. In this study, the results of image enhancement improved the action camera results, but not for the compact camera.

The turbidity, as indicated as an NTU value, of the sites were similar to the reported range of turbidity the Exmouth Gulf experiences [29]. The turbid coral reefs of the islands in the Exmouth Gulf, for example, Eva Island's northern reef, is on average 1.9 NTU throughout 9 months (Table S4.1), including the time where the survey in Chapter 2 occurred (October 2020). Therefore, the resulting workflow and recommendations can be applied to surveys of the Gulf's turbid reefs.

Our results on image enhancement techniques used to improve 3D models reflect those of previous studies [e.g.,18,19,20,21,22] However, as our image enhancement only improved the results from the action camera, it appears that the CLAHE method used requires more investigation to optimise its use in turbid underwater environments. However, the simplistic histogram equalisation improves the close altitude photos and is suited improving image quality and subsequent 3D models for photos taken in turbid water environments.

### **Uncertainty in findings**

The models created of the Apollo structure at Coogee Maritime Trail show variable surface area measurements, that highly under or overestimated the surface area. The 3D model produced from the original images was overlaid in CloudCompare with the image enhanced models from that camera. It was found that the 3D models which had a lot of visual noise (i.e., the mesh had areas which were not the Apollo structure) (e.g., Figure S4.1), produced a higher surface area measurement. This could be attributed to the histogram

stretching of the photos causing the SfM photogrammetry program to create pseudo-features, which is shown as noise in the model. In contrast, the models which were incomplete (i.e., had holes) (e.g., Figure S4.2) had a lower surface area measurement. Therefore, the surface area measurements for some of the models cannot be taken at face value, as the numbers indicate a higher or lower surface area for the Apollo structure, without omitting either the parts of the model which are not the Apollo structure, or not accounting for the holes in the model. As the Apollo structure has been in its current location for several years, we would also expect its surface area to have increased, due to growth of marine organisms such as algae, tunicates and sponges. Whilst two of the models, the CLAHE model for both ranges from GoPro Hero 8 and the histogram model for Canon G7X Mark II at 1 m altitude, produced surface area measurements slightly higher but still close to the original surface area measurement from the engineering model, it is unclear whether the SfM photogrammetry software accurately modelled the structure in terms of including the growth on the structure.

#### **4.6 Conclusion**

Image enhancement of photos taken in turbid underwater environments can improve the accuracy of 3D models, however measurements such as surface area can be obscured by inaccurate visual representations of the object as a 3D model. It is still unclear why some models created a visually complete and measurably accurate model, whilst other models were incomplete and the distortion of the model gave inaccurate surface area measurements. A more dedicated study of the effect of image enhancement on photos from turbid underwater environments is needed to determine if image enhancement is required for a more accurate 3D model to be produced, or if the original photos provide an adequate model without enhancement.

## 4.7 References

1. Lange ID, Perry CT. A quick, easy and non-invasive method to quantify coral growth rates using photogrammetry and 3D model comparisons. *Methods Ecol. Evol.*, **2020**, *11*, 714-726
2. Figueira W, Ferrari R, Weatherby E, Porter A, Hawes S, Byrne M. Accuracy and precision of habitat structural complexity metrics derived from underwater photogrammetry. *Remote Sens.*, **2015**, *7*, 16883-16900
3. Ferrari R, McKinnon D, He H, Smith RN, Corke P, Gonzalez-Rivero M, Mumby PJ, Upcroft B. Quantifying multiscale habitat structural complexity: A cost-effective framework for underwater 3D modelling. *Remote Sens.*, **2016**, *8*, 113
4. Ferrari R, Figueira WF, Pratchett MS, Boube T, Adam A, Kobelkowsky-Vidrio T, Doo SS, Brooke Atwood T, Byrne M. 3D photogrammetry quantifies growth and external erosion of individual coral colonies and skeletons. *Sci. Rep.*, **2017**, *7*, 16737
5. Cresswell AK, Orr M, Renton M, Haywood MDE, Giraldo Ospina A, Slawinski D, Austin R, Thomson DP. Structure-from-motion reveals coral growth is influenced by colony size and wave energy on the reef slope at Ningaloo Reef, Western Australia. *J. Exp. Mar. Biol. Ecol.*, **2020**, 530-531
6. Roach TNF, Yadav S, Caruso C, Dilworth J, Foley CM, Hancock JR, Huckeba J, Huffmyer AS, Hughes K, Kahkejian VA, Madin EMP, Matsuda SB, McWilliam M, Miller S, Santoro EP, Rocha de Souza M, Torres-Pullizaa D, Drury C, Madin JS. A field primer for monitoring benthic ecosystems using Structure-from-Motion photogrammetry. *J. Vis. Exp.*, **2021**, 170
7. Shi W, Wang M. Characterization of global ocean turbidity from Moderate Resolution Imaging Spectroradiometer ocean color observations. *J. Geophys. Res. Oceans*, **2010**, 115
8. Sully S, van Woesik R. Turbid reefs moderate coral bleaching under climate-related temperature stress. *Glob. Chang. Biol.*, **2020**, *26*, 1367-1373



9. Zweifler A, O'Leary M, Morgan K, Browne NK. Turbid coral reefs: Past, present and future-A review. *Diversity*, **2021**, 13, 251
10. Dynamsoft. Available online: <https://www.dynamsoft.com/blog/insights/image-processing/image-processing-101-image-enhancement/#:~:text=Image%20enhancement%20refers%20to%20the%20process%20of%20highlighting,adjusting%20levels%20to%20highlight%20features%20of%20an%20image> (Accessed on 08 August 2022)
11. Sharma V, Kulshrestha A, Barot P. A study on underwater image enhancement using histogram equalization. *Int. J. Sci. Eng. Res.*, **2019**, 10
12. Abd-Al Ameer ZS, Daway HG, Kareem HH. Enhancement underwater image using histogram equalization based on color restoration. *J. Eng. Appl. Sci.*, **2019**, 14, 641-647.
13. Hitam MS, Awalludin EA, Jawahir Hj Wan Yussof WN, Bachok Z. Mixture contrast limited adaptive histogram equalization for underwater image enhancement. *2013 International Conference on Computer Applications Technology*. 1-5
14. Jawahir Hj Wan Yussof WN, Hitam MS, Awalludin EA, Bachok Z. Performing contract limited adaptive histogram equalization technique on combined color models for underwater image enhancement. *Int. J. Interact. Dig. Media*, **2013**, 1
15. Yang W, Xu Y, Qiao X, Rao W, Li D, Li Z. Method for image intensification of underwater sea cucumber based on contrast-limited adaptive histogram equalization. *Transactions of the Chinese Society of Agricultural Engineering*, **2016**, 32, 197-203
16. Kanthamma K, Geetha G, Keerthi D, Uday Kiran D, Vinod Kumar CH. Improved CLAHE enhancement technique for underwater images. *International journal of Engineering Research and Technology*, **2020**, 9
17. Geeks for Geeks. Available online: <https://www.geeksforgeeks.org/clahe-histogram-equalization-opencv/> (Accessed on 08 August 2022)

18. Li Z, Tan P, Tan RT, Zou D, Zou SZ, Cheong L. Simultaneous video defogging and stereo reconstruction. **2015**, 10.1109/CVPR.2015.729913
19. Xu X, Che R, Nian R, He B, Chen M, Lendasse A. Underwater 3D object reconstruction with multiple views in video stream via structure from motion. *Oceans 2016-Shanghai*. 1-5
20. Alasal SA, Alsmirat M, Baker QB, Jararweh Y. Improving passive 3D model reconstruction using image enhancement. *2018 6<sup>th</sup> International Conference on Multimedia Computing and Systems (ICMCS)*, **2018**, 1-7
21. Qiao X, Ji Y, Yamashita A, Asama H. Structure from Motion of underwater scenes considering image degradation and refraction. *IFAC-PapersOnLine*, **2019**, 52, 78-82
22. Xu H, Qian W, Xu D, Pu Y, Yuan G. 3D reconstruction of multi-view images based on modified histogram equalization. *4<sup>th</sup> International Conference on Modelling, Simulation and Applied Mathematics (MSAM)*, **2020**
23. Mertes J, Thomsen T, Gulley J. Evaluation of Structure from Motion software to create 3D models of late Nineteenth Century Great Lakes shipwrecks using archived diver-acquired video surveys. *J. Marit. Archaeol.*, **2014**, 9, 173-189
24. Google Earth Pro V 7.3.48642. (June 8<sup>th</sup>, 2022). Map of South Fremantle and Coogee, Perth.
25. Seniorocity. Available online: <https://seniorocity.com.au/coogee-maritime-trail-and-omeo-shipwreck/> (Accessed on 08 August 2022)
26. West Travel Club. Available online: <https://westtravelclub.com.au/stories/new-dive-snorkel-trail-for-coogee> (Accessed on 08 August 2022)
27. Subcon. (Subcon, Perth, Western Australia, Australia). Image of Apollo Structure at Coogee Maritime Trail, 2022. (Company photograph)

28. Saunders R. (Curtin University, Perth, Western Australia, Australia).  
Three-dimensional modelling of coral reef using underwater photogrammetry,  
2020. (Unpublished work)
29. Sutton AL, Shaw JL. Cumulative pressures on the distinctive values of  
Exmouth Gulf. First draft report to the Department of Water and  
Environmental Regulation by the Western Australian Marine Science  
Institution, Perth, Western Australia. **2021**. 272 pages

## 4.8 Supplementary material

### Data S4.1. HistogramEqualisation

Histogram equalisation of photos was executed in MATLAB prior to alignment. Relevant code is available on figshare

[<https://doi.org/10.6084/m9.figshare.20509122.v1>]

### Data S4.2. CLAHE

CLAHE of photos was executed in Jupyter Notebook prior to alignment.

Relevant code is available on figshare

[<https://doi.org/10.6084/m9.figshare.20509122.v1>]

**Table S4.1.** NTU and SD of Eva Island, Exmouth Gulf, Western Australia for 9 months of the year in 2020/2021.

Location	Month/Year	Average NTU	SD
Eva Island	October 2020	1.90	± 1.13
Eva Island	November 2020	1.21	± 0.35
Eva Island	December 2020	1.55	± 1.05
Eva Island	January 2021	1.33	± 0.79
Eva Island	February 2021	2.49	± 2.31
Eva Island	March 2021	2.46	± 4.87
Eva Island	April 2021	3.77	± 5.57
Eva Island	May 2021	1.72	± 1.83
Eva Island	June 2021	1.14	± 0.41

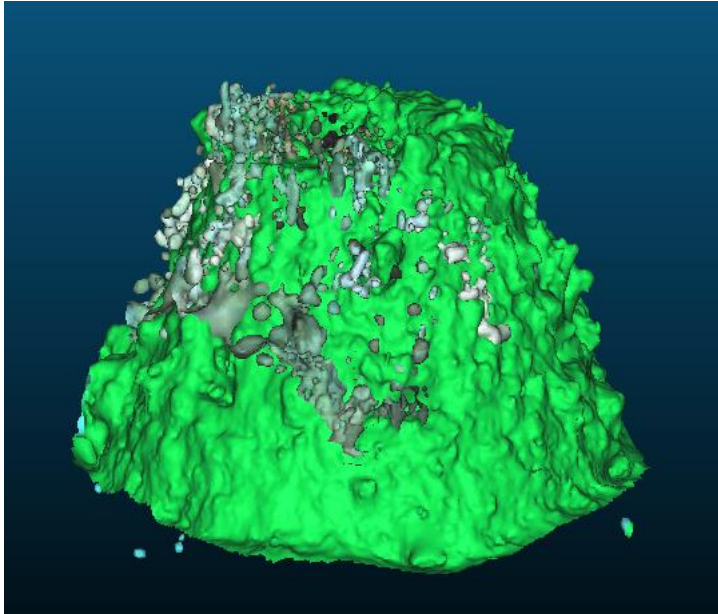


**Figure S4.1.** Example of the original model (light green) at 1m from Canon G7X Mark II overlaid with CLAHE model (dark green) at 1m. The CLAHE model can be seen as “noisy” due to the mesh including not just the structure itself.

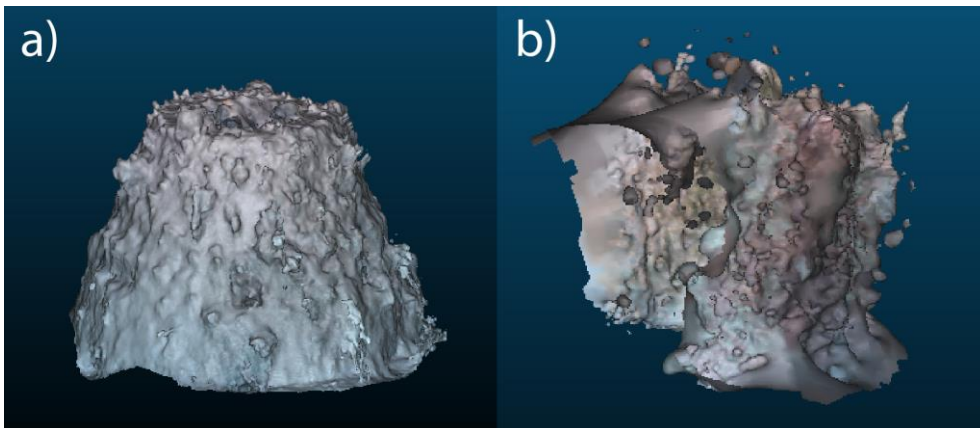


**Figure S4.2.** Models from combined altitudes for 1m and 2m for **a.** GoPro Hero 8 original photos. **b.** GoPro Hero 8 Histogram photos.

# Chapter 5

## General discussion

### 5.1 Summary of findings

This thesis examined the use of SfM photogrammetry in turbid benthic environments to determine the accuracy of the methodology to collect key coral metrics (i.e., coral cover and species composition) against traditional methods (Chapter 2), if camera type and altitude from the survey area/target significantly impacted the accuracy of the 3D model (Chapter 3) and if image enhancement techniques improve the accuracy of 3D models (Chapter 4). This final chapter consolidates the main aims and results of each data chapter, and discusses the limitations and significance of this thesis and identifies future research opportunities (Figure 5.1). Key findings from this thesis are summarised below.

#### **5.1.1 Research finding #1. Currently SfM photogrammetry does not provide better estimates of coral metrics for carbonate budgets than traditional methods.**

Chapter 2 found that in a turbid reef environment, measurements for species richness was greater using outputs from SfM photogrammetry than LIT's, yet mean coral cover was significantly higher for LIT's. It was determined that differences in coral cover estimates was driven by SfM photogrammetry's limitation to resolve small, low-lying coral colonies. Key factors that impacted the accuracy of SfM photogrammetry data acquisition were low visibility combined with the complex surface topography of the reef. It was therefore concluded that the SfM photogrammetry workflow used (as described in Chapter 2) in turbid reef environments, with patchy coral reefs dominated by weedy coral species, will not provide a more accurate assessment of coral metrics for carbonate budget calculations than the traditional LIT method. SfM photogrammetry also requires a large budget for initial setup and is more intensive post-processing of data than LIT's, so it may not be practical in many research studies and monitoring projects where time and money is

sparse. However, SfM photogrammetry does not require divers trained in coral identification like LIT's require, and it allows for repeatability assessments without needing to go back in the field. Furthermore, if the 3D model is accurately scaled, measurements such as rugosity and coral volume calculations could be extracted, to improve carbonate budget assessments.

### **5.1.2 Research finding #2. Camera type and altitude affects the accuracy of SfM photogrammetry 3D models.**

Camera type and altitude were investigated in Chapter 3. It was found that a camera with a large sensor size and high sensor resolution (in this case 13.2 x 8.8 mm) performed better in turbid benthic environments. In addition, it was more beneficial to use customised camera settings to suit the environment, rather than using the camera's automatic settings, which will slightly vary between photos. This allows for high quality photos to be taken, assisting in the photo alignment process, where similar features from sequential photos are aligned based on similar points between photos.

In this study, photos taken at both 1 m and 2 m above the survey target provided the most accurate 3D model, compared to just using one set altitude. Model accuracy increased with the addition of photos from either altitude. However, it was also found that a log function based on number of photos could be used to adequately account for 3D model accuracy, suggesting the increase in accuracy with number of photos eventually results in diminishing returns. These results suggest using photos taken at more than one altitude, can improve accuracy of 3D models produced, which could be because it improves the estimation of the camera's interior orientation parameters. However, if surveying a large area and time is scarce, photos taken at a closer altitude, e.g., 1 m, can provide a more accurate model than a model with only photos taken further away from the survey area. As this would not suit every survey site, time needs to be taken at the start of each survey to establish the optimal altitude.

### **5.1.3 Research finding #3. Image enhancement can improve the accuracy of 3D models.**

Image enhancement of photos taken in turbid benthic environments was investigated in Chapter 4. It was found that image enhancement can improve the accuracy of 3D models created from SfM photogrammetry software, however measurements derived from the models, such as surface area, can be obscured by inaccurate representations of the survey target as a 3D model. Improvements in 3D model creation from image enhancement were seen most in the camera with the lowest sensor size. Also, it should be noted that while some of the 3D models created were visually complete and measurably accurate, others were visually incomplete and measurably inaccurate. This suggests that further studies on the effect of image enhancement on photos from turbid benthic environments be investigated to provide a definitive answer if image enhancement is significantly beneficial to the SfM photogrammetry workflow in these environments or if the original photos provide an adequate model with the need for enhancement.



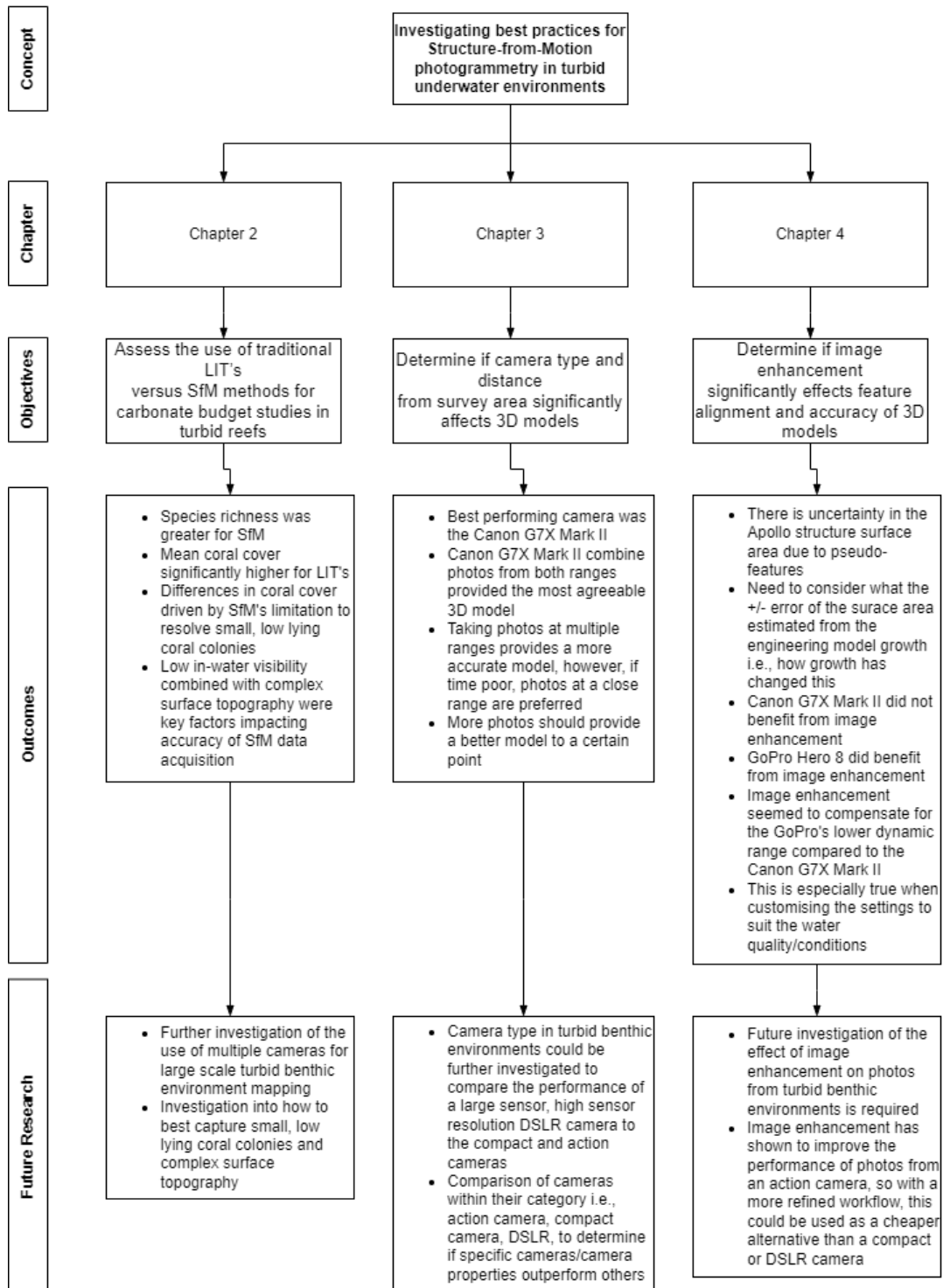


**Figure 5.1.** Concept diagram outlining the outcomes and future research opportunities generated from this thesis.

## 5.2 Limitations and future opportunities

This thesis demonstrates the application of SfM photogrammetry in turbid benthic environments, however, several limitations still apply to this research. Firstly, the camera array used in Chapter 2 consisted of four action cameras in a 1.5 m<sup>2</sup> array. This design was used to provide high coverage of the area that consisted of patchy reef dominated by weedy coral species and variable depths due to the reef's structure. This technique did not work as intended and only images from two of the four cameras were able to be aligned to create several orthophoto mosaics of different parts of the survey area. Although orthomosaics of parts of the reef were created, we were unable to create an orthophoto or 3D model of the entire area. However, multiple camera arrays and their footprint have been investigated and published and therefore can be used to rectify the issues we encountered with our array.

Secondly, the DSLR camera used in this study was outdated which could have affected the performance of the camera against the action camera and the compact camera. Whilst the compact camera with a large sensor size and high sensor resolution was found to be most suitable to turbid benthic environments, further research comparing a newer DSLR camera model against a similar compact camera used in this study could be investigated. This could determine whether an inexpensive camera (e.g., Canon G7X Mark II) is better suited for specific research questions for turbid benthic environments over the more expensive DSLR camera, provided its specifications (i.e., sensor size and sensor resolution) are suitable for use in low-light underwater environments.

Finally, the image enhancement techniques used in this study tended to create pseudo-features due to the stretching of the histogram in each of the photos. This affected the surface area measurements significantly. Further research to refine these techniques, including the process of modelling after post-processing of the photos, should be conducted to confidently determine if image enhancement improves the accuracy of the 3D models in turbid

benthic environments. Further, this should be considered as part of the workflow for future studies in similar environments.

### **5.3 Significance of thesis**

Coral reefs are biodiverse and productive ecosystems that not only provide a habitat for a vast number of species, but also provide coastal protection and are economically valuable, producing billions of dollars each year through tourism and fisheries industries (Cornwall et al., 2021). Recent models suggest that an increase of 1.5°C in sea surface temperatures, which is currently predicted to be reached by early 2030's, will cause 99% of global reefs to experience heatwave events that reefs are unlikely to recover from due to their frequency (Dixon et al., 2022). There is evidence to suggest that turbid coral reefs, which represent 12% of reefs globally (Zweifler et al., 2021) are more resilient to effects of increasing sea surface temperatures than clear water reefs (Perry et al., 2008; Morgan et al., 2017; Browne et al., 2019), and could become critical refuge sites for coral larvae. Despite the importance of these ecosystems, they are relatively understudied. Clear water reefs are commonly studied due to their range and ease of studying, as opposed to turbid reefs which are logistically harder to study, due to their limited visibility and low light conditions. As methods for monitoring coral reefs develop and new technologies arise, the application of these novel methods needs to be developed to suit a range of environments, from clear water to semi-turbid to turbid reefs.

This thesis demonstrates the application of SfM photogrammetry in turbid benthic environments and the considerations and current limitations due to the lack of studies using this technique in turbid environments. The main findings this thesis presents is suggested considerations for using SfM photogrammetry in turbid water environments. This includes selecting a camera with a good sensor size and resolution (within budget), spend time determining the optimal altitude(s) that photos should be taken, and consider applying image enhancement for processing of photos from these

environments. It also highlights the need of further research in optimising the use of SfM photogrammetry in turbid benthic environments which will allow for a quick, easy and non-invasive survey which can be used in a variety of environments (e.g., coral reefs, shipwrecks, seagrass meadows). It can also provide a multitude of data that can be extracted from a single dive as opposed to multiple, labour intensive dives using traditional methodology (e.g., multiple types of transect surveys are required to collect data, such as rugosity and coral cover, for carbonate budget calculations)

#### **5.4 Overall thesis conclusion**

Turbid benthic environments are important ecosystems which may be more resilient to the effects of local stressors and anthropogenic climate change. Understanding their health and function is crucial to future management and conservation initiatives in order to preserve the world's turbid benthic ecosystems, specifically turbid coral reefs as warming ocean temperatures are predicted to severely effect their clear water counterparts. SfM photogrammetry has proven to be an effective approach to monitoring benthic environments in clear water environments and with the appropriate workflow, can be successfully applied to turbid environments.

#### **5.5 References**

- Browne N, Braoun C, McIlwain J, Ramasamy N, Zinke J. 2019. Borneo coral reefs subject to high sediment loads show evidence of resilience to various environmental stressors. *PeerJ*. 8, e7382
- Cornwall CE, Comeau S, Kornder NA, Perry CT, van Hooidek R, DeCarlo TM, Pratchett MS, Anderson KD, Browne N, Carpenter R, Diaz-Pulido G, D'Olivo JP, Doo SS, Figueiredo J, Fortunato SAV, Kennedy E, Lantz CA, McCulloch MT, Gonzalez-Rivero M, Schoepf V, Smithers SG, Lowe RJ. 2021. Global declines in coral reef calcium carbonate production under ocean acidification and warming. *PNAS*. 118 (21), e2015265118

- Dixon A, Beger M, Kalmus P, Heron S. 2022. Safe havens for coral reefs will be almost non-existent at 1.5 of global warming-new study. *The Conversation*. <https://theconversation.com/safe-havens-for-coral-reefs-will-be-almost-non-existent-at-1-5-c-of-global-warming-new-study-176084>
- Morgan KM, Perry CT, Johnson JA, Smither SG (2017) Nearshore turbid-zone corals exhibit high bleaching tolerance on the Great Barrier Reef following the 2016 ocean warming event. *Front Mar Sci* 4:224
- Perry, C.T.; Smithers, S.G.; Palmer, S.E.; Larcombe, P.; Johnson, K.G. 2008. 1200 year paleoecological record of coral community development from the terrigenous inner shelf of the Great barrier reef. *Geology*. 36, 691–694
- Zweifler A, O'Leary M, Morgan K, Browne NK. 2021. Turbid coral reefs: Past, present and future-A review. *Diversity*. 13(6), 251

# **Appendix A: Copyright statements**

## **Chapter 2**

As first author, permission is automatically granted to use this manuscript in this thesis.

To whom it may concern, I, Kesia Louise Savill, contributed to the design of this study, analysed the data and wrote and edited the following manuscript:

Savill, K.L., Browne, N.K., Parnum, I, Helmholz, P. A comparative and cost-benefit analysis of Structure-from-Motion of determining coral cover and diversity in turbid reef environments.

I, as a co-author, endorse that the level of contribution by the candidate stated above is appropriate.

Dr. Nicola Browne

Dr. Iain Parnum

Dr. Petra Helmholz

### **Chapter 3**

As first author, permission is automatically granted to use this manuscript in this thesis.

To whom it may concern, I, Kesia Louise Savill, contributed to the design of this study, analysed the data and wrote and edited the following manuscript:

Savill, K.L., Parnum, I. McIlwain, J., Belton, D. Effect of camera type and altitude on SfM photogrammetry for application in turbid benthic environments.

I, as a co-author, endorse that the level of contribution by the candidate stated above is appropriate.

Dr. Iain Parnum

Dr. Jennifer McIlwain

Dr. David Belton

## Chapter 4

As first author, permission is automatically granted to use this manuscript in this thesis.

To whom it may concern, I, Kesia Louise Savill, contributed to the design of this study, analysed the data and wrote and edited the following manuscript:

Savill, K.L., Parnum, I. McIlwain, J., Belton, D. Image enhancement can improve the accuracy of 3D models in turbid benthic environments.

I, as a co-author, endorse that the level of contribution by the candidate stated above is appropriate.

Dr. Iain Parnum

Dr. Jennifer McIlwain

Dr. David Belton